

ABSTRACT

Title of Dissertation: PHYSICAL LAYER ISSUES AND CROSS-LAYER DESIGN IN WIRELESS NETWORKS

Yun Li, Doctor of Philosophy, 2004

Dissertation Directed By: Professor Anthony Ephremides,
Department of Electrical and Computer
Engineering

Comparing to wired networks, wireless networks have some special features in the physical layer, medium access control (MAC) layer, and the network layer. This work discusses several research topics in the physical layer, and studies the cross-layer design of wireless networks.

First, we consider a Code-division multiple-access (CDMA) system with multiuser detection when the presence of a subset of the users is unknown to the receiver. The performance of the system in terms of Signal-to-Interference and noise-Ratio (SIR) and user capacity is given, by assuming symmetric signals. Then, we study the power control problem with multiple flow types. Each node has multiple flow types requiring different QoS, (for example in a multimedia system,) and has the constraint of using the same

power level for all of the flow types. The conditions for solution to exist are given; and the characteristics of the solution are provided. Next, we propose a passive rate adaptation, in which some bits are dropped at the receiver end of a link, for the ad hoc network to use in the temporary channel fluctuation. We study the performance of this passive rate control scheme in terms of both symbol error probability and mean square distortion.

Finally, we study the coupling between layers of the network structure, and the cross-layer design. We explore the coupling between the physical layer and the MAC sublayer first, and propose the scheduling algorithm with power control. Then we consider the coupling between MAC sublayer and the network layer, and propose the joint scheduling and routing algorithm. The simulation results demonstrate that the joint algorithm improves the performance significantly.

PHYSICAL LAYER ISSUES AND CROSS-LAYER DESIGN
IN WIRELESS NETWORKS

by

Yun Li

Thesis or Dissertation submitted to the Faculty of the Graduate School of the
University of Maryland, College Park, in partial fulfillment
of the requirements for the degree of
Doctor of Philosophy
2004

Advisory Committee:

Professor Anthony Ephremides, Chairman/Advisor
Professor Ashok K. Agrawala
Professor John Baras
Professor Prakash Narayan
Assistant Professor Sennur Ulukus

© Copyright by

Yun Li

2004

Dedication

To my husband and sons.

Acknowledgements

I am greatly indebted to my advisor Dr. Anthony Ephremides for his invaluable guidance and enthusiastic support during the course of this work. He gave me great freedom in choosing my research topics, and also enthusiastic guidance during my work. I gained a lot of knowledge and valuable experience while working with him. I appreciate his detailed discussion with me about research, his great help in reading my papers, his generous financial support for me to attend conferences, and his strong encouragement for me to pursue my career.

I am grateful to Prof. Agrawala, Prof. Baras, Prof. Narayan, and Prof. Ulukus for their serving on my defense committee.

I would also like to thank my husband, my parents, and my parent-in-laws for their great support and love.

Table of Contents

Dedication	ii
Acknowledgements	iii
Table of Contents	iv
List of Tables	vii
List of Figures	viii
Chapter 1 Introduction	1
1.1 CDMA and Multiuser Detection.....	1
1.2 Power Control and Sequence Optimization.....	3
1.3 Rate Control for Fluctuating Links.....	4
1.4 Cross-layer Design of Ad-hoc Networks.....	6
Chapter 2: Linear Multiuser Detectors for Incompletely Known Symmetric Signals in CDMA Systems	8
2.1 Introduction.....	8
2.2 Signal Model.....	11
2.3 Performance of Linear Multiuser Detectors	15
2.3.1 Matched filter.....	15
2.3.2 Decorrelator	16
2.3.3 MMSE detector	20
2.3.4 Comparison of linear multiuser detectors	21
2.4 Single-class Case and User Capacity.....	26
2.4.1 Matched filter.....	27
2.4.2 (K,0) Decorrelator.....	28
2.4.3 (M,N) Decorrelator	29
2.4.4 (K,0) MMSE detector	33
2.4.5 (M,N) MMSE detector.....	34
2.4.6 Comparisons	36
2.5 Multiple-class Case and Effective Bandwidth.....	38
2.5.1 Matched filter.....	39
2.5.2 (K,0) Decorrelator.....	40
2.5.3 (M,N) Decorrelator	42
2.5.4 Comparisons	42
2.6 Summary.....	43
Chapter 3 Power Control in Uplink and Downlink CDMA System with Multiple Flow Types.....	45
3.1 Introduction.....	45
3.2 Uplink	48

3.2.1 Special Case of $F=1$	49
3.2.2 Special Case of $N=2$, with Common Flow Types at Two Nodes	51
3.2.3 Special Case of $N=2$, with Different Flow Types at Two Nodes.....	56
3.2.4 General Case of $N>1$	59
3.3 Downlink	62
3.3.1 Special Case of $F=1$	63
3.3.2 Special Case of $N=1$	65
3.3.3 General Case of $N>1$ and $F>1$	67
3.4 Effect of the One Power Level Constraint.....	67
3.4.1 Special Case of $N=1$	69
3.4.2 Special Case of $\beta_1 = \beta_2 = \dots = \beta_F$	71
3.4.3 Numerical Example for General N And F	72
3.5 Summary	73
Chapter 4 Simple Rate Control for Fluctuating Channels in Ad Hoc Wireless Networks	75
4.1 Introduction.....	75
4.2 Model and Analysis	80
4.3 PAM Example in a Gaussian Channel.....	85
4.3.1 Symbol Error Probability	85
4.3.2 Mean Square Distortion	88
4.4 QAM Example in a Gaussian Channel	92
4.4.1 Symbol Error Probability	92
4.4.2 Mean Square Distortion	93
4.5 Rayleigh Fading Channel.....	96
4.6 Non-uniform Constellation	100
4.7 Summary and Conclusions	102
Chapter 5 Joint Scheduling, Power Control, and Routing Algorithm for Ad-Hoc Wireless Networks.....	104
5.1 Introduction.....	104
5.2 Network Model	107
5.3 Jointly Scheduling and Power Control	108
5.3.1 Scheduling Metric	108
5.3.2 Scheduling Rules	109
5.3.3 Scheduling Algorithms and Power Control	110
5.3.4 Simulation Results	113
5.4 Jointly Scheduling and Routing.....	122
5.4.1 Routing Distance.....	122
5.4.2 Rerouting.....	123
5.4.3 Simulation Results	124
5.5 Distributed Algorithm.....	128
5.5.1 With Simplified Scheduling.....	130
5.5.2 With Joint Scheduling and Power Control.....	131
5.6 Future Work and Extension	132
5.7 Conclusions.....	132

Chapter 6 Summary	133
Appendices.....	135
A. Proof of Restriction 1	135
B. Proof of Restriction 2	136
C. Derivation of (2.5).....	138
D. Derivation of (2.15) and (2.16)	139
E. Monotonicity of $SIR_{\text{mmse}}^{(K,0)}(P, K)$ and $SIR_{\text{mmse}}^{(M,N)}(P, M)$	141
F. Proof of Proposition 1.....	142
G. Proof of (3.10).....	144
H. Proof of Proposition 3	145
I. Proof of Proposition 4	146
J. Proof of Proposition 7	147
K. Derivation of (4.7)	149
References.....	150

List of Tables

Table 2.1: User capacity and effective bandwidth for linear multiuser detectors	44
Table 3.1: Comparison of the power for the power control problem with and without the constraint of one power level. $N=3$; $F=2$; $L=20$	73
Table 5.1: The throughput, delay, and power of the 10-node network with simplified scheduling for different values of α *.....	115
Table 5.2: Minimum number of iteration needed for joint scheduling and power control algorithms with 0.1% failure rate.....	116
Table 5.3: Threshold rates for scheduling algorithms	117

List of Figures

Figure 2.1: SIR of $(K,0)$ linear multiuser detectors, when $\rho=0.5$	24
Figure 2.2: SIR of (M,N) linear multiuser detectors, when $\rho=0.5$ and $P_u/\sigma^2=10$	25
Figure 2.3: Function $F(M)$ for (M,N) decorrelator.....	30
Figure 2.4: Constraint on number of known users M for (M,N) decorrelator.....	33
Figure 2.5: Power allocation of (M,N) MMSE detector for $P_u/\sigma^2=0, 4$, and 10 , when $\rho=0.5, \beta=10$	36
Figure 3.1: Examples of $N=2, F=2$ power control problem. Solutions do not exist.....	55
Figure 3.2: Examples of $N=2, F=2$ power control problem. Solutions exist.....	55
Figure 3.3: Examples of the convergence of iterative algorithm in the 2-D plane.	57
Figure 4.1: Signal space constellation of 8-PAM and 8-PAM- \rightarrow 4.....	81
Figure 4.2: Signal space constellation of 16-QAM and 16-QAM- \rightarrow 4.	82
Figure 4.3: SEP of PAM example, for a uniform source, in a Gaussian channel.....	87
Figure 4.4: SEP of PAM example, for a Gaussian source, in a Gaussian channel.....	87
Figure 4.5: MSD of PAM example, for a uniform source, in a Gaussian channel.....	91
Figure 4.6: MSD of QAM example, for a Gaussian source, in a Gaussian channel.....	91
Figure 4.7: SEP of QAM example, for a uniform source, in a Gaussian channel.	93
Figure 4.8: MSD of QAM example, for a uniform source, in a Gaussian channel.	95
Figure 4.9: MSD of QAM example, for a Gaussian source, in a Gaussian channel.....	95
Figure 4.10: SEP of PAM example, for a uniform source, in a Gaussian channel and a Rayleigh fading channel with $\Omega=1$	97
Figure 4.11: SEP of QAM example for a uniform source, in a Gaussian channel and a Rayleigh fading channel with $\Omega=1$	98
Figure 4.12: MSD of PAM example, for a Gaussian source, in a Gaussian channel and a	

Rayleigh fading channel with $\Omega=1$	99
Figure 4.13: MSD of QAM example, for a Gaussian source, in a Gaussian channel and a Rayleigh fading channel with $\Omega=1$	99
Figure 4.14: Signal space constellation of non-uniform 4-QAM and 4-QAM->2.	100
Figure 4.15: SEP of uniform and non-uniform 4-QAM and 4-QAM->2, for a uniform source in a Gaussian channel.	101
Figure 4.16: MSD of uniform and non-uniform 4-QAM and 4-QAM->2, for a Gaussian source in a Gaussian channel.	102
Figure 5.1: The 10-node network and 20-node network used in simulation.	114
Figure 5.2: Throughput, power, delay, and complexity of scheduling algorithms, for the 10-node network.	119
Figure 5.3: Throughput, power, delay, and complexity of scheduling algorithms, for the 20-node network.	121
Figure 5.4: Throughput, delay, and power for different routing parameters, 10-node example.	126
Figure 5.5: Throughput, delay, and power for different routing parameters, 20-node example.	128

Chapter 1 Introduction

Wireless communication networks are widely used nowadays. Cellular networks, wireless LANs, and mobile ad hoc networks are a few examples. Wireless networks have an air interface rather than a wireline interface. This wireless characteristic provides special features to the network, and has a profound impact on the lower layers of the network.

First, in the physical layer, the channels are noisy and unstable, and usually have very limited bandwidth. Then in the MAC layer, the broadcasting nature introduces interference to other users in the nearby area, and therefore, generates new challenge for the multi access schemes. Also, wireless networks include mobile users which are powered by battery. Therefore, the energy efficiency is very important to the wireless networks. Finally, there are coupling between network layers, especially in ad hoc wireless networks.

In this dissertation, the following issues in the wireless networks are discussed.

1.1 CDMA and Multiuser Detection

Code-division multiple-access (CDMA) is a method of multiple-access in which all the users occupy the given time-frequency space simultaneously. Each user is given a unique signature sequence (code) at the transmitter with which to spread its signal. The receiver de-spreads the received signal if it knows the signature sequences of the

transmitter. As long as the codes are orthogonal, all signals can be separated. CDMA has superior performance over time-division multiple access (TDMA) or frequency division multiple access (FDMA) in mobile communication systems [1] and in harsh channel environments [2]. However, in non-orthogonal CDMA systems the traditional single-user receiver suffers from the near-far problem caused by multi-access interference and performance degrades.

Multiuser receivers suppress the interference between users in spread-spectrum CDMA systems by making use of the structure of the multi-access interference [3]-[5] and of the knowledge of the code sequences. Linear multiuser detectors are more attractive than nonlinear ones because of their reduced complexity. Much of the work on multiuser detection has focused on the multiuser efficiency and the near-far resistance [6]-[7] of multiuser receivers. Since improving network capacity is an important design goal [8], increased attention is paid to receiver performance in power-controlled CDMA systems and to the resulting user capacity [9]-[11].

The effective bandwidth characterization of the user capacity was first derived in [9]. Specifically, it was proved that the SIR requirements of all users can be met if and only if the sum of the effective bandwidths of the users is less than the total number of degrees of freedom in the system. Simple expressions are derived for systems with matched filter, decorrelator, or linear minimum mean square error (MMSE) receiver, assuming the users are assigned random sequences. Then a synchronous power-controlled CDMA system with a MMSE linear receiver was studied in [10], and the optimal signature sequences and power allocation scheme were identified to meet the SIR requirement with minimum total power.

The multiuser detector needs to know which of the users are active and what their signature sequences are in order to detect the signals correctly. But in some instances, the detector may not know exactly all of the transmitting users and their sequences. One solution to this problem is the group-blind multiuser detection [12,13]. The interference from users with unknown signatures may affect the performance in a different way than the interference from known users and the noise. If we have some information about the unknown users, like sequence crosscorrelation and power, we may be able to track their effect on the performance of the system.

In Chapter 2 we evaluate the performance degradation caused by unknown interference if there is no blind multiuser detection. The performance indices we study include SIR, user capacity and effective bandwidth. Although random sequences are often used in analysis (as in [9]), meaningful results are not possible for a system with a finite number of users. Here, we use symmetric sequences to simplify the analysis and obtain one data point of reference in the study of finite-user system performance.

1.2 Power Control and Sequence Optimization

Power control is used to balance the received powers of the users of a CDMA system, so that no single user creates excessive interference that can destroy the quality of the communication of other users. At the same time it is desirable to use power levels as low as possible, provided they satisfy the quality of service (QoS) objective defined by fixed signal-to-interference ratio (SIR) requirements.

In previous papers [15,16], the optimum power vector was found by inversion of a non-negative matrix [14,17] related to the channel gains and crosscorrelation. For $N < L$, (N is number of users and L is the processing gain.) the optimal sequences are orthogonal

sequences. For $N > L$, the optimal sequences are found to be the WBE sequences [18,19]. Optimal sequence sets for synchronous and asynchronous CDMA systems are studied in [20] and [21]. An iterative power control algorithm to calculate the optimum power vector was given in [22], and the convergence of the algorithm was proved if the interference function satisfies some conditions.

However, all the studied models assume only one flow type at each node. In practice, users may have multiple flow types that have different QoS requirements. In Chapter 3 we consider a synchronous CDMA system with a base station and N nodes. At each node, there are F flow types and they transmit simultaneously to the base station. Each node has only one transmitter, i.e., only one power level is available in the uplink for all F flow types. Such a transmitter structure is simpler than the one in which the power levels of the multiplexed flow types are adjusted by appropriate weights or baseband processing, or the one in which separate transceivers and power amplifiers are used for each flow.

The objective of Chapter 3 is to evaluate the performance degradation that results from this simple and inexpensive transmitter structure. For the uplink, we studied the conditions for this power control problem to have solutions, the minimum power vector, and if possible, the optimal sequences to achieve the minimum total power. For the downlink, we studied the power assignment at the base station, and obtained some properties of the optimal sequences.

1.3 Rate Control for Fluctuating Links

The link quality of a wireless connection may vary considerably due to noise burst, fades, and the mobility of transmitter and/or receiver nodes. Therefore a fixed modulation scheme and a fixed data rate will lead to variable link quality. When the Signal-to-Noise

Ratio (SNR) of the received signal drops significantly, there are many ways to maintain the link quality. One way is to increase the transmission power [23]. Another way is to change the channel coding rate or choice of code, and therefore change the received data rate indirectly [24,25]. It can also be done by adapting the data rate directly [26,27,28], or some combination of the methods listed above [29,30,31].

However, all these methods require feedback channels from the receiver to the source. Some may require buffering of traffic at the source, which may cause longer delay and/or buffer overflows or underflows. Some methods may also require increased complexity in the transmitter design.

In Chapter 4, we consider a passive rate adaptation scheme at the receiver in which only part of the transmitted bits are detected (i.e., some bits are intentionally dropped). For example, if the transmitter uses 8-PAM (PAM modulation with 8-point constellation), then when the channel is in poor condition, the receiver uses a detector with 4 output levels after the demodulator. We denote the procedure by 8-PAM->4. Another example is 16-QAM->4.

This method is motivated by the need to have a quick and simple rate adaptation scheme when a link in an ad hoc wireless network fluctuates for very brief periods. The advantage of the proposed method is that no feedback is needed; and the receiver alone makes the decision according to the channel status. It is also fairly simple at the receiver, while there is no buffer and complicated transmitter design at the transmitter.

With our method, when the receiver detects few of the transmitted bits, it decreases the symbol error probability. At the same time, the dropped bits take away some signal information and cause additional quantization noise. In terms of the mean square

distortion metric, there is a trade-off between the error probability and the detected data rate. This trade-off is identified and illustrated. In fact, it is the main focus of Chapter 4. The question is precisely whether the overall distortion, with fewer bits but with smaller symbol error probability, exceeds or not that achieved with more bits but with larger symbol error probability.

In Chapter 4 we consider two examples of the modulation schemes, PAM and QAM, and study the performance of the rate adaptation in terms of symbol error probability and mean square distortion, in both a Gaussian channel and a Rayleigh fading channel.

1.4 Cross-layer Design of Ad-hoc Networks

An ad-hoc wireless network is a collection of wireless mobile hosts forming a temporary network. Connections of mobile hosts are via multihop wireless connection without the support from a fixed infrastructure (“Base Station”). Its classical applications are battlefield communications, disaster recovery, search and rescue, and so on. Due to the mobility of nodes, the status of a communication link is a function of the location and transmission power of the source and destination nodes, and the channel interference from other links.

The traditional layered structure of networks simplifies the design and implementation, and allows end systems manufactured by different vendors to share the information seamlessly. Recently, more and more people realize that in wireless networking there is strong coupling among the traditional layers of the OSI (open systems interconnection) architecture and that these interactions can not be ignored. These couplings are most obvious in the ad hoc networks. Cross-layer design is able to improve the network performance [38,39,40].

One example of the coupling is between the routing in the network layer and the access control in the MAC sublayer. The selection of routes clearly affects the flows and, hence, the requirement of bandwidth allocation at each wireless link. On the other hand, the choice of bandwidth allocation and access control affects the accumulation of queuing at links, and therefore changes the distance of each link and the route selection. Many works on routing in such networks (see, e.g., [41,42]) assume a fixed underlying protocol for access control, and most of the researches on multiple access assume fixed routes and flow requirements [43]. In the past several years, the problem of coupling routing with medium access control in ad-hoc wireless networks has been addressed [44,45,46]. Another example of the coupling between layers is the coupling of power control in the physical layer and the scheduling in the MAC layer. The power assignment of links changes the link status, and the topology of the network, and hence the scheduling result. On the other hand, the scheduling decides the link activation and the interference generated, and therefore changes the power required at each link to achieve the QoS. Joint scheduling and power control algorithm are studied in [47,48].

In Chapter 5, we assume a TDMA-based wireless ad-hoc network, where each node has one receiver and one transmitter. We study both scheduling algorithms with joint power control and without joint power control, and conclude that with joint power control, the network achieves significantly larger throughput and less delay in the cost of slightly higher energy consumption. We also study the joint routing and scheduling algorithm. The simulation results show that there is a trade-off between the energy consumption and the network performance, and the network performance improves significantly by the joint algorithm.

Chapter 2: Linear Multiuser Detectors for Incompletely Known Symmetric Signals in CDMA Systems

2.1 Introduction

Code-division multiple-access (CDMA) is a method of multiple-access in which all the users occupy the given time-frequency space simultaneously. Each user is given a unique signature sequence (code) at the transmitter with which to spread its signal. The receiver de-spreads the received signal if it knows the signature sequences of the transmitter. As long as the codes are orthogonal, all signals can be separated. CDMA has superior performance over time-division multiple access (TDMA) or frequency division multiple access (FDMA) in mobile communication systems [1] and in harsh channel environments [2]. However, in non-orthogonal CDMA systems the traditional single-user receiver suffers from the near-far problem caused by multi-access interference and performance degrades.

Multiuser receivers suppress the interference between users in spread-spectrum CDMA systems by making use of the structure of the multi-access interference [3]-[5] and of the knowledge of the code sequences. Linear multiuser detectors are more attractive than nonlinear ones because of their reduced complexity. Much of the work on

multiuser detection has focused on the multiuser efficiency and the near-far resistance [6]-[7] of multiuser receivers. Since improving network capacity is an important design goal [8], increased attention is paid to receiver performance in power-controlled CDMA systems and to the resulting user capacity [9]-[11].

The effective bandwidth characterization of the user capacity was first derived in [9]. Specifically, it was proved that the SIR requirements of all users can be met if and only if the sum of the effective bandwidths of the users is less than the total number of degrees of freedom in the system. Simple expressions are derived for systems with matched filter, decorrelator, or linear minimum mean square error (MMSE) receiver, assuming the users are assigned random sequences. The corresponding user capacity and effective bandwidth (as the processing gain and the number of users approach to infinity) were found to be a function of the SIR requirement β . Specifically, it was shown that

$$C_{\text{mf}}(\beta) = \frac{1}{\beta}, \quad C_{\text{dec}}(\beta) = 1, \quad C_{\text{mmse}}(\beta) = 1 + \frac{1}{\beta},$$

$$e_{\text{mf}}(\beta) = \beta, \quad e_{\text{dec}}(\beta) = 1, \quad e_{\text{mmse}}(\beta) = \frac{\beta}{1 + \beta}.$$

Then a synchronous power-controlled CDMA system with a MMSE linear receiver was studied in [10], and the optimal signature sequences and power allocation scheme were identified to meet the SIR requirement with minimum total power. The user capacity and effective bandwidth of the MMSE linear receiver were found to be given by $C_{\text{mmse}}(\beta) = 1 + 1/\beta$ and $e_{\text{mmse}}(\beta) = \beta/(1 + \beta)$ respectively. After that, the user capacity of power-controlled CDMA systems with linear receivers in fading channels was evaluated in [11].

In this chapter, we consider a synchronous CDMA system that uses BPSK

modulation and is equipped with a multiuser receiver. We assume that all of the users have symmetric signature sequences, i.e., the crosscorrelation between any two signature waveforms from different users are the same: $\rho_{ij} = \rho$, $0 \leq \rho < 1$, for all $i \neq j$. Although random sequences are often used in analysis (as in [9]), meaningful results are not possible for a system with a finite number of users. Here, we use symmetric sequences to simplify the analysis and obtain one data point of reference in the study of finite-user system performance.

The multiuser detector needs to know which of the users are active and what their signature sequences are in order to detect the signals correctly. But in some instances, the detector may not know exactly all of the transmitting users and their sequences. For example, in some CDMA systems, the receiver detects which of the users are transmitting from the analysis of the received signal; so some error in this detection may cause some of the users' identity to remain unknown to the receiver. Another example is the out-of-cell interference in a cellular network. One solution to this problem is the group-blind multiuser detection [12] that is based on stochastic approximation or subspace tracking techniques. When the set of codes of all possible users is known, an algorithm was proposed in [13] that make use of the knowledge of the codes to identify the interference and achieve faster convergence of the group-blinded multiuser detection. These blind multiuser detection schemes improve the performance, but introduce additional complexity.

The interference from users with unknown signatures may affect the performance in a different way than the interference from known users and noise. If we have some information about the unknown users, like sequence crosscorrelation and power, we may

be able to track their effect on the performance of the system. In this chapter we are NOT trying to detect or identify the unknown users; instead, we evaluate the performance degradation caused by unknown interference if there is no blind multiuser detection. The performance indices we study include SIR, user capacity and effective bandwidth. Note that the detector is operated without the knowledge of the unknown users; however, the performance analysis is exact in that it accounts for all the active users.

The organization of this chapter is as follows: In Section 2.2, we introduce the DS-CDMA signal model and the multiuser receivers when some users are unknown. In Section 2.3, the SIR of the matched filter, the decorrelator, and the MMSE detector are derived and compared. In Section 2.4, the single-class case is considered and user capacity for the matched filter, the decorrelator, and the MMSE detector are given. In Section 2.5, the multiple-class case is studied and effective bandwidth for the matched filter and decorrelator are computed. Finally in Section 2.6, we summarize our conclusions. The detailed derivations of some formulas are given in Appendices A to E.

2.2 Signal Model

Assume a BPSK modulated, synchronized CDMA system with a total of K possible users. Each user has a specific SIR requirement and is assigned a unique signature sequence with processing gain L . There are two kinds of users:

Known users: For these, the receiver knows their signature sequences, and uses them in the detector structure. The system can control their transmission power.

Unknown users: For these, the receiver does not know their signature sequences, and can not control their transmission power. The system does not detect their signals.

Let there be M known users ($1 \leq M \leq K$) and N ($N=K-M$) unknown users. The

notation (M,N) is used to denote the corresponding detection problem. Since in this case the receiver does not know that the N unknown users are actually transmitting, the detector operates as if there were only M users. That is, the (M,N) detector has the same structure as the $(M,0)$ detector, although, of course, its performance will be different. The special case of $N=0$, i.e., the $(K,0)$ receiver, is the regular multiuser detector discussed in [3], where all the users are known to the receiver.

User i ($i=1,2,\dots,K$) has power P_i , transmitted bit $b_i=\pm 1$, and signature waveform $S_i(t)$, $0\leq t\leq T$, which satisfies $\int_0^T S_i^2(t)dt=1$. The waveform $S_i(t)$ can also be represented by its corresponding signature sequence $\mathbf{s}_i=[s_{i1} \ s_{i2} \ \dots \ s_{iL}]$, where $S_i(t)=\sum_{j=1}^L s_{ij}\psi_j(t)$ is based on an orthonormal basis $\{\psi_j(t), j=1,\dots,L\}$. We assume that the crosscorrelation between any two users' sequences is given by a constant ρ between 0 and 1.

$$\rho_{ij} = \int_0^T S_i(t) \cdot S_j(t) dt = \rho, \quad 0 \leq \rho < 1, \text{ for all } i \neq j.$$

This symmetry assumption leads to some restrictions on the possible values of L , K , and ρ .

Restriction 1: *In L -dimensional space, K ($K \leq L$) symmetric vectors with unit length and crosscorrelation ρ exist, if and only if*

$$-\frac{1}{K-1} \leq \rho \leq 1. \quad (2.1)$$

Restriction 2: *In L -dimensional space (L finite), the number of symmetric vectors K satisfies $K \leq L+1$; and for K to have the maximum value $L+1$, the value of ρ must be equal to $-L^{-1}$.*

The proofs of these statements are in Appendices A and B respectively. From these

two restrictions, if $K=L+1$, the only possible value of ρ is $\rho = -L^{-1}$; while if $K \leq L$, the possible values of ρ satisfy (2.1). Negative values of ρ , namely the interval $\left[-(K-1)^{-1}, 0\right]$, have a very limited range, which actually vanishes as K gets large. So we assume $0 \leq \rho < 1$ in our calculations; and therefore, the number of users K has to satisfy $K \leq L$.

A natural question that arises is that, since the number of users is always less than or equal to the processing gain, why not let $\rho = 0$. In this way the same user capacity would be achieved and better performance would be realized. The answer is that in assigning sequences (and, hence, the value of ρ), the designer deals with a number of subscribers much greater than L and orthogonal sequences are not possible. In general, fewer than L users are simultaneously active in the system at any given moment. In a cellular case, the base station assigns codes to active users as they enter the system, hence orthogonal codes are possible. But for military and other ad hoc environments, codes are pre-assigned and hence the option of orthogonal codes to only active users does not exist, if the population of potential users is very large. The case we are considering corresponds to a subset of a large number of users who cannot have orthogonal sequences in L dimensions. Why should they be symmetric then? They need not be. Another popular assumption about sequences is that they be random. Analysis of the random sequence case for a finite number of users is very difficult. Hence, we assume symmetric sequences here, both for simplifying the analysis and for obtaining one data point in the space of performance evaluation of multiuser detectors.

We impose two constraints on the maximal admissible number of users. The first is from the power consumption point of view; i.e., the power allocation to any of the users

must be finite. This is similar to the assumption made in [9] and [10]. The other is from our assumption that the K users are symmetric. Assuming an L -dimensional space and $0 \leq \rho < 1$, there are at most L symmetric users with crosscorrelation ρ (i.e., $K \leq L$). This constraint was not needed in [9] and [10], since there could be arbitrary numbers of random sequences or optimum sequences.

The received signal at the receiver is given by $y(t) = \sum_{i=1}^K \sqrt{P_i} b_i S_i(t) + \sigma \cdot n(t)$, where $n(t)$ is the white Gaussian noise with unit power spectral density. The $(K,0)$ receiver passes the received signal through K matched filters, the outputs of which can be written in matrix form as

$$\mathbf{y}_K = \mathbf{R}_K \cdot \mathbf{A}_K \cdot \mathbf{b}_K + \sigma \cdot \mathbf{n}_K. \quad (2.2)$$

Here the $K \times 1$ vectors \mathbf{y}_K , \mathbf{n}_K , and \mathbf{b}_K , the $K \times K$ crosscorrelation matrix \mathbf{R}_K , and the diagonal matrix \mathbf{A}_K are defined as:

$$(\mathbf{y}_K)_i = \int_0^T y(t) \cdot S_i(t) dt,$$

$$(\mathbf{n}_K)_i = \int_0^T n(t) \cdot S_i(t) dt,$$

$$(\mathbf{b}_K)_i = b_i, \quad i=1,2,\dots,K,$$

$$(\mathbf{R}_K)_{ij} = 1 \text{ if } i = j, \quad (\mathbf{R}_K)_{ij} = \rho \text{ if } i \neq j,$$

$$\text{and } \mathbf{A}_K = \text{diag}\{\sqrt{P_1}, \sqrt{P_2}, \dots, \sqrt{P_K}\}.$$

After the matched filters, a multiuser detector is used to detect the signal from the vector \mathbf{y}_K . The signal from user i is detected by $\hat{b}_i = \text{sgn}((\mathbf{H}_K \mathbf{y}_K)_i)$. The choice of the matrix \mathbf{H}_K distinguishes the different linear multiuser detectors. The matched filter has the form of $\mathbf{H}_K = \mathbf{I}_K$, and is a single-user detector. The decorrelator has the form of

$\mathbf{H}_K = \mathbf{R}_K^{-1}$, it eliminates the multi-access interference by projecting the signal onto the orthogonal space of the interference. The MMSE multiuser detector is designed to be the optimal linear detector by minimizing MSE (maximizing SIR). As derived in [3], it has the form of $\mathbf{H}_K = (\mathbf{R}_K + \sigma^2 \mathbf{A}_K^{-2})^{-1}$.

For the (M,N) detector, the receiver passes the signal through M matched filters based on the waveform of the M known users. The outputs in matrix form are given by

$$\mathbf{y}_M = \mathbf{R}_M \mathbf{A}_M \mathbf{b}_M + \Delta \mathbf{A}_N \mathbf{b}_N + \sigma \cdot \mathbf{n}_M. \quad (2.3)$$

Here \mathbf{y}_M , \mathbf{R}_M , \mathbf{A}_M , \mathbf{b}_M , and \mathbf{n}_M are defined as above, except that the dimension of the matrix is different. The matrix Δ represents the crosscorrelation between unknown users and known users, with $\Delta_{ij} = \rho$ for all $1 \leq i \leq M, 1 \leq j \leq N$. And $(\mathbf{A}_N \mathbf{b}_N)_i = \sqrt{P_{M+i}} \cdot b_{M+i}$, $i=1,2,\dots,N$, represents the signal from unknown users.

Since the receiver assumes only the M known users are active, it has the same structure as the $(M,0)$ detector. The signal from user i is detected by $\hat{b}_i = \text{sgn}((\mathbf{H}_M \mathbf{y}_M)_i)$. The matrix \mathbf{H}_M is equal to \mathbf{I}_M for the matched filter, \mathbf{R}_M^{-1} for the decorrelator, and $(\mathbf{R}_M + \sigma^2 \mathbf{A}_M^{-2})^{-1}$ for the MMSE detector.

2.3 Performance of Linear Multiuser Detectors

2.3.1 Matched filter

In the (M,N) matched filter detector, the user i is detected by $\hat{b}_i = \text{sgn}((\mathbf{y}_M)_i)$, $i=1,2,\dots,M$. Therefore the SIR for user i is given by

$$SIR_{mf,i}^{(M,N)} = \frac{P_i}{\sigma^2 + \sum_{\substack{j=1 \\ j \neq i}}^M \rho^2 P_j + \sum_{j=M+1}^{M+N} \rho^2 P_j}, \quad i=1,2,\dots,M. \quad (2.4)$$

We notice that $SIR_{mf,i}^{(M,N)} = SIR_{mf,i}^{(M+N,0)}$, $i=1, 2, \dots, M$. This means that the interference from unknown users affects the SIR in the same way as the interference from known users. Actually, the interference from unknown users affects the SIR in the same way as noise with power $\rho^2 P_u$. The SIR for user i in the $(K,0)$ matched filter detector can be obtained from (2.4) by letting $M=K$ and $N=0$.

2.3.2 Decorrelator

For the (M,N) decorrelator, we have

$$\hat{b}_i = \text{sgn}\left((\mathbf{R}_M^{-1} \mathbf{y}_M)_i\right) = \text{sgn}\left(\sqrt{P_i} b_i + (\mathbf{R}_M^{-1} \Delta \mathbf{A}_N \mathbf{b}_N)_i + \sigma (\mathbf{R}_M^{-1} \mathbf{n}_M)_i\right).$$

Here $(\mathbf{R}_M^{-1} \mathbf{n}_M)_i$ is the colored Gaussian noise with variance $(\mathbf{R}_M^{-1})_{ii}$. The term $\mathbf{R}_M^{-1} \Delta \mathbf{A}_N \mathbf{b}_N$ represents the extra interference from the N unknown users. After some matrix calculation (Appendix C), we obtain the SIR of user i , which is given by

$$SIR_{dec,i}^{(M,N)} = \frac{P_i}{\frac{\sigma^2}{1-\rho} \cdot \frac{1+\rho(M-2)}{1+\rho(M-1)} + \left[\frac{\rho}{1+\rho(M-1)}\right]^2 \sum_{j=M+1}^{M+N} P_j}, \quad i=1,2,\dots,M. \quad (2.5)$$

The error probability of user i is obtained by conditioning on all interference bits \mathbf{b}_N and making use of the symmetry of Gaussian distribution. We obtain

$$P_{err,dec,i}^{(M,N)}(\sigma) = 2^{-N} \sum_{b_{M+1}=\{+1,-1\}} \cdots \sum_{b_{M+N}=\{+1,-1\}} \mathcal{Q}\left(\frac{\sqrt{P_i}}{\sigma} \left(1 + \frac{\rho}{1+\rho(M-1)} \sum_{j=M+1}^{M+N} \sqrt{\frac{P_j}{P_i}} \cdot b_j\right) \sqrt{\frac{(1+\rho(M-1))(1-\rho)}{1+\rho(M-2)}}\right). \quad (2.6)$$

Let us review some of the concepts defined in [3] in order to evaluate the multiuser

performance of the (M,N) decorrelator.

Effective energy: $e_k(\sigma)$, is the energy that user k would require to achieve bit-error-rate equal to $P_k(\sigma)$ in a single-user Gaussian channel with the same noise level. i.e.,

$$P_k(\sigma) = Q(e_k(\sigma)/\sigma).$$

Multuser efficiency: $e_k(\sigma)/P_k$, is the ratio between the effective and actual energies.

Asymptotic multuser efficiency: $\eta_k = \lim_{\sigma \rightarrow 0} e_k(\sigma)/P_k$. It measures the slope with which $P_k(\sigma)$ goes to 0 in logarithmic scale in the high signal-to-noise (SNR) region; that is

$$\eta_k = \sup \left\{ 0 \leq r \leq 1 : \lim_{\sigma \rightarrow 0} \frac{P_k(\sigma)}{Q(\sqrt{r}\sqrt{P_k}/\sigma)} = 0 \right\} = \frac{2}{P_k} \lim_{\sigma \rightarrow 0} \sigma^2 \log \frac{1}{P_k(\sigma)}.$$

From the error probability expression (2.6), the expression of the asymptotic multuser efficiency is obtained from the largest term of the Q function among all possible combinations in \mathbf{b}_N . That is,

$$\eta_{\text{dec},i}^{(M,N)} = \max^2 \left\{ 0, \left(1 - \frac{\rho}{1 + \rho(M-1)} \cdot \sum_{j=M+1}^{M+N} \sqrt{\frac{P_j}{P_i}} \right) \cdot \sqrt{\frac{(1 + \rho(M-1))(1 - \rho)}{1 + \rho(M-2)}} \right\}. \quad (2.7)$$

Equations (2.6) and (2.7) are derived by analogy with the matched filter receiver in [3, Ch. 1].

From (2.7) it is seen that the asymptotic multuser efficiency of the (M,N) case is smaller than that of the $(M,0)$ case, and the reduction depends on the sum of the unknown users' signal amplitudes. When the unknown signal amplitudes exceed a certain value, the asymptotic multuser efficiency reduces to zero. Specifically, when

$$\sum_{j=M+1}^{M+N} \sqrt{P_j/P_i} \geq [1 + \rho(M-1)]/\rho$$

is true, then $\eta_{\text{dec},i}^{(M,N)} = 0$ holds. This means that when the unknown power is very large, the (M,N) decorrelator is not near-far resistant, and the bit

error rate does not vanish as the noise level goes to zero.

For the $(K,0)$ decorrelator, we let $M=K$ and $N=0$ in (2.5), (2.6) and (2.7), and thus the SIR, error probability, and asymptotic multiuser efficiency, (which is also multiuser efficient in this case,) are given by

$$SIR_{\text{dec},i}^{(K,0)} = \frac{P_i}{\frac{\sigma^2}{1-\rho} \left[\frac{1+\rho(K-2)}{1+\rho(K-1)} \right]}, \quad (2.8)$$

$$P_{\text{err}}^{(K,0)}(\sigma) = Q \left(\frac{\sqrt{P_i}}{\sigma} \sqrt{\frac{(1+\rho(K-1))(1-\rho)}{1+\rho(K-2)}} \right), \quad (2.9)$$

$$\text{and } \eta_{\text{dec},i}^{(K,0)} = \frac{(1+\rho(K-1))(1-\rho)}{1+\rho(K-2)}. \quad (2.10)$$

Asymptotic Performance of the (M,N) decorrelator: The asymptotic performance can be calculated from (2.5) and (2.7), by letting

$$L \rightarrow \infty, \quad K \rightarrow \infty, \quad \frac{K}{L} = \alpha, \quad \text{and} \quad \frac{M}{K} = \phi.$$

We find that

$$SIR_{\text{dec},i}^{(M,N)} \rightarrow \frac{P_i}{\sigma^2} (1-\rho).$$

Notice that $\lim_{L \rightarrow \infty} SIR_{\text{dec},i}^{(M,N)} = \lim_{L \rightarrow \infty} SIR_{\text{dec},i}^{(K,0)}$, i.e., the interference from the unknown users vanishes asymptotically. This is caused by the factor $[\rho/(1+(M-1)\rho)]^2$ in (2.5), which goes to 0 as fast as M^{-2} , and therefore faster than $\sum_{j=M+1}^{M+N} P_j$, which is of order M if the average powers of the unknown users are the same.

For simplicity, we assume that the average relative amplitude of any unknown user (with respects to user i) is one. i.e.,

$$\lim_{K \rightarrow \infty} \frac{1}{N} \sum_{j=M+1}^{M+N} \sqrt{P_j/P_i} = 1.$$

We observe that if ρ is constant and $0 \leq \rho < 1$, then

$$\eta_{\text{dec},i}^{(M,N)} \rightarrow (1-\rho) \max^2 \left\{ 0, 2 - \frac{1}{\phi} \right\}. \quad (2.11)$$

Equation (2.11) implies that, in order to have $\eta_{\text{dec},i}^{(M,N)} > 0$, we must have $\phi > 1/2$, i.e., at least half of the transmitting users must be known by the receiver.

Effective Interference: The following expression of SIR is an approximation for a large system [9].

$$SIR_i = \frac{P_i}{\sigma^2 + \frac{1}{L} \sum_{\substack{j=1 \\ j \neq i}}^K I_{ji}(P_j, P_i, SIR_i)}. \quad (2.12)$$

The quantity $I_{ji}(P_j, P_i, SIR_i)$ is the *effective interference* that user j imposes on user i .

We rewrite the SIR of the (M,N) decorrelator as

$$SIR_{\text{dec},i}^{(M,N)} = P_i / \left\{ \sigma^2 + (M-1) \frac{\sigma^2 \rho^2}{[1 + \rho(M-1)](1-\rho)} + \left[\frac{\rho}{1 + \rho(M-1)} \right]^2 \sum_{j=M+1}^{M+N} P_j \right\}. \quad (2.13)$$

In this equation, the three terms in the denominator are identified to be respectively (i) the noise, (ii) the effective interference from the other $M-1$ known users except user i , and (iii) the interference from the N unknown users. By analogy between (2.12) and (2.13), we define the effective interference from each of the $K-1$ users to user i as:

$$I_{\text{dec},ji}^{(M,N)} = \begin{cases} \frac{\sigma^2 \rho^2 L}{[1 + \rho(M-1)](1-\rho)} & j \neq i, j = 1, 2, \dots, M, \\ \left[\frac{\rho}{1 + \rho(M-1)} \right]^2 L P_j & j = M+1, \dots, M+N. \end{cases} \quad (2.14)$$

Notice that the effective interference from known user j is independent from its power, while the effective interference of the unknown users is proportional to their

power. This is because the decorrelator uses the projection of \mathbf{y}_M onto the orthogonal space of $\{\mathbf{s}_1, \mathbf{s}_2, \dots, \mathbf{s}_{i-1}, \mathbf{s}_{i+1}, \dots, \mathbf{s}_M\}$ to detect b_i , so the performance in detecting user i is independent of the power in the direction of \mathbf{s}_j . Actually, the ‘‘effective interference’’ is not the real interference; it is the noise enhancement that corresponds to the power reduction in the desired signal in the process of projection. For $(K,0)$ case, (2.14) becomes

$$I_{\text{dec},ji}^{(K,0)} = \frac{\sigma^2 \rho^2 L}{[1 + \rho(K-1)](1-\rho)} = \frac{P_i}{\beta_i} \frac{\rho^2 L}{[1 + \rho(K-2)]}, \quad j \neq i, j=1,2,\dots,K.$$

In [9], the effective interference in the decorrelator is given by P_i/β_i for a large system and for the case of random sequences, which is also independent of the interfering power.

2.3.3 MMSE detector

The (M,N) MMSE detector minimizes the MSE assuming only users $1, \dots, M$ are active. We let $\mathbf{G} = (\mathbf{R}_M + \sigma^2 \mathbf{A}_M^2)^{-1}$. Since this is hard to calculate for a general \mathbf{A}_M matrix, we assume equal power for all the users, i.e., $P_1 = \dots = P_M = P$. Define the $M \times 1$ vector \mathbf{u}_M as $\mathbf{u}_M = [1 \ \dots \ 1]^T$. Now, $\mathbf{G} = (\mathbf{R}_M + (\sigma^2/P) \cdot \mathbf{I}_M)^{-1}$, and

$$\begin{aligned} \hat{b}_i &= \text{sgn}((\mathbf{G}\mathbf{y}_M)_i) \\ &= \text{sgn}\left((\mathbf{G}\mathbf{R}_M)_{ii} \sqrt{P} \cdot b_i + \sum_{\substack{j=1 \\ j \neq i}}^M (\mathbf{G}\mathbf{R}_M)_{ij} \sqrt{P} \cdot b_j + \left(\rho \sum_{j=M+1}^{M+N} \sqrt{P_j} \cdot b_j\right) \cdot (\mathbf{G}\mathbf{u}_M)_i + \sigma \cdot (\mathbf{G}\mathbf{n}_M)_i\right). \end{aligned}$$

Here, $(\mathbf{G}\mathbf{R}_M)_{ii} \sqrt{P} \cdot b_i$ is the desired signal; $\sum_{\substack{j=1 \\ j \neq i}}^M (\mathbf{G}\mathbf{R}_M)_{ij} \sqrt{P} \cdot b_j$ is the interference from the $M-1$ known users; $\left(\rho \sum_{j=M+1}^{M+N} \sqrt{P_j} \cdot b_j\right) (\mathbf{G}\mathbf{u}_M)_i$ is the interference from the N unknown

users; and finally, $(\mathbf{Gn}_M)_i \sim N(0, (\mathbf{GR}_M \mathbf{G})_{ii})$ is the colored Gaussian noise.

Define $\delta = 1 + \rho(M-1)$, $\gamma = 1 - \rho$, and $P_u = \sum_{j=M+1}^{M+N} P_j$. We obtain the SIR as follows

(Appendix D).

$$SIR_{\text{mmse}}^{(M,N)} = P(\delta\gamma P + \sigma^2)^2 \sqrt{[(\delta-1)\rho P\sigma^4 + \sigma^2(\sigma^4 + 2\delta\gamma\sigma^2 P + \delta\gamma(\delta-\rho)P^2) + P_u \cdot \rho^2(\gamma P + \sigma^2)^2]} \quad (2.15)$$

For the $(K,0)$ MMSE detector, let $M=K$ and $P_u = 0$ in (2.15); we then obtain

(Appendix D)

$$SIR_{\text{mmse}}^{(K,0)} = \frac{P((1+\rho(K-1))(1-\rho)P + \sigma^2)}{\sigma^2((1+\rho(K-2))P + \sigma^2)}. \quad (2.16)$$

We reorganize (2.15) as follows

$$SIR_{\text{mmse}}^{(M,N)} = \frac{P}{\sigma^2 + (M-1)\frac{\rho^2 P\sigma^2}{(\delta\gamma P + \sigma^2)} + \left(\sum_{j=M+1}^{M+N} P_j\right)\rho^2 \frac{(\gamma P + \sigma^2)^2}{(\delta\gamma P + \sigma^2)^2}} \quad (2.17)$$

By analogy between (2.12) and (2.17), we define the effective interference from each of the $K-1$ users to user i as:

$$I_{\text{dec},ji}^{(M,N)} = \begin{cases} \frac{\sigma^2 \rho^2 LP}{[1 + \rho(M-1)](1-\rho)P + \sigma^2} & j \neq i, j = 1, 2, \dots, M, \\ \frac{\rho^2 ((1-\rho)P + \sigma^2)^2 LP_j}{([1 + \rho(M-1)](1-\rho)P + \sigma^2)^2} & j = M+1, \dots, M+N. \end{cases} \quad (2.18)$$

2.3.4 Comparison of linear multiuser detectors

Based on the above analysis we can now compare the matched filter, the decorrelator and the MMSE detector, for both the $(K,0)$ and the (M,N) cases, in the special case of equal power P and equal SIR requirement β for all known users. The symmetry constraint

still has to be satisfied.

(K,0) Linear Multiuser Detectors: From equations (2.4), (2.8), and (2.16), we obtain Figure 2.1, which shows the comparative behavior of the SIR of these detectors for $\rho=0.5$. From Figure 2.1-a) and 2.1-b), we observe that:

a) The MMSE detector has the best performance in terms of the SIR, because its design is based on SIR maximization.

b) As $P \rightarrow \infty$, or $K \rightarrow \infty$, the performance difference between the MMSE and the decorrelator detector vanishes. The reason is that the decorrelator focuses on canceling interference from other users, while the MMSE works on both noise and interference in an optimal way. As $P \rightarrow \infty$, or $K \rightarrow \infty$, the effect of noise is negligibly small compared to the interference, therefore the difference between MMSE and the decorrelator reduces to 0.

c) As $P \rightarrow \infty$, we have $SIR_{\text{mmse}}^{(K,0)} \rightarrow \infty$, $SIR_{\text{dec}}^{(K,0)} \rightarrow \infty$, but $SIR_{\text{mf}}^{(K,0)} \rightarrow \rho^{-2}(K-1)^{-1} < \infty$.

Therefore, any SIR requirement β is feasible for the decorrelator and the MMSE detectors, but there is a maximum value of SIR requirement that the matched filter can achieve no matter how large the power is. Also, as $K \rightarrow \infty$, we have $SIR_{\text{mf}}^{(K,0)} \rightarrow 0$, which means there is a constraint on maximum number of users in the matched filter case. However, there is no constraint on the maximum number of users in the decorrelator and in the MMSE detector, because the SIR requirement can always be satisfied by using large enough power.

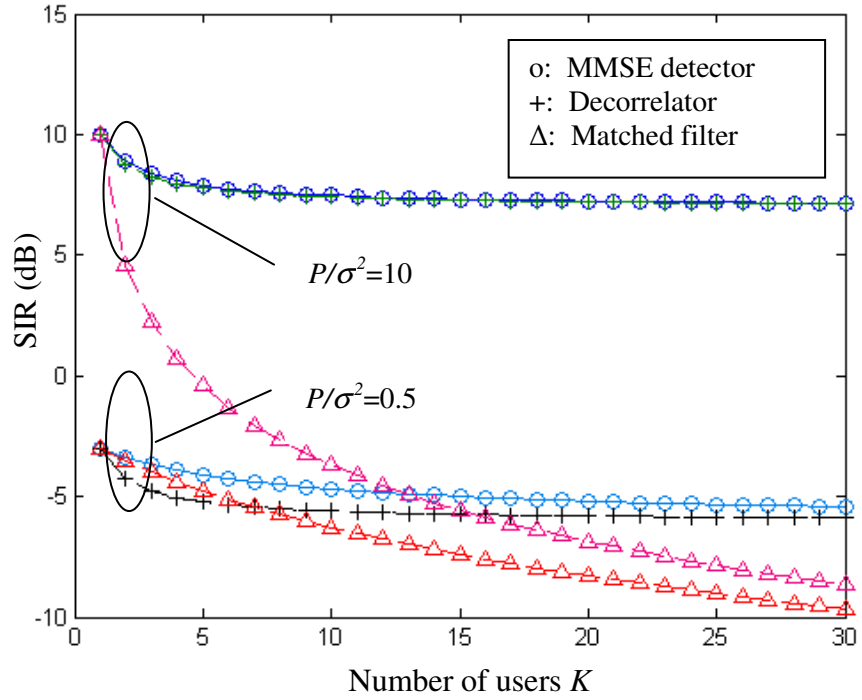
d) When power P is small, we have $SIR_{\text{mf}}^{(K,0)} > SIR_{\text{dec}}^{(K,0)}$; but as P increases, this order switches. Because the matched filter treats both interference and noise as noise, it performs well if the interference is much smaller than the noise (when P is small),

and poorly if the interference is dominant (when P is large). On the contrary, the decorrelator focuses on canceling interference from other users, and it works better when the interference is much stronger than the noise. The MMSE detector represents the compromised solution and it is actually a decorrelator when the noise is 0, and becomes a matched filter when the interference is 0.

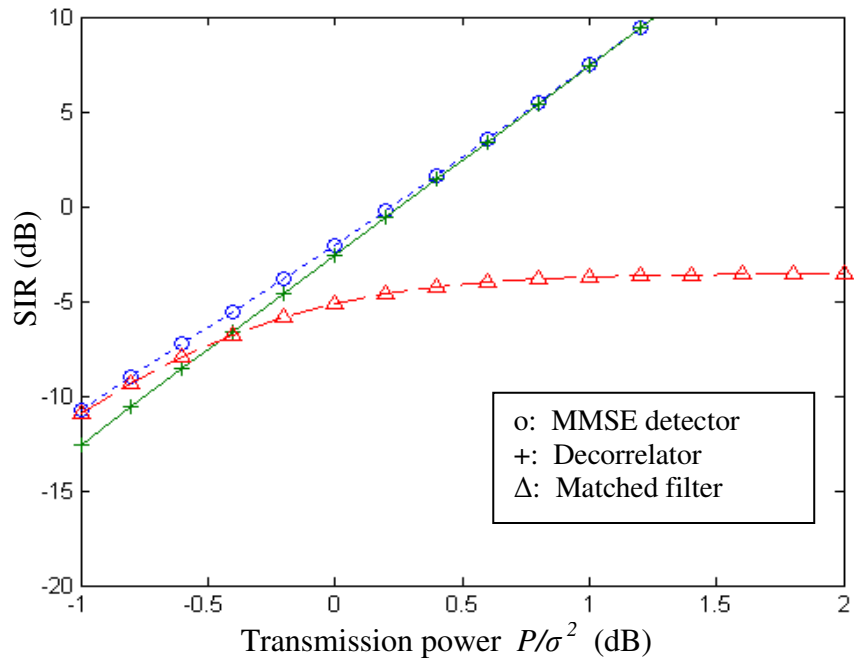
All these observations for the $(K,0)$ linear detectors agree with the behavior described in [3].

(M,N) Linear Multiuser Detectors: The SIR of the (M,N) matched filter, decorrelator, and MMSE detector, from equations (2.4), (2.5), and (2.15), is plotted by Figure 2.2, for the case of $\rho=0.5$ and $P_i/\sigma^2=10$. From these figures, we observe that:

- a) For the (M,N) decorrelator and the MMSE detector, the SIR increases with M , which is contrary to the $(K,0)$ case. The reason is that for $P_i/\sigma^2=10$, the interference from the unknown users is stronger than the noise. The more the known users, the less the effect of the unknown users on the detection. In the matched filter, however, the knowledge of the known users is not used to mitigate the interference from the unknown user and the noise, and its SIR is always decreasing with M .
- b) Sometimes the MMSE detector loses its optimality. We consider $P/\sigma^2=0.5$ and observe the SIR versus M , or consider $M=10$ and observe SIR versus P/σ^2 . For these examples, the performance of the decorrelator is clearly better than that of the MMSE detector. This is not surprising, because the MMSE detector is optimal when all users are known; the presence of the interference from unknown users is responsible for this suboptimality.

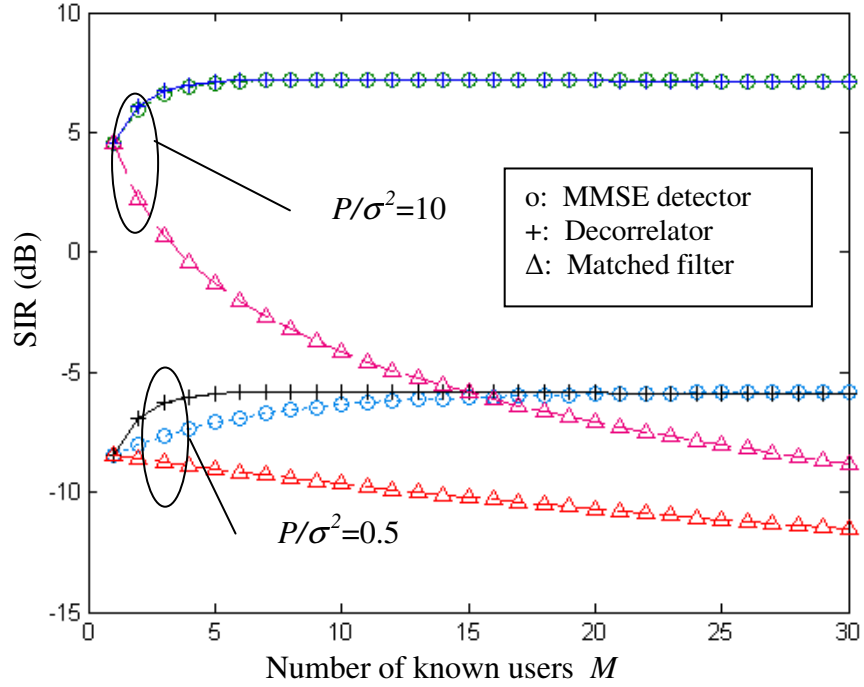


(a) SIR versus number of users, when $P/\sigma^2=0.5$ and 10.

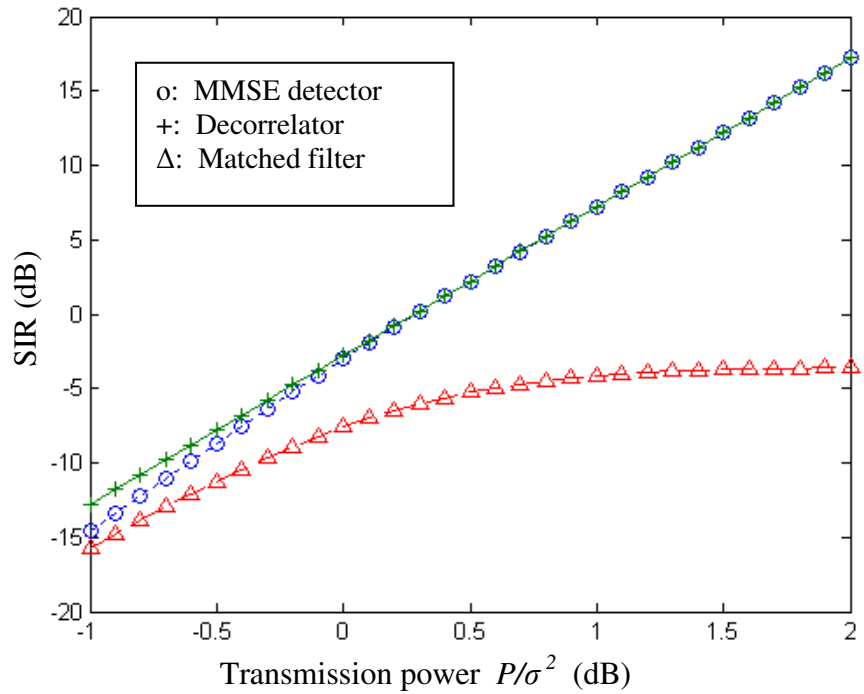


(b) SIR versus transmission power P/σ^2 , when $K=10$

Figure 2.1: SIR of $(K,0)$ linear multiuser detectors, when $\rho=0.5$.



(a) SIR versus number of known users M , when $P/\sigma^2=0.5$, or 10.



(b) SIR versus transmission power P/σ^2 , when $M=10$.

Figure 2.2: SIR of (M,N) linear multiuser detectors, when $\rho=0.5$ and $P_u/\sigma^2=10$.

- c) As $P \rightarrow \infty$, or $M \rightarrow \infty$, the differences between the MMSE detector and the decorrelator vanish.
- d) The matched filter has limited user capacity from the viewpoint of power.

2.4 Single-class Case and User Capacity

In the so-called single-class case, all the users have the same SIR requirement, i.e., $SIR_i \geq \beta$ (β is the target SIR), and the same power constraint $P_i \leq \bar{P}$ (\bar{P} is the maximum allowable power). We consider two kinds of power constraint:

Infinity power constraint: $\bar{P} = \infty$ (extreme, or ideal, case).

Finite power constraint: $\bar{P} < \infty$ (practical case).

For the (M,N) detector, we assume that the unknown users have power $P_j, j = M+1, \dots, M+N$ and total power $\sum_{j=M+1}^{M+N} P_j = P_u$.

In a power-controlled system, we need to find the minimum power allocation for the system to satisfy the SIR requirements. Since all the users have symmetric sequences and same SIR requirements, their minimal allocated power should be the same. This is easy to prove mathematically. Because the inequality $SIR_i \geq \beta$ is a function of only ρ^2, β, P_u , and $P_i, i = 1, \dots, M$, the minimum power allocation P_i of different users satisfy exactly the same equations; therefore their solutions should be the same.

For both the $(K,0)$ and the (M,N) detector, we consider the user capacity for the single-class case. For the $(K,0)$ case, the K users are admissible into the system if a power allocation scheme can be found such that the SIR requirements of all K users are satisfied. The maximal admissible number of users per degree of freedom (in the single-class case) with infinity power constraint is called the *user capacity*. For the (M,N) case,

this definition is changed to identify the known users.

User capacity for (M,N) detector: The M known users are admissible into the system if there exists a power allocation scheme for the M known users such that their SIR requirements are satisfied. The maximum admissible number of *known* users per degree of freedom with infinite power constraint is called the user capacity.

2.4.1 Matched filter

Analysis for the matched filter is simple. Since known and unknown users affect the performance in the same way, the $(K,0)$ and the (M,N) detector behave similarly. So we only give results for the (M,N) case here; the $(K,0)$ case can be easily obtained by simply letting $M=K$, $N=0$, and $P_u=0$.

Infinite Power Constraint: From symmetry, all M users should have the same power; we let $P_1 = \dots = P_M = P$ and $SIR_1 = \dots = SIR_M = \beta$ in (2.4), and the power allocation to satisfy SIR requirements of all M known users is given by

$$P_{mf,i}^{(M,N)} = \frac{\beta(\sigma^2 + \rho^2 P_u)}{1 - (M-1)\beta\rho^2}, \quad i=1,2,\dots,M.$$

Therefore in order to have $P_i < \infty$, M must satisfy

$$M < 1 + \frac{1}{\beta\rho^2}.$$

Another constraint from the symmetric property gives $M \leq L - N$. Hence the user capacity is

$$C_{mf}^{(M,N)}(\beta) = \min \left\{ 1 - \frac{N}{L}, \frac{1}{L} + \frac{1}{\beta\rho^2 L} \right\} \text{ user / degree of freedom.} \quad (2.19)$$

Finite Power Constraint: The power allocation is the same as before, but from

$P_i \leq \bar{P}$, we now have $M \leq 1 + 1/\beta\rho^2 - (\sigma^2 + \rho^2 P_u)/(\bar{P}\rho^2)$, which yields a smaller region than that of the infinite power constraint case. Therefore the admissible number of known users satisfies:

$$M \leq \min \left\{ L, 1 + \frac{1}{\beta\rho^2} - \frac{\sigma^2 + \rho^2 P_u}{\rho^2 \bar{P}} \right\}. \quad (2.20)$$

2.4.2 (K,0) Decorrelator

Infinite Power Constraint: The minimal power allocation is the same for all users and is given by

$$P_{\text{dec},i}^{(K,0)} = \frac{\beta\sigma^2}{1-\rho} \left[\frac{1+\rho(K-2)}{1+\rho(K-1)} \right], \quad i=1,2,\dots,K.$$

The allocated power increases as the number of users K increases. Since $P_i < \beta\sigma^2/(1-\rho) < \infty$ is true for any value of K , there is no constraint imposed on the number of users from the viewpoint of the allocated power. However, the assumption of the existence of K users with symmetric sequences requires that $K \leq L$. Therefore,

$$C_{\text{dec}}^{(K,0)}(\beta) = 1 \text{ user / degree of freedom.} \quad (2.21)$$

Finite Power Constraint: We must have $\bar{P} \geq \beta\sigma^2$ if there is at least one user. Remember that there is the additional constraint that $K \leq L$ from the symmetry assumption. Therefore, the admissible number of users satisfies:

$$\left\{ \begin{array}{ll} K=0, & \text{if } \bar{P} < \beta\sigma^2, \\ K \leq \min \left\{ 1 - \frac{1}{\rho} + \frac{\beta\sigma^2}{\beta\sigma^2 - (1-\rho)\bar{P}}, L \right\} & \text{if } \beta\sigma^2 \leq \bar{P} < \frac{\beta\sigma^2}{1-\rho}, \\ K \leq L, & \text{if } \bar{P} \geq \frac{\beta\sigma^2}{1-\rho}. \end{array} \right. \quad (2.22)$$

2.4.3 (M,N) Decorrelator

Infinite Power Constraint: The power allocation is the same for all M users and is given by

$$P_{dec,i}^{(M,N)} = \beta \frac{\sigma^2}{1-\rho} \left[\frac{1+\rho(M-2)}{1+\rho(M-1)} \right] + \beta \left[\frac{\rho}{1+\rho(M-1)} \right]^2 P_u, \quad i=1,2,\dots,M. \quad (2.23)$$

Since $\beta\sigma^2 < P_i < \beta\sigma^2/(1-\rho) + \beta\rho^2 P_u < \infty$ holds for any value of M , there is no constraint imposed on M from the viewpoint of power. From the symmetry condition we have $M \leq L - N$, and, hence, the user capacity is given by:

$$C_{dec}^{(M,N)}(\beta) = 1 - \frac{N}{L} \text{ user / degree of freedom.} \quad (2.24)$$

To study the behavior of power allocation $P(M)$ versus M , we define $\Delta(M)$, Δ^* , and $F(M)$ as follows

$$\Delta(M) \equiv \frac{1}{1+\rho(M-1)},$$

$$\Delta^* \equiv \frac{\sigma^2}{2\rho(1-\rho)P_u},$$

$$\begin{aligned} F(M) &\equiv -\frac{\sigma^2\rho}{1-\rho}\Delta(M) + \rho^2 P_u \Delta^2(M) \\ &= \rho^2 P_u \Delta(M) (\Delta(M) - 2\Delta^*) \end{aligned}$$

Then from (2.23) we obtain the power allocation to any one of the known users given by

$$P(M) = \beta \left[\frac{\sigma^2}{1-\rho} + F(M) \right].$$

We see that this power depends on the value of M . The function $F(\Delta(M))$ is a parabolic function of $\Delta(M)$ ($0 < \Delta(M) \leq 1$) with the minimum at Δ^* . There are three critical points

for this function as listed below:

$$F(M=1) = \frac{\sigma^2 \rho}{1-\rho} \left(-1 + \frac{1}{2\Delta^*} \right),$$

$$F(\Delta(M) = \Delta^*) = -\frac{\rho \Delta^*}{2} \frac{\sigma^2}{1-\rho},$$

$$\text{and } F(M = \infty) = 0.$$

The behavior of the quantity $F(M)$ is based on the relative position of Δ^* in the range of $\Delta(M)$, that is, whether $\Delta^* \geq 1$, or $\frac{1}{2} \leq \Delta^* < 1$, or $0 < \Delta^* \leq \frac{1}{2}$. This is illustrated in Figure 2.3.

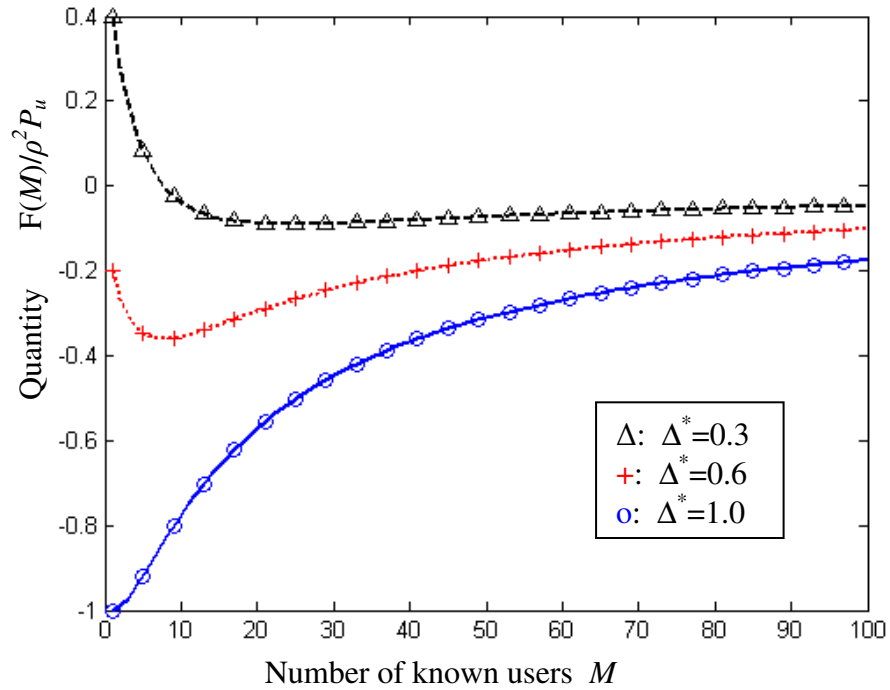


Figure 2.3: Function $F(M)$ for (M,N) decorrelator.

Specifically,

- a) $\Delta^* \geq 1$ implies that $F(M)$ increases monotonically from a minimum of $F(M=1)$ to a maximum of $F(M = \infty)$.

b) $\frac{1}{2} \leq \Delta^* < 1$ implies that $F(M)$ decreases first from $F(M=1)$ to the minimum $F(\Delta = \Delta^*)$, and then it increases to a maximum of $F(M = \infty)$.

c) $0 < \Delta^* \leq \frac{1}{2}$ implies that $F(M)$ first decreases from the maximum of $F(M=1)$ to the minimum of $F(\Delta = \Delta^*)$, and then increases to $F(M = \infty)$.

Note that $F(M)$, and therefore $P(M)$ are not always monotonic with M . This is different from the case of the $(K,0)$ decorrelator and the matched filter detector. The explanation of the difference is as follows. The first term in the power allocation of (2.23) is the power to overcome the noise and the $M-1$ other known users; this term is monotonically increasing with M . The second term in (2.23) is the power to overcome the interference from N unknown users; this term is decreasing monotonically with M . The reason is that for a fixed number and power of unknown users, if we let the number of known users increase, the ratio of the power from the unknown users to the power of known users is decreasing, and hence it enhances the detection process. Therefore, the curve shape of $P(M)$ is determined by the relative values of the increasing term and of the decreasing term, which, in turn, depend on the parameter Δ^* . When $\Delta^* \geq 1$, i.e., when $\sigma^2 \rho / (1 - \rho) \geq \rho^2 P_u$, the noise term is dominant, and $P(M)$ is increasing with M . When $\Delta^* < 1$, the unknown interference term is dominant for small M and the noise term becomes dominant as M becomes large. Therefore the power needed to satisfy the SIR requirement will decrease first as M increases, and then will start increasing when M becomes large enough.

Finite Power Constraint: We only discuss the constraint on the number of known users M from the power point of view here. The constraint from the symmetry property,

i.e., the constraint that $M \leq L - N$, can be incorporated easily. We have to compare the possible values of P_i with that of \bar{P} to obtain the constraint on M . The number of known users M has to satisfy $P(M) \leq \bar{P}$. Let

$$F(M) = \frac{\bar{P}}{\beta} - \frac{\sigma^2}{1-\rho}. \quad (2.25)$$

We denote the value of M that solves (2.25) by M_0 if there is a unique solution. If there are two solutions, we denote them by M_1 and M_2 ($M_1 < M_2$). Then the constraint on M depends on the values of Δ^* (i.e., the behavior of $F(M)$) and of \bar{P} , as shown in Figure 2.4. The following possibilities arise.

- a) If $\bar{P} < \min \left\{ \frac{\beta\sigma^2}{1-\rho} \left(1 - \frac{\rho}{2} \Delta^* \right), \frac{\beta\sigma^2}{1-\rho} \left(1 - \rho + \frac{\rho}{2\Delta^*} \right) \right\}$, then $M=0$.
- b) If $\bar{P} > \max \left\{ \frac{\beta\sigma^2}{1-\rho} \left(1 - \rho + \frac{\rho}{2\Delta^*} \right), \frac{\beta\sigma^2}{1-\rho} \right\}$, then $M < \infty$ (No constraint).
- c) If $0 \leq \Delta^* < \frac{1}{2}$, and $\frac{\beta\sigma^2}{1-\rho} \leq \bar{P} < \frac{\beta\sigma^2}{1-\rho} \left(1 - \rho + \frac{\rho}{2\Delta^*} \right)$, then $M \geq M_0$.
- d) If $0 \leq \Delta^* < 1$ and $\frac{\beta\sigma^2}{1-\rho} \left(1 - \frac{\rho}{2} \Delta^* \right) \leq \bar{P} < \min \left\{ \frac{\beta\sigma^2}{1-\rho}, \frac{\beta\sigma^2}{1-\rho} \left(1 - \rho + \frac{\rho}{2\Delta^*} \right) \right\}$, then $M_1 \leq M \leq M_2$.
- e) If $\Delta^* \geq \frac{1}{2}$ and $\frac{\beta\sigma^2}{1-\rho} \left(1 - \rho + \frac{\rho}{2\Delta^*} \right) \leq \bar{P} < \frac{\beta\sigma^2}{1-\rho}$, then $M \leq M_0$.

M_0 is solution of (2.25) when only one solution exists. M_1 and M_2 are solutions of (2.25) when two solutions exist.

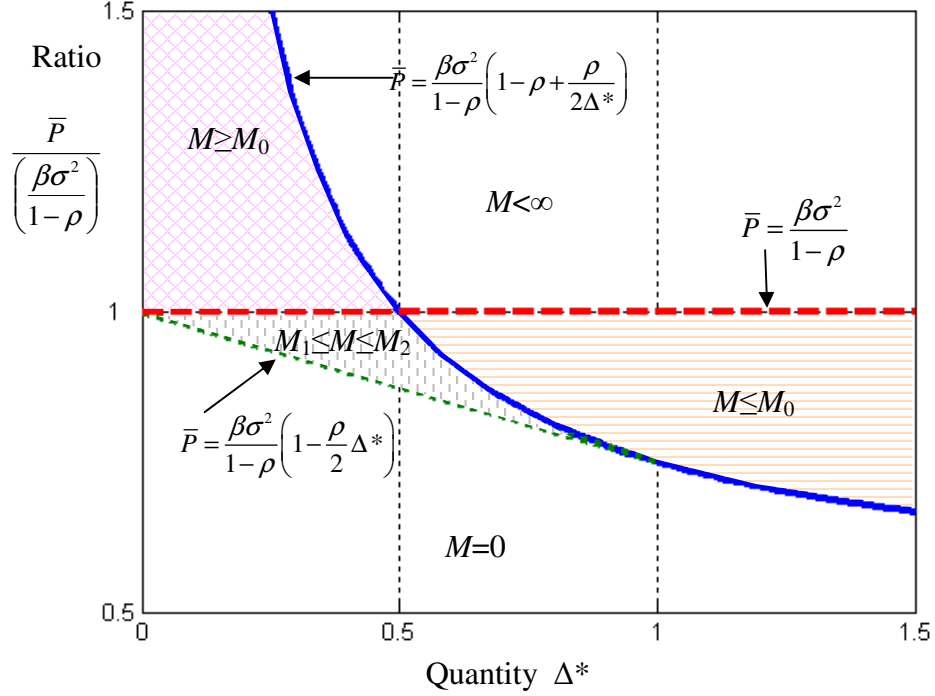


Figure 2.4: Constraint on number of known users M for (M,N) decorrelator.

2.4.4 (K,0) MMSE detector

For any fixed value of the power P , the function of SIR versus K is monotonically decreasing (Appendix E) from P/σ^2 to $\gamma P/\sigma^2$. Also for any fixed number of users $K \geq 1$, the function of SIR versus P is monotonically increasing (Appendix E) from 0 to ∞ . Therefore, any $\beta > 0$ is a feasible SIR requirement as far as the power constraint is concerned. However, the symmetry constraint still has to be satisfied.

Infinite Power Constraint: Our assumption of equal powers for all users is reasonable here because the allocated power to each user will be the same as follows from the assumed symmetry of their sequences.

To calculate the minimum power needed for K users with SIR requirement β , we let $SIR_{\text{mmse}}^{(K,0)} = \beta$ and find the positive solution of the quadratic equation that P satisfies. It is

given by

$$P_{\text{mmse}}^{(K,0)}(K, \beta) = 2\sigma^2 / \left\{ \rho + \frac{1}{\beta} - (1 + \rho(K-1)) + \sqrt{\left(1 + \rho(K-2) - \frac{1}{\beta}\right)^2 + 4 \frac{(1-\rho)(1+\rho(K-1))}{\beta}} \right\}.$$

This is an increasing function of K from $P(K=1) = \sigma^2 \beta$ to $P(K \rightarrow \infty) = \sigma^2 \beta / (1-\rho)$.

Since $P < \infty$ is always true and independent of K , there is no constraint on the number of users from the power allocation viewpoint. However the symmetry property of sequences requires $K \leq L$, and thus the user capacity is

$$C_{\text{mmse}}^{(K,0)} = 1 \text{ user / degree of freedom.} \quad (2.26)$$

Finite Power Constraint: Define K^* such that $SIR_{\text{mmse}}^{(K,0)}(\bar{P}, K^*) = \beta$; then the admissible number of users satisfies

$$\begin{cases} K \leq L, & \text{if } \bar{P} \geq \frac{\beta\sigma^2}{1-\rho}, \\ K \leq \min\{K^*, L\}, & \text{if } \beta\sigma^2 \leq \bar{P} < \frac{\beta\sigma^2}{1-\rho}, \\ K = 0, & \text{if } \bar{P} < \beta\sigma^2. \end{cases} \quad (2.27)$$

2.4.5 (M,N) MMSE detector

The behavior of the SIR function of the (M,N) MMSE detector versus M (K varies along with M) depends on the value of the constant P_u/σ^2 , that is, the ratio between the total unknown powers and the noise. We observe that as $P_u/\sigma^2 > 0$, the SIR is no longer a monotonically decreasing function of M . An example is shown in Figure 2.2-a). When $P_u/\sigma^2 = 10$ and $\rho = 0.5$, the SIR is an increasing function of M . The reason is that the interference from the unknown users decreases with M ; while the interference from the known users and the noise increases with M . For very large P_u/σ^2 , (which means that the

interference from the unknown users is dominant,) the more known users there are, the better it is in order to counterbalance the interference from the unknown users.

For any fixed number of known users $M \geq 1$, the function of SIR versus the transmission power P is monotonically increasing from 0 to ∞ as P increases from 0 to ∞ (Appendix E). So, the quantity $\min_{1 \leq M < \infty} SIR_{\text{mmse}}^{(M,N)}(P, M)$ is also monotonically increasing with P from 0 to ∞ . Therefore, any $\beta > 0$ is a feasible SIR requirement as far as the power constraint is concerned; again, however, the symmetry constraint still has to be satisfied.

Infinite Power Constraint: To satisfy the SIR requirement, we can always use large enough power allocation P , so that $\min_{1 \leq M < \infty} SIR_{\text{mmse}}^{(M,N)}(P, M) = \beta$. In this way, $SIR_{\text{mmse}}^{(M,N)}(P, M) \geq \min_{1 \leq M < \infty} SIR_{\text{mmse}}^{(M,N)}(P, M) = \beta$ is satisfied for any M . Since $P < \infty$ is always true, the only constraint on the number of users is from the symmetry property of the sequences, which yields $M \leq L - N$. Therefore the user capacity is given by

$$C_{\text{mmse}}^{(M,N)} = 1 - \frac{N}{L} \text{ user / degree of freedom.} \quad (2.28)$$

To find the minimal power allocation, we let $SIR_{\text{mmse}}^{(M,N)} = \beta$, and find that P satisfies a cubic equation. The solution is too complex to derive analytically, instead we provide a numerical evaluation for 3 cases, namely, $P_u / \sigma^2 = 0$ (the $(K, 0)$ case), $P_u / \sigma^2 = 4$, and $P_u / \sigma^2 = 10$, shown in Figure 2.5. Notice that when $P_u / \sigma^2 = 10$, the power allocation is decreasing with the number of users. Again this phenomenon arises from the interference the unknown users cause.

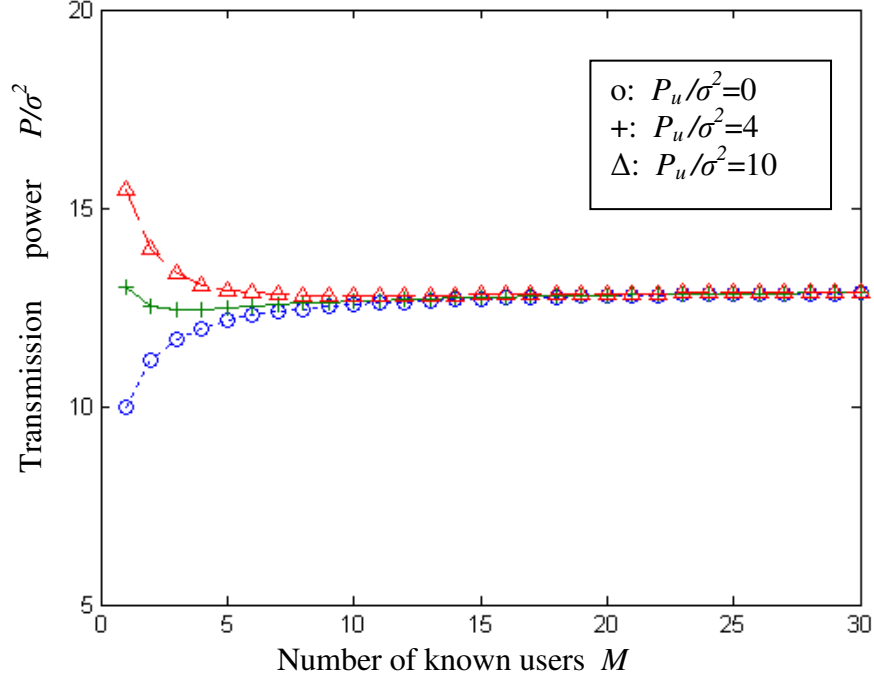


Figure 2.5: Power allocation of (M,N) MMSE detector for $P_u/\sigma^2=0, 4,$ and $10,$ when $\rho=0.5, \beta=10.$

Finite Power Constraint: The number of users depends on the value of \bar{P} and on the behavior of the function $P(M,\beta)$. We observe that M has to satisfy $M \leq L-N$ and $P(M) \leq \bar{P}$. From the similarity between Figure 2.3 and Figure 2.5, we know that the constraint on M is similar to that of the (M,N) decorrelator with finite power constraint. There are 5 possible constraints on M : (i) $M = 0$, (ii) $M < \infty$, (iii) $M \geq M_0$, (iv) $M \leq M_0$, and (v) $M_1 \leq M \leq M_2$, with $M_0, M_1,$ and M_2 solutions of $P(M) = \bar{P}$. Which kind of constraint applies to a specific problem depends on the values of \bar{P} and $P_u/\sigma^2=10$. Since we do not have the analytical form of the function $P(M,\beta)$, we cannot provide exact analytical results. But the idea is the same as in the analysis of Section 2.4.3.

2.4.6 Comparisons

(M,N) Detector Versus (K,0) Detector for Symmetric Sequences: Comparing the (M,N) to the $(K,0)$ case for all three detectors (i.e., matched filter, decorrelator, and MMSE), we see that $C^{(M,N)}(\beta) \leq C^{(K,0)}(\beta)$. For the matched filter, although the knowledge of N does not change the SIR of the known users, the unknown users do occupy and, hence, waste resources, and, therefore reduce the user capacity. For the decorrelator and the MMSE detector, the observed user capacity of the (M,N) detector is less than that of the $(K,0)$ detector by a factor of N/L .

Symmetric Sequences Versus Random Sequences for the (K,0) Case: The results given in [9] for random sequences are asymptotic results, while our results for symmetric sequences are for finite values of K and L , and depend on the crosscorrelation ρ . In order to make a valid comparison, we let $L \rightarrow \infty$, and let ρ depend on L , so that both cases have approximately the same level of multiple access interference. Since $\rho_{ij}^2 P_j$ is the interference from user j to user i in the matched filter, $E\{\rho_{ij}^2\}$ is a good representation of the interference level. The crosscorrelation between any two random sequences is a random variable, with $E\{\rho_{ij}^2\} = L^{-1}$. Hence we let $\rho = L^{-\frac{1}{2}}$, so that the crosscorrelation between any two symmetric sequences also satisfies $E\{\rho_{ij}^2\} = L^{-1}$.

From (2.19), the user capacity of the matched filter for symmetric sequences is given by $\min\{1, \beta^{-1}\}$, as compared to β^{-1} in [9]. Of these asymptotic results, the dimension corresponding to the symmetry property is not applicable to the random sequence case; however, the dimension corresponding to the power constraint is the same as that of the random sequence case.

The user capacity of the $(K,0)$ decorrelator using symmetric sequences is the same as

that of the case of random sequences as given in [9]. But here the constraint is actually imposed by the symmetry property rather than from the power constraint.

The user capacity is equal to 1 for the $(K,0)$ MMSE detector using symmetric sequences, which is less than that of the random sequence case, which is $1 + \beta^{-1}$. But the constraint for symmetric sequences case is imposed by the symmetric sequence assumption, while for random sequence case it is imposed by the power allocation.

Symmetric Sequences Versus Optimum Sequences for the $(K,0)$ MMSE Detector: The results for both symmetric sequences and optimum sequences are for a finite system. The user capacity is given by 1 for the $(K,0)$ MMSE detector using symmetric sequences, which is less than that of the optimum sequence case, which is given by $1 + \beta^{-1}$. But, again, the constraint for the symmetric sequences case is imposed by the symmetric sequence assumption, while for optimum sequence case it is imposed by the power allocation.

2.5 Multiple-class Case and Effective Bandwidth

In the multiple-class case, each of the J classes of users has its own SIR requirement and power constraint. The j th class, $j=1,2,\dots,J$, has number of users K_j (or M_j for the (M,N) case), (where $\sum_{j=1}^J K_j = K$, or $\sum_{j=1}^J M_j = M$), SIR requirements β_j , ($\beta_1 < \beta_2 < \dots < \beta_J$), and power constraint \bar{P}_j . We consider two kinds of power constraint, infinite power constraint with $\bar{P}_j = \infty$, and finite power constraint with $\bar{P}_j < \infty$. Just as in the single-class case, since all the users in one class have symmetric sequences and identical SIR requirement, their powers should be the same.

We consider the multi-class case for the effective bandwidth calculation. The MMSE detector is not considered here, because the SIR values in (2.15) and (2.16), are only for valid for the equal-power case, which is correct for the single-class case, but not for multiple-class case.

The original definition of effective bandwidth in [9] works for the $(K,0)$ case. For the (M,N) case, we modify it slightly to focus on the known users. Besides, since we have two constraints on the number of users, effective bandwidth can NOT be written in a scalar form. So we introduce a two-dimensional vector effective bandwidth quantity, whose two components correspond to the symmetric correlation constraint and to the power constraint respectively. Now the SIR of all users can be satisfied if and only if the sum of the effective bandwidth *vectors* of all the users is less than the total number of degrees of freedom for both components; which can be written formally as

$$\sum_{j=1}^J K_j \cdot \mathbf{e}(\beta_j) \leq L \cdot \mathbf{u}_2,$$

where \mathbf{u}_2 is the vector $[1 \ 1]$.

Effective Bandwidth for the (M,N) detector: The effective bandwidth *vector* of a *known* user can be defined so that the SIR requirements of all the *known* users can be met if and only if the sum of the effective bandwidth *vectors* of the *known* users is less than the total number of degrees of freedom for each component.

2.5.1 Matched filter

Infinite Power Constraint: Let $SIR_j = \beta_j$ for $j=1,2,\dots,J$ in (2.4); we obtain the power allocation for class j to be

$$P_{\text{mf},j}^{(M,N)} = \frac{\beta_j}{1 + \beta_j \rho^2} \frac{\sigma^2 + \rho^2 P_u}{1 - \sum_{i=1}^J M_i \frac{\beta_i \rho^2}{1 + \beta_i \rho^2}}, \quad j=1,2,\dots,J.$$

From $P_j < \infty$ and the symmetric property, the user capacity constraint for the matched filter receiver with J classes is given by:

$$\sum_{j=1}^J M_j \frac{\beta_j \rho^2 L}{1 + \beta_j \rho^2} < L,$$

$$\text{and } \sum_{j=1}^J M_j \leq L - N.$$

According to the new definition, the effective bandwidth vector of the (M,N) matched filter can be written as

$$\mathbf{e}_{\text{mf}}^{(M,N)}(\beta) = \left[\begin{array}{cc} 1 & \beta \rho^2 L \\ 1 - \frac{N}{L} & 1 + \beta \rho^2 \end{array} \right] \text{ degree of freedom / user.} \quad (2.29)$$

Finite Power Constraint: The power allocation is as before, but we now have $P_j < \bar{P}_j$, $j=1,2,\dots,J$. Thus M_j satisfies

$$\sum_{j=1}^J M_j \frac{\beta_j \rho^2}{1 + \beta_j \rho^2} \leq 1 - \max_i \left[\frac{\beta_i (\sigma^2 + \rho^2 P_u)}{\bar{P}_i (1 + \beta_i \rho^2)} \right]. \quad (2.30)$$

This equation, together with $\sum_{j=1}^J M_j \leq L - N$, defines the restricted user capacity region of the system, which is obviously smaller than that of the infinite power constraint case.

2.5.2 (K,0) Decorrelator

Infinite Power Constraint: The power allocation to class- j user is given by

$$P_{\text{dec},j}^{(K,0)} = \frac{\beta_j \sigma^2}{1 - \rho} \left[\frac{1 + \rho(K-2)}{1 + \rho(K-1)} \right], \quad j=1,2,\dots,J.$$

Note that P_j satisfies $\beta_j \sigma^2 \leq P_j < \beta_j \sigma^2 / (1 - \rho)$. Define $\bar{\beta} = \max_j \beta_j$. Just as in the single-class case, the inequality $P_j < \bar{\beta} \sigma^2 / (1 - \rho) < \infty$ is true for any number of users. So, the user capacity constraint is just given by $\sum_{j=1}^J K_j \leq L$. From this, we can identify the effective bandwidth to be 1. To be consistent with the matched filter case, we still write it as the form of effective bandwidth vector, that is

$$\mathbf{e}_{\text{dec}}^{(K,0)}(\boldsymbol{\beta}) = [1 \quad 0] \text{ degree of freedom / user.} \quad (2.31)$$

Finite Power Constraint: If we have J power constraints $P_j \leq \bar{P}_j < \infty$, $j=1,2,\dots,J$, we first need to partition the J classes into three sets according to the value of \bar{P} as follows:

$$J_1 = \left\{ j : \bar{P}_j \geq \frac{\beta_j \sigma^2}{1 - \rho} \right\}, \quad J_2 = \left\{ j : \sigma^2 \beta_j \leq \bar{P}_j < \frac{\beta_j \sigma^2}{1 - \rho} \right\}, \quad \text{and} \quad J_3 = \left\{ j : \bar{P}_j < \beta_j \sigma^2 \right\}.$$

For set J_3 , it is not possible to satisfy the power constraint, so we must have $\sum_{j \in J_3} K_j = 0$. For set J_1 , the power constraints are satisfied automatically. So the only real constraint arises from classes $j \in J_2$.

If J_2 is a null set, there is actually no constraint on the number of total users from either the SIR requirement or from the power constraint; the user capacity is given accordingly by:

$$\sum_{j \in J_1} K_j \leq L, \quad \text{and} \quad \sum_{j \in J_3 \cup J_2} K_j = 0.$$

If J_2 is not a null set, it follows from $P_j \leq \bar{P}_j$ that

$$K \leq 1 - \frac{1}{\rho} + \frac{\beta_j \sigma^2}{\beta_j \sigma^2 - \bar{P}_j (1 - \rho)}, \quad \text{for each } j \in J_2.$$

Therefore the user capacity constraint can be written as:

$$\sum_{j \in J_2 \cup J_1} K_j \leq \min \left(L, 1 - \frac{1}{\rho} + \frac{1}{1 - (1 - \rho) \min_{j \in J_2} (\bar{P}_j / \beta_j \sigma^2)} \right), \text{ and } \sum_{j \in J_3} K_j = 0. \quad (2.32)$$

2.5.3 (M,N) Decorrelator

Infinite Power Constraint: Define $\bar{\beta} = \max_j \beta_j$. The power allocation to the class j users is given by

$$P_{\text{dec},j}^{(M,N)} = \frac{\beta_j \sigma^2}{1 - \rho} \left[\frac{1 + \rho(M - 2)}{1 + \rho(M - 1)} \right] + \beta_j P_u \left[\frac{\rho}{1 + \rho(M - 1)} \right]^2, \quad j = 1, 2, \dots, J.$$

Since $P_i < \bar{\beta} \sigma^2 / (1 - \rho) + \bar{\beta} P_u \rho^2 < \infty$ holds for any value of M , the user capacity constraint is given by $\sum_{j=1}^J M_j \leq L - N$. Thus, we can identify the effective bandwidth vector as

$$\mathbf{e}_{\text{dec}}^{(M,N)}(\beta) = \begin{bmatrix} \frac{1}{1 - \frac{N}{L}} & 0 \end{bmatrix} \text{ degree of freedom / user.} \quad (2.33)$$

Finite Power Constraint: Now the number of known users M has to satisfy the J inequalities of the form $P_j(M) \leq \bar{P}_j$. For those classes j for which $\min_M P_j(M) > \bar{P}_j$ is true, we need to require $M_j = 0$. For each of the other classes, we obtain a region of acceptable values of M . The overall acceptable region of M is the intersection of all regions obtained in this way. The results depend on Δ^* and on the value of \bar{P}_j , and are rather complicated to derive. We omit the detailed discussion of this case here.

2.5.4 Comparisons

(M,N) Detector Versus (K,0) Detector for Symmetric Sequences: Comparing the

(M,N) to the $(K,0)$ case for symmetric sequences, for the matched filter and the decorrelator cases, the effective bandwidth vector is clearly larger than that of the $(K,0)$ decorrelator. This is because the unknown users waste the resources.

Symmetric Sequences Versus Random Sequences for the $(K,0)$ Case: For the matched filter, the effective bandwidth is $[1 \ \beta]$, as compared to β in [9]. Of these asymptotic results, the dimension corresponding to the symmetry property is not applicable to the random sequence case; however, the dimension corresponding to the power constraint is the same as that of the random sequence case.

For the decorrelator case using symmetric sequences, the effective bandwidth vector can be actually reduced to the original scalar form, because the constraint $P_i < \infty$ is satisfied all the time. Therefore, the effective bandwidth of the $(K,0)$ decorrelator using symmetric sequences is the same as that of the random sequences case as given in [9]; both are equal to 1. However, here the constraint is actually imposed by the symmetry property rather than from the power constraint.

2.6 Summary

In summary, for the CDMA system with symmetric sequences, we found the user capacity and the effective bandwidth for the $(K,0)$ and the (M,N) matched filter and decorrelator detectors, by assuming fixed total power from unknown users. By making the equal power assumption for all known users, we obtained the user capacity for the $(K,0)$ and the (M,N) MMSE detectors. Our conclusions about the user capacity and effective bandwidth for these detectors are listed in Table 2.1, and are compared to the results for the case of random sequences [9] and optimum sequences [10].

Table 2.1: User capacity and effective bandwidth for linear multiuser detectors

Sequence	Detector	User Capacity [#]		Effective Bandwidth	
		Finite L	As $L \rightarrow \infty$ *	Finite L	As $L \rightarrow \infty$ *
Symmetric Sequence ($K,0$)	Matched Filter	$\min\left\{1, \frac{1}{L} + \frac{1}{\beta\rho^2 L}\right\}$	$\min\left\{1, \frac{1}{\beta}\right\}$	$\left[1, \frac{\beta\rho^2 L}{1 + \beta\rho^2}\right]$	$[1, \beta]$
	Decorrelator	$\min\{1, \infty\}$	$\min\{1, \infty\}$	$[1, 0]$	$[1, 0]$
	MMSE Detector	$\min\{1, \infty\}$	$\min\{1, \infty\}$	————	————
Symmetric Sequence (M,N)	Matched Filter	$\min\left\{1 - \frac{N}{L}, \frac{1}{L} + \frac{1}{\beta\rho^2 L}\right\}$	$\min\left\{1, \frac{1}{\beta}\right\}$	$\left[\frac{1}{1 - N/L}, \frac{\beta\rho^2 L}{1 + \beta\rho^2}\right]$	$[1, \beta]$
	Decorrelator	$\min\left\{1 - \frac{N}{L}, \infty\right\}$	$\min\{1, \infty\}$	$\left[\frac{1}{1 - N/L}, 0\right]$	$[1, 0]$
	MMSE Detector	$\min\left\{1 - \frac{N}{L}, \infty\right\}$	$\min\{1, \infty\}$	————	————
Random Sequence ($K,0$)	Matched Filter	————	$1/\beta$	————	β
	Decorrelator	————	1	————	1
	MMSE Detector	————	$1 + \frac{1}{\beta}$	————	$\frac{\beta}{1 + \beta}$
Optimum Sequence ($K,0$)	Matched Filter, MMSE	$1 + \frac{1}{\beta}$	————	$\frac{\beta}{1 + \beta}$	————

[#]: In the user capacity, the first term inside of the $\min\{ , \}$ is from the symmetry property of the sequences; the second term is from the power constraint. We leave the ∞ there to make it clear where does the constraint on the number of user come from. Similarly, in the effective bandwidth, the first dimension in the 2-dimensional vector is from the symmetry property and the second term is from the power constraint.

*: As $L \rightarrow \infty$, we assume $\rho^2 = L^{-1} \rightarrow 0$. We also assume N , the number of unknown users is fixed and $\lim_{L \rightarrow \infty} (N/L) = 0$ is used. If we assume $\lim_{L \rightarrow \infty} (N/L) = \alpha$, then the user capacity and effective bandwidth of (M,N) detectors as $L \rightarrow \infty$ should be changed accordingly.

Chapter 3 Power Control in Uplink and Downlink CDMA

System with Multiple Flow Types

3.1 Introduction

Power control is used to balance the received powers of the users of a code division multiple access (CDMA) system, so that no single user creates excessive interference that can destroy the quality of the communication of other users. At the same time it is desirable to use power levels as low as possible, provided they satisfy the quality of service (QoS) objective defined by fixed signal-to-interference ratio (SIR) requirements. In previous papers [15,16], the optimum power vector was found by inversion of a non-negative matrix related to the channel gains and crosscorrelation. But all the studied models assume only one flow type at each node. In practice, users may have multiple flow types that have different QoS requirements. Here we consider a synchronous CDMA system with a base station and N nodes. At each node, there are F flow types with SIR requirements $\beta_1 \leq \beta_2 \leq \dots \leq \beta_f$. Each flow type is assigned a code with processing gain L , and they transmit simultaneously to the base station. Each node has only one transmitter, i.e., only one power level is available in the uplink for all F flow types. So when a node sets its power, it has to satisfy all of the SIR requirements of its flow types.

Such a transmitter structure is simpler than the one in which the power levels of the multiplexed flow types are adjusted by appropriate weights or baseband processing, or the one in which separate transceivers and power amplifiers are used for each flow. The objective of this chapter is to evaluate the performance degradation that results from this simple and inexpensive transmitter structure. In the downlink, the base station transmits to N nodes simultaneously using NF different codes. Its power level P can be adjusted to satisfy the SIR requirements of the users. We assume that the distances from the nodes to the base station are equal; therefore the gain factors are ignored. This simplification must be eventually removed to establish the feasibility of the proposed transmitter design in practical systems. We also assume matched filter receivers. We can think of the system having NF virtual users, i.e., N sets of F users with the same power in each set, or F sets of N users with the same SIR requirements in each set.

For the uplink, the questions are:

(i) For fixed codes, the conditions for the power control problem to have solutions; i.e., when are the SIR requirements met?

If this question is answered and the power control problem has solutions, then the next question is:

(ii) What is the optimum (minimum) power vector to satisfy all the SIR requirements?

If the above two questions are answered, the natural question followed is

(iii) What are the optimal sequences so that the total power of all users is minimum, suppose the optimum power vectors are used?

For the downlink, the questions are:

(i) For fixed codes, what is the minimum power assignment of the base station to satisfy the SIR requirements?

Since the base station only has one power level, the power assignment is relatively easy to obtain; then the next question is

(ii) What are the optimal sequences to minimize that power assignment of the base station?

The organization of this chapter is as follows. In Section 3.2, we first formulate the problem for the uplink case, then we organize the rest of this section from the most simple $F=1$ special case (Section 3.2.1), to the $F>1, N=2$ special case (Section 3.2.2 and 3.2.3), and then to the general $F>1, N>1$ case (Section 3.2.4). The special case of $F=1$ is the typical power control problem already solved in the literature. We revisit this problem and find the optimal sequences to minimize the total power. For $F>1$, the condition to have solutions is completely solved for the special case $N=2$ and partially solved for the general $N>1$ case. An iterative algorithm to find the optimum power vector for the general $N>1$ case is given with the proof of the convergence.

In Section 3.3, we solve the power assignment of the base station and write it as the maximum of F terms. We first obtain the optimal sequences for the $F=1$ special case in Section 3.3.1, then we provide a partial solution of the optimal sequences for the special case of $N=1$ in Section 3.3.2 and general case of $N>1$ in Section 3.3.3. In particular, we have obtained some properties of the optimal sequences.

In Section 3.4, we compare the performance achieved by the optimal solution in the proposed constrained problem with the performance of the same system if each flow type can have its own power level chosen without the assumed constraint. Three examples are

given in Section 3.4.1, 3.4.2 and 3.4.3.

Finally, we summarize our work in Section 3.5.

3.2 Uplink

In the uplink CDMA system, the signal received at the base station [3] is given by

$$y(t) = \sum_{i=1}^N \sqrt{P_i} \cdot \left(\sum_{f=1}^F b_{if} S_{if}(t) \right) + \sigma \cdot n(t),$$

which consists of the signals from the NF virtual users and the noise. Here P_i is the power of node i , b_{if} and $S_{if}(t)$ are the transmitted bits and the signature waveform of type f at node i . We assume Additive White Gaussian Noise (AWGN) with power spectral density σ^2 .

The SIR requirements of flow type f at node i can be written as

$$SIR_{i,f} = \frac{P_i}{\sigma^2 + \sum_{(j,g) \neq (i,f)} P_j \cdot \rho_{if,jg}^2} \geq \beta_f, \quad f = 1, 2, \dots, F, \quad i = 1, 2, \dots, N.$$

The notation $\rho_{if,jg}$ denotes the crosscorrelation between flow type f at node i and flow type g at node j , that is,

$$\rho_{if,jg} = \mathbf{s}_{jg}^T \cdot \mathbf{s}_{if} = \int_0^T S_{if}(t) \cdot S_{jg}(t) dt.$$

Define the total squared crosscorrelation between flow type f at node i and all flow types at node j as

$$\alpha_{ij}^f = \sum_{g=1}^F \rho_{if,jg}^2.$$

Then the SIR requirements become

$$P_i \geq \beta_f \sigma^2 + \beta_f \sum_{j=1}^N (P_j \alpha_{ij}^f) - \beta_f P_i, \quad f = 1, 2, \dots, F, \quad i = 1, 2, \dots, N. \quad (3.1)$$

Or in matrix form,

$$\mathbf{P} \geq \beta_f \mathbf{A}^{(f)} \cdot \mathbf{P} + \beta_f \sigma^2 \mathbf{1}, f = 1, 2, \dots, F, \quad (3.2)$$

$$\text{with } \mathbf{A}^{(f)} = \begin{bmatrix} \alpha_{11}^f - 1 & \alpha_{12}^f & \cdots & \alpha_{1N}^f \\ \alpha_{21}^f & \alpha_{22}^f - 1 & \cdots & \alpha_{2N}^f \\ \vdots & \vdots & \ddots & \vdots \\ \alpha_{N1}^f & \alpha_{N1}^f & \cdots & \alpha_{NN}^f - 1 \end{bmatrix}, \quad \mathbf{P} = \begin{bmatrix} P_1 \\ P_2 \\ \vdots \\ P_N \end{bmatrix}, \quad \mathbf{1} = \begin{bmatrix} 1 \\ 1 \\ \vdots \\ 1 \end{bmatrix}_{N \times 1}.$$

3.2.1 Special Case of $F=1$

This goes back to the typical power control problem considered in [15] and [16], i.e.,

$$\mathbf{P} \geq \beta \mathbf{A} \cdot \mathbf{P} + \beta \sigma^2 \mathbf{1}. \quad (3.3)$$

Now the symmetric non-negative matrix \mathbf{A} has entries $a_{ij} = \rho_{ij}^2$ for $i \neq j$, and $a_{ij} = 0$ for $i = j$. The solutions to this problem with fixed sequences are well known from the properties of the non-negative matrices [17]. If $\beta < 1/\rho_A$ is true, then solutions exist. Here ρ_A is the largest eigenvalue of the matrix \mathbf{A} (Perron-Frobenius eigenvalue). Therefore the feasible β satisfies $\beta < 1/\rho_A$, and the optimum power vector is given by

$$\mathbf{P}^* = \sigma^2 \beta (\mathbf{I} - \beta \mathbf{A})^{-1} \cdot \mathbf{1}.$$

Notice that this optimum power vector is component-wise minimum over all feasible power vectors. So it also reaches the minimum total power over all feasible power vectors.

Here we wish to find the optimal codes, which minimize $\mathbf{1}^T \cdot \mathbf{P}^*$, the total power of the optimum power vector. The minimization by the sequence assignment now reduces to the problem of $\min_{\mathbf{S}} (\mathbf{1}^T \cdot (\mathbf{I} - \beta \mathbf{A})^{-1} \cdot \mathbf{1})$. Here $\mathbf{S} = [\mathbf{s}_{11}, \dots, \mathbf{s}_{1F}, \dots, \mathbf{s}_{N1}, \dots, \mathbf{s}_{NF}]$ is the matrix that consists of column sequence vectors. Using the properties of the matrix $(\mathbf{I} - \beta \mathbf{A})$

(which is positive definite and Hermitian [14,17]), and the Welch Bound of total squared correlation [18], we obtain the following conclusion.

Proposition 1: *For $N > L$, the optimal sequences to minimize the total power in an uplink power-controlled CDMA system with SIR requirement β are the WBE sequences and the corresponding optimum power vector is*

$$\mathbf{P} = \frac{\sigma^2}{1 + \frac{1}{\beta} - \frac{N}{L}} \cdot \mathbf{1}.$$

And for $N \leq L$, the optimal sequences are orthogonal with optimum power vector

$$\mathbf{P} = \beta \sigma^2 \cdot \mathbf{1}.$$

Therefore the total power for $N > L$ case is

$$P_{total} = \frac{N \sigma^2}{1 + \frac{1}{\beta} - \frac{N}{L}}.$$

Since this total power is for the optimum power assignment and optimal code assignment, it is the least possible total power needed to satisfy a SIR requirement β . This total power should be positive, i.e., $0 < P_{total} < \infty$. This implies that

$$\frac{N}{L} < 1 + \frac{1}{\beta}.$$

Therefore $1 + 1/\beta$ is the maximum number of users per degree of freedom the system can hold, provided the SIR requirement β is satisfied. It is the so-called user capacity for the uplink CDMA system with matched filter for $N > L$ case.

The conclusions about the optimal sequences, the optimum power vector, and the user capacity of the uplink CDMA system with a matched filter were also given in [10] following a different approach. In [10], the power and sequence assignment were jointly optimized to maximize the user capacity for a synchronous CDMA system with linear

MMSE multiuser receiver. Then the optimal sequences were found to be the WBE sequences, which also minimize the total power. Moreover, the MMSE receiver for the optimal sequences and optimum power assignment was found to be a matched filter. Here we first optimize the power vector for any sequences; then we optimize the sequence assignment for a CDMA cell (which uses the optimum power vector) to minimize the total power. We also have a separate proof (Appendix F), which is much simpler than the one given in [10]. It is interesting that the same result is obtained by looking at this problem from different angles.

The WBE sequences satisfy $\mathbf{S}\mathbf{S}^T = (N/L)\mathbf{I}$, and $\sum_{j=1}^N \rho_{ij}^2 = N/L, i=1,2,\dots,N$. This means that the matrix \mathbf{S} , whose columns are the sequences, has orthogonal rows. The matrix \mathbf{A} therefore has equal row summations. This symmetry comes from the symmetry between all the N users, in the sense of having the same SIR requirement and adjustable sequences. The WBE sequences are known to be the optimal sequences for several problems when $N > L$. Reference [19] showed that the overall information capacity of a multi-access channel with equal power is maximized by the WBE sequences. In [10], the author proved that the user capacity of a single cell synchronous CDMA system is maximized by the WBE sequences. The sequence sets to minimize the total squared correlation and maximize the common achievable SIR are also found to be the WBE sequences [20]. An iterative algorithm for the construction of the WBE sequences is introduced in [21].

3.2.2 Special Case of $N=2$, with Common Flow Types at Two Nodes

We now study thoroughly the case of two nodes because it is the simplest case that

reveals the different character of our problem. We start from the special case of $N=2$, with common flow types at the two nodes, and give an example of $N=2, F=2$ to show the details.

For the special case of $N=2$, recall from (3.1) that the SIR requirements for the flow types at node 1 and at node 2 are as follows

$$P_1 \geq \beta_f \sigma^2 + \beta_f P_1 (\alpha_{11}^f - 1) + \beta_f P_2 \alpha_{12}^f, f = 1, 2, \dots, F,$$

$$P_2 \geq \beta_f \sigma^2 + \beta_f P_1 \alpha_{21}^f + \beta_f P_2 (\alpha_{22}^f - 1), f = 1, 2, \dots, F.$$

Let us rewrite them as

$$P_1 \geq a_f + b_f P_2, \text{ and } P_2 \geq c_f + d_f P_1, f = 1, 2, \dots, F, \quad (3.4)$$

$$a_f = \frac{\sigma^2}{1 + \frac{1}{\beta_f} - \alpha_{11}^f}, \quad b_f = \frac{\alpha_{12}^f}{1 + \frac{1}{\beta_f} - \alpha_{11}^f}, \quad c_f = \frac{\sigma^2}{1 + \frac{1}{\beta_f} - \alpha_{22}^f}, \quad d_f = \frac{\alpha_{21}^f}{1 + \frac{1}{\beta_f} - \alpha_{22}^f}.$$

Because of the non-negativity of α_{ij}^f , if positive solutions (P_1, P_2) exist, then we have

$$P_1 \left(1 + \frac{1}{\beta_f} - \alpha_{11}^f \right) \geq \sigma^2 + P_2 \alpha_{12}^f > 0, f = 1, 2, \dots, F,$$

$$P_2 \left(1 + \frac{1}{\beta_f} - \alpha_{22}^f \right) \geq \sigma^2 + P_1 \alpha_{21}^f > 0, f = 1, 2, \dots, F.$$

Therefore we have the following necessary conditions in order for the problem to have solutions.

$$\alpha_{11}^f < 1 + \frac{1}{\beta_f}, \quad \alpha_{22}^f < 1 + \frac{1}{\beta_f}, f = 1, 2, \dots, F.$$

And then the coefficients defined in (3.4) satisfy

$$a_f > 0, \quad b_f \geq 0, \quad c_f > 0, \quad d_f \geq 0.$$

If $\alpha_{11}^f < 1 + \frac{1}{\beta_f}, \alpha_{22}^f < 1 + \frac{1}{\beta_f}, f = 1, 2, \dots, F$, are satisfied, the straight lines $P_2 = c_f + d_f P_1$

have non-negative slope d_f and positive ordinate intersection c_f ; and lines $P_1 = a_f + b_f P_2$ have positive slope $1/b_f$ and positive abscissa intersection a_f .

Further more, (3.4) can be written as

$$\begin{aligned} P_1 &\geq \max_f \{a_f + b_f P_2\}, \\ P_2 &\geq \max_f \{c_f + d_f P_1\}. \end{aligned} \quad (3.5)$$

The area $P_1 \geq \max_{f=1,2,\dots,F} (a_f + b_f P_2)$ is the infinite area to the right of all the lines $P_1 = a_f + b_f P_2, f=1,2,\dots,F$. Its behavior when P_1 and P_2 are large enough is determined by the minimum slope $\min_{f=1,\dots,F} (1/b_f)$. The area $P_2 \geq \max_{f=1,2,\dots,F} (c_f + d_f P_1)$ is the infinite area above all the lines $P_2 = c_f + d_f P_1, f=1,2,\dots,F$. Its behavior when P_1 and P_2 are large enough is determined by the largest slope $\max_{f=1,\dots,F} (d_f)$. If solutions exist, the power vectors that satisfy (3.5) are in the overlapping area of $P_1 \geq \max_{f=1,2,\dots,F} (a_f + b_f P_2)$ and $P_2 \geq \max_{f=1,2,\dots,F} (c_f + d_f P_1)$ on the (P_1, P_2) plane. Therefore the existence of solutions can be completely determined by the coefficients. Specifically, we need $\max_{f=1,\dots,F} (d_f)$ and $\min_{f=1,\dots,F} (1/b_f)$.

Proposition 2: *In the $N=2$ uplink power control problem with common SIR requirements $\beta_1 \leq \beta_2 \leq \dots \leq \beta_F$, the solutions exist if and only if*

$$\alpha_{11}^f < 1 + \frac{1}{\beta_f}, \quad \alpha_{22}^f < 1 + \frac{1}{\beta_f}, \quad f = 1, 2, \dots, F, \quad \text{and} \quad \max_{f=1,2,\dots,F} (b_f) \cdot \max_{f=1,2,\dots,F} (d_f) < 1.$$

The proof can be obtained from the proof of the later Proposition 3 as a special case of $N=2$ with different flow types at the two nodes. The optimum power vector \mathbf{P}^* should be the intersection of the two curves $P_1 = \max_{f=1,2,\dots,F} \{a_f + b_f P_2\}$ and $P_2 = \max_{f=1,2,\dots,F} \{c_f + d_f P_1\}$. An iterative algorithm can be used to find the minimum power solution in this fixed-point

problem. Namely,

$$\begin{aligned} P_1^{(i+1)} &= \max_{f=1,2,\dots,F} \{a_f + b_f P_2^{(i)}\}, \\ P_2^{(i+1)} &= \max_{f=1,2,\dots,F} \{c_f + d_f P_1^{(i)}\}. \end{aligned} \quad (3.6)$$

This algorithm converges to the optimum power vector very fast. The proof of the convergence is discussed later in Section 3.2.4 as a special case of $N>1$.

Example of $N=2, F=2$: To make it clear in the 2-D (P_1, P_2) space, we rewrite (3.4) as:

$$P_1 \geq a_1 + b_1 P_2 \quad \text{and} \quad P_2 \geq c_1 + d_1 P_1, \quad (3.7a)$$

and

$$P_1 \geq a_2 + b_2 P_2 \quad \text{and} \quad P_2 \geq c_2 + d_2 P_1. \quad (3.7b)$$

The coefficients are the same as in (3.4) with $f=1$ and 2. Then the solution area of flow type 1 (defined by (3.7a)) is bounded by two lines, one with a smaller slope d_1 , and the other with a larger slope $1/b_1$. The solution area of flow type 2 (defined by (3.7b)) is also bounded by two lines, one with a smaller slope d_2 , and the other with a larger slope $1/b_2$. Whether the two solution areas of flow type 1 and 2 overlap depends on the value of the 8 coefficients defined above. Some examples are shown in Figure 3.1 and Figure 3.2.

When $1/b_2 \leq d_1$ is true, the smaller slope of the solution area of flow type 1 is larger than the larger slope of the solution area of flow type 2, as shown in Figure 3.1a. Since the solution area of flow type 1 is always above the solution area of flow type 2, the two solution areas do not overlap. When $1/b_1 \leq d_2$ is the case, as shown in Figure 3.1b, the two solution areas also do not overlap because the solution area of flow type 1 is always below the solution area of flow type 2. Therefore $1/b_2 > d_1$ and $1/b_1 > d_2$ are the necessary conditions for both flow types to have solutions simultaneously.

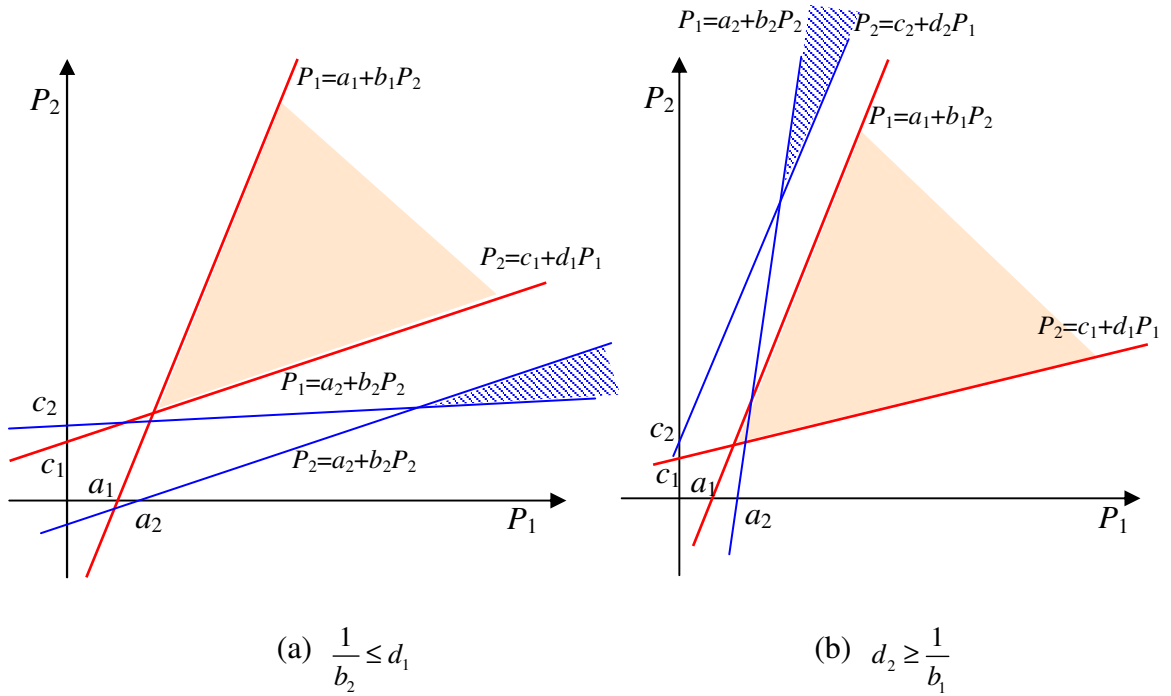


Figure 3.1: Examples of $N=2, F=2$ power control problem. Solutions do not exist.

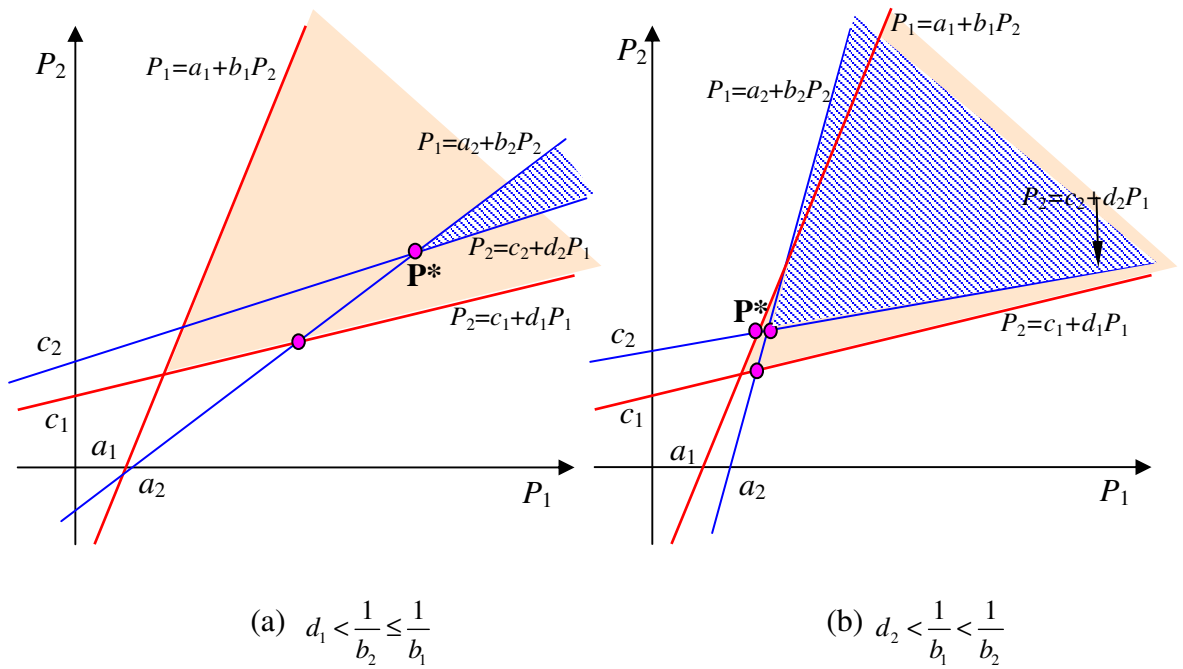


Figure 3.2: Examples of $N=2, F=2$ power control problem. Solutions exist.

When $1/b_2 > d_1$ and $1/b_1 > d_2$ are satisfied, there are two possible cases. One is

$d_1 < 1/b_2 \leq 1/b_1$ (the larger slope of the solution area of flow type 2 is between the smaller and larger slopes of the solution area of flow type 1). The other is $d_2 < 1/b_1 < 1/b_2$ (the larger slope of area 1 is between the smaller and larger slopes of area 2). For either case, by studying Figure 3.2, we can guarantee the overlap of the two areas.

The solution area (if it exists) is also the overlapping area of the two curves $P_1 \geq \max\{a_1 + b_1 P_2, a_2 + b_2 P_2\}$ and $P_2 \geq \max\{c_1 + d_1 P_1, c_2 + d_2 P_1\}$. The minimum power vector \mathbf{P}^* is actually the intersection of these two curves. Since this is a fixed-point problem, we can use an iterative algorithm to find this intersection. Let us start from $\mathbf{P}_0 = [0 \ 0]$, and iterate as follows,

$$\begin{aligned} P_1^{(i+1)} &= \max\{a_1 + b_1 P_2^{(i)}, a_2 + b_2 P_2^{(i)}\}, \\ P_2^{(i+1)} &= \max\{c_1 + d_1 P_1^{(i)}, c_2 + d_2 P_1^{(i)}\}. \end{aligned} \tag{3.8}$$

Figure 3.3 gives two examples of the convergence of the iteration in (3.8) on the (P_1, P_2) plane. We can see that this algorithm converges to the right solution very fast.

3.2.3 Special Case of $N=2$, with Different Flow Types at Two Nodes

Up to now we have assumed that there are F flow types, and they are common to all nodes. Now we remove this assumption and look at the case of $N=2$ again. Assume at node 1, there are F_1 flow types with $\beta_{11} \leq \beta_{12} \leq \dots \leq \beta_{1F_1}$; and at node 2, there are F_2 flow types with $\beta_{21} \leq \beta_{22} \leq \dots \leq \beta_{2F_2}$. With some minor modifications, this problem can fit into the previous structure.

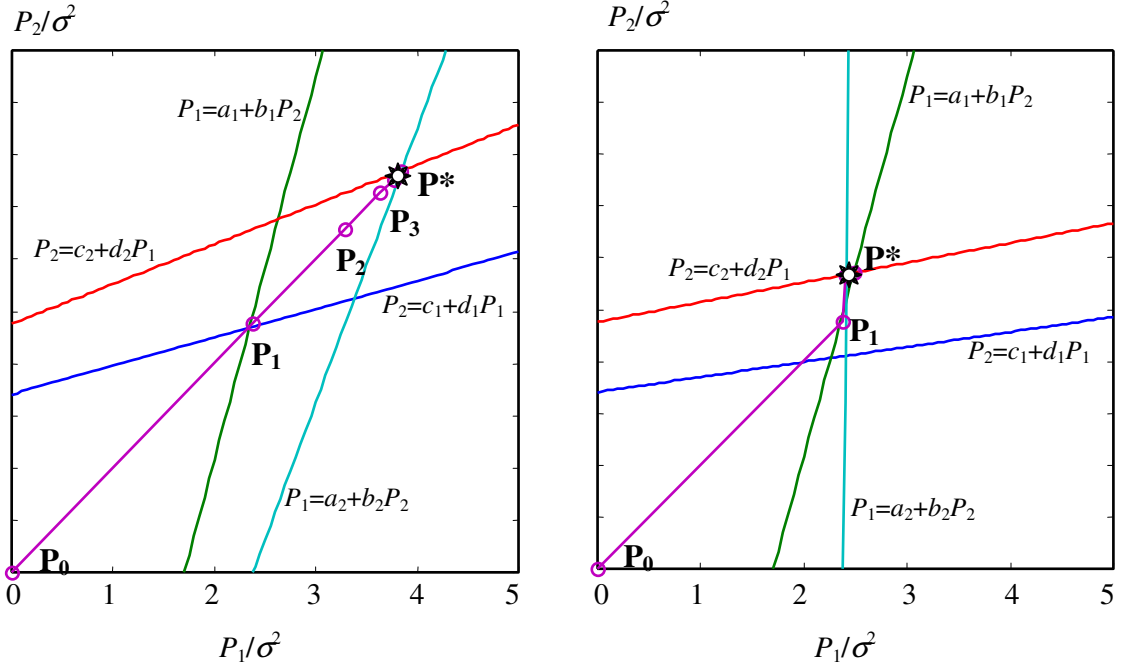


Figure 3.3: Examples of the convergence of iterative algorithm in the 2-D plane.

The SIR requirements for node 1 and node 2 can be written as

$$P_1 \geq \beta_{1f} \sigma^2 + \beta_{1f} P_1 (\alpha_{11}^f - 1) + \beta_{1f} P_2 \alpha_{12}^f,$$

where $\alpha_{11}^f = \sum_{g=1}^{F_1} \rho_{1f,1g}^2$, $\alpha_{12}^f = \sum_{g=1}^{F_2} \rho_{1f,2g}^2$, $f = 1, 2, \dots, F_1$, and

$$P_2 \geq \beta_{2f} \sigma^2 + \beta_{2f} P_1 \alpha_{21}^f + \beta_{2f} P_2 (\alpha_{22}^f - 1),$$

where $\alpha_{21}^f = \sum_{g=1}^{F_1} \rho_{2f,1g}^2$, $\alpha_{22}^f = \sum_{g=1}^{F_2} \rho_{2f,2g}^2$, $f = 1, 2, \dots, F_2$.

Finally, we get an expression similar to that of (3.4), i.e.,

$$P_1 \geq a_f + b_f P_2, \tag{3.9a}$$

if we let $a_f = \frac{\sigma^2}{1 + \frac{1}{\beta_{1f}} - \alpha_{11}^f}$, $b_f = \frac{\alpha_{12}^f}{1 + \frac{1}{\beta_{1f}} - \alpha_{11}^f}$, $f = 1, 2, \dots, F_1$, and

$$P_2 \geq c_f + d_f P_1, \tag{3.9b}$$

if we let $c_f = \frac{\sigma^2}{1 + \frac{1}{\beta_{2f}} - \alpha_{22}^f}$, $d_f = \frac{\alpha_{21}^f}{1 + \frac{1}{\beta_{2f}} - \alpha_{22}^f}$, $f = 1, 2, \dots, F_2$.

Similarly to the case of $N=2$ with common flow types in Section 3.2.2, we have a necessary condition from the positivity of (P_1, P_2) and non-negativity of α_{ij}^f as follows (Appendix G).

$$\alpha_{11}^f < 1 + \frac{1}{\beta_{1f}}, f = 1, 2, \dots, F_1, \text{ and } \alpha_{22}^f < 1 + \frac{1}{\beta_{2f}}, f = 1, 2, \dots, F_2. \quad (3.10)$$

And when these conditions are satisfied, the coefficients satisfy

$$a_f > 0, b_f \geq 0, f = 1, 2, \dots, F_1; \quad c_f > 0, d_f \geq 0, f = 1, 2, \dots, F_2.$$

Now the solution area for node 1 (described in (3.9a)) is bounded by F_1 straight lines with non-negative slopes $1/b_f$ and the solution area for node 2 (described in (3.9b)) is bounded by F_2 straight lines with non-negative slope d_f . Similarly to the discussion in Section 3.2.2, the existence of the solutions can be completely determined by the coefficients. Specifically, it depends on $\max_{f=1,2,\dots,F_2} (d_f)$, the largest slope of lines $P_2 = c_f + d_f P_1$, $f = 1, 2, \dots, F_2$, and $\min_{f=1,2,\dots,F_1} (1/b_f)$, the smallest slope of lines $P_1 = a_f + b_f P_2$, $f = 1, 2, \dots, F_1$.

Proposition 3: *In the $N=2$ uplink power control problem with SIR requirements $\beta_{11} \leq \beta_{12} \leq \dots \leq \beta_{1F_1}$ at node 1 and $\beta_{21} \leq \beta_{22} \leq \dots \leq \beta_{2F_2}$ at node 2, the solutions exist if and only if (Appendix H)*

$$\alpha_{11}^f < 1 + \frac{1}{\beta_{1f}}, f = 1, 2, \dots, F_1, \quad \alpha_{22}^f < 1 + \frac{1}{\beta_{2f}}, f = 1, 2, \dots, F_2, \quad \text{and} \quad \max_{f=1,2,\dots,F_1} (b_f) \cdot \max_{f=1,2,\dots,F_2} (d_f) < 1.$$

If solutions exist, then the solution area is the overlapping area of $P_1 \geq \max_{f=1,2,\dots,F_1} \{a_f + b_f P_2\}$

and $P_2 \geq \max_{f=1,2,\dots,F_2} \{c_f + d_f P_1\}$. And the optimum power vector \mathbf{P}^* should be the intersection of the two curves $P_1 = \max_{f=1,2,\dots,F_1} \{a_f + b_f P_2\}$ and $P_2 = \max_{f=1,2,\dots,F_2} \{c_f + d_f P_1\}$. Similarly, the same iterative algorithm introduced earlier can be used to find the optimum power vector, i.e.,

$$\begin{aligned} P_1^{(i+1)} &= \max_{f=1,\dots,F_1} \{a_f + b_f P_2^{(i)}\}, \\ P_2^{(i+1)} &= \max_{f=1,\dots,F_2} \{c_f + d_f P_1^{(i)}\}. \end{aligned} \quad (3.11)$$

This algorithm converges to the optimum power vector. The proof of the convergence is discussed later in Section 3.2.4 as a special case of $N>1$.

3.2.4 General Case of $N>1$

Recall that for the general case of $N>1$ with common F flow types at each node, the power assignment should satisfy (3.2). Define the interference function $\mathbf{I}(\mathbf{P})$ as follows,

$$\mathbf{I}(\mathbf{P}) = \max_{f=1,2,\dots,F} \left\{ \beta_f (\mathbf{A}^{(f)} \mathbf{P})_i + \beta_f \sigma^2 \right\}, i=1,2,\dots,N. \quad (3.12)$$

Then (3.2) is now

$$\mathbf{P} \geq \mathbf{I}(\mathbf{P}).$$

For general case of $N>1$ with different F flow types at each node, we assume that at node i , there are F_i flow types with $\beta_{i1} \leq \beta_{i2} \leq \dots \leq \beta_{iF_i}$. The SIR requirements at node i can be rewritten as

$$P_i \geq \beta_{if} \sigma^2 + \beta_{if} P_i (\alpha_{ii}^f - 1) + \beta_{if} \sum_{j \neq i} P_j \alpha_{ij}^f, \quad f = 1, 2, \dots, F_i,$$

$$\text{with } \alpha_{ij}^f = \sum_{g=1}^{F_j} \rho_{if,jg}^2, \quad f = 1, 2, \dots, F_i.$$

Since the flow types are different at each node, there is no matrix form like that of (3.2) here. But we can still define a similar interference function $\mathbf{I}(\mathbf{P})$ as follows:

$$\mathbf{I}_i(\mathbf{P}) = \max_{f=1,2,\dots,F_i} \left\{ \beta_{if} \sigma^2 + \beta_{if} P_i (\alpha_{ii}^f - 1) + \beta_{if} \sum_{j \neq i} P_j \alpha_{ij}^f \right\}, \quad i=1,2,\dots,N. \quad (3.13)$$

Then the SIR requirements can still be written as $\mathbf{P} \geq \mathbf{I}(\mathbf{P})$.

Let us suppose the solutions exist first, and consider the existence later. The problem is now to find the minimum \mathbf{P} , such that $\mathbf{P} \geq \mathbf{I}(\mathbf{P})$ is satisfied. The iterative algorithm we used in (3.6) and (3.11) can all be written as

$$\mathbf{P}^{(i+1)} = \mathbf{I}(\mathbf{P}^{(i)}).$$

We use the conclusions from [22] to prove the convergence of the algorithm. Reference [22] defined an interference function $\mathbf{I}(\mathbf{P})$ to be *standard* if for all $\mathbf{P} > \mathbf{0}$, the following properties are satisfied:

1. Positivity: $\mathbf{I}(\mathbf{P}) > \mathbf{0}$.
2. Monotonicity: If $\mathbf{P} \geq \mathbf{P}'$, then $\mathbf{I}(\mathbf{P}) \geq \mathbf{I}(\mathbf{P}')$.
3. Scalability: For all $\alpha > 1$, $\alpha \mathbf{I}(\mathbf{P}) > \mathbf{I}(\alpha \mathbf{P})$.

The algorithm $\mathbf{P}^{(i+1)} = \mathbf{I}(\mathbf{P}^{(i)})$ with standard $\mathbf{I}(\mathbf{P})$ is called a standard power control algorithm. From [22] it follows that if there is a fixed point, then it is unique and it is the optimum power vector (component-wise minimum) that we are looking for. Furthermore, if $\mathbf{P} \geq \mathbf{I}(\mathbf{P})$ has solutions, then, for any initial power vector \mathbf{P} , the standard power control algorithm converges to the optimum power vector \mathbf{P}^* . Since the proof of convergence was given in [22], we only need to verify here that the interference function defined above is standard. This can be verified in a straightforward way.

Proposition 4: *The algorithm $\mathbf{P}^{(i+1)} = \mathbf{I}(\mathbf{P}^{(i)})$ with the interference function defined in either (3.12) or (3.13) converges to the optimum power vector \mathbf{P}^* , if solutions of*

$\mathbf{P} \geq \mathbf{I}(\mathbf{P})$ exist (Appendix I).

Notice that, by letting $N=2$, we come back to the special case of $N=2$. Therefore the proof of Proposition 4 also proves the convergence of the algorithm in (3.6) and (3.11).

Now we discuss the existence of the solutions for the general case of $N>1$. Similarly to the $N=2$ case, we have the following necessary condition from the positivity of the power vector.

Proposition 5: *If the $N>1$ uplink power control problem with SIR requirements $\beta_{i1} \leq \beta_{i2} \leq \dots \leq \beta_{iF_i}$ at node i has solutions, then,*

$$\alpha_{ii}^f < 1 + \frac{1}{\beta_{if}}, \quad f = 1, 2, \dots, F_i, \quad i = 1, 2, \dots, N.$$

Let us assume that these necessary conditions are satisfied. Then under what condition do solutions exist? In the N -D space (P_1, P_2, \dots, P_N) , the requirements are not as clear and direct as those in the 2-D (P_1, P_2) space. We have not obtained a complete answer to the question of the existence of the solutions. However, we can relate the $N>2$ case with the $N=2$ case and obtain some insights.

For a necessary condition, let us simplify the problem to $N=2$, assuming other nodes are not transmitting, that is, for any i, j ($i \neq j$), let P_k ($k \neq i, j$) = 0, and then only 2 inequality sets for P_i and P_j are left in $\mathbf{P} \geq \mathbf{I}(\mathbf{P})$. If the original $N>2$ problem has solutions, then this simplified less demanding $N=2$ problem has solutions. Therefore, one necessary condition for the original $N>2$ problem to have solutions is that any simplified $N=2$ problem, as described, satisfies $\max_{f=1,2,\dots,F_1} (b_f) \cdot \max_{f=1,2,\dots,F_2} (d_f) < 1$.

For a sufficient condition, let us partition the N nodes into two distinct sets, one with

N_1 nodes i_1, i_2, \dots, i_{N_1} , and the other with N_2 nodes j_1, j_2, \dots, j_{N_2} , ($N = N_1 + N_2$). Let nodes in set 1 have same power P_1 and nodes in set 2 have same power P_2 . Set 1 has a total of F_1 flow types with $F_1 = F_{i_1} + F_{i_2} + \dots + F_{i_{N_1}}$; set 2 has a total of F_2 flow types with $F_2 = F_{j_1} + F_{j_2} + \dots + F_{j_{N_2}}$. Then re-index the flow types in set 1 from 1 to F_1 , and flow types in set 2 from 1 to F_2 , and define an α factor and coefficients a, b, c, and d as in the $N=2$ case. Since the $N=2$ problem defined in this way is almost the same as the original problem, except that it has additional constraints on P , the original problem has solutions if the corresponding $N=2$ problem has solutions. If for any partition, as described above, the coefficients of the corresponding $N=2$ problem satisfy $\max_{f=1,2,\dots,F_1} (b_f) \cdot \max_{f=1,2,\dots,F_2} (d_f) < 1$, then the original power control problem has solutions. And if the optimum power vector of the corresponding $N=2$ problem is $\mathbf{P}_{N=2}$, and then the optimum power vector of the original power control problem satisfies $\mathbf{P}^* \leq \mathbf{P}_{N=2}$.

3.3 Downlink

In the downlink case, the base station transmits to all the flow types at all the nodes simultaneously. Its power level P can be adjusted to satisfy the SIR requirements of all flow types. The signal received at the multiuser receiver of any node [3] is given by

$$y(t) = \sqrt{P} \sum_{i=1}^N \sum_{f=1}^F b_{if} S_{if}(t) + \sigma \cdot n(t).$$

The SIR requirement of flow type f at node i is given by

$$SIR_{i,f} = \frac{P}{\sigma^2 + \sum_{(j,g) \neq (i,f)} P \cdot \rho_{if,jg}^2} \geq \beta_f, \quad f = 1, 2, \dots, F, \quad i = 1, 2, \dots, N.$$

Define the total squared crosscorrelation between flow type f at node i and all flow

types at all nodes as

$$\alpha_{if} = \sum_{j=1}^N \sum_{g=1}^F \rho_{if,jg}^2.$$

Then the SIR requirements become

$$\frac{\sigma^2}{P} \leq 1 + \frac{1}{\beta_f} - \alpha_{if}, \quad f=1,2,\dots,F, \quad i=1,2,\dots,N.$$

Hence, the power assignment P has to satisfy $P \geq P^*$, with P^* the minimum power level of the base station, which satisfies

$$\frac{\sigma^2}{P^*} = \min_f \left(1 + \frac{1}{\beta_f} - \max_i \alpha_{if} \right). \quad (3.14)$$

In order to have positive solutions P , we need $1 + 1/\beta_f - \alpha_{if} > 0$ for all i and f . That is, the feasible β_f (which means that β_f alone can be satisfied by power control if the SIR requirements of other flow types are not considered) should satisfy

$$\max_i \alpha_{if} < 1 + \frac{1}{\beta_f}, \quad f=1,2,\dots,F.$$

Now we wish to minimize P^* by selecting the appropriate sequences. That is,

$$\max_{\mathbf{s}} \left\{ \min_f \left(1 + \frac{1}{\beta_f} - \max_i \alpha_{if} \right) \right\},$$

with $\mathbf{S} = [\mathbf{s}_{11}, \dots, \mathbf{s}_{1F}, \dots, \mathbf{s}_{N1}, \dots, \mathbf{s}_{NF}]$, the matrix that consists of the column sequence vectors. The optimal sequences to minimize the power are now a max-min problem.

3.3.1 Special Case of $F=1$

For $F=1$, (3.14) becomes

$$\frac{\sigma^2}{P^*} = 1 + \frac{1}{\beta} - \max_i \sum_j \rho_{ij}^2. \quad (3.15)$$

The problem to minimize P^* is now

$$\max_s \left(1 + \frac{1}{\beta} - \max_i \sum_j \rho_{ij}^2 \right) = 1 + \frac{1}{\beta} - \min_s \left(\max_i \sum_j \rho_{ij}^2 \right).$$

For $N \leq L$, obviously $\min_s \left(\max_i \sum_j \rho_{ij}^2 \right) = 1$, and the minimum power is obtained by orthogonal sequences.

For $N > L$, The Welch Bound of total squared crosscorrelation is [18]

$$\sum_{i=1}^N \sum_{j=1}^N \rho_{ij}^2 \geq \frac{N^2}{L}. \quad (3.16)$$

The sequences which satisfy (3.16) with equality are the WBE sequences [20] which satisfy $\mathbf{S}\mathbf{S}^T = \frac{N}{L}\mathbf{I}$, and $\sum_{j=1}^N \rho_{ij}^2 = \frac{N}{L}$, $i=1,2,\dots,N$. Since the maximum value is always greater than or equal to the average, we also have

$$\max_i \sum_j \rho_{ij}^2 \geq \frac{1}{N} \sum_{i=1}^N \left(\sum_{j=1}^N \rho_{ij}^2 \right). \quad (3.17)$$

The equality is satisfied when $\sum_{j=1}^N \rho_{ij}^2$ is the same for all $i=1,2,\dots,N$. It happens that the WBE sequences that satisfy equality in (3.16) also reach equality in (3.17). Using (3.16) and (3.17) in succession we find

$$\max_i \sum_j \rho_{ij}^2 \geq \frac{N}{L},$$

and the equality is satisfied by the WBE sequences. After calculating the minimum power level from (3.15), we have the following conclusion.

Proposition 6: For $N > L$, the optimal sequences that minimize the power in a

downlink CDMA system with SIR requirement β are the WBE sequences and the minimum power assignment is

$$P^* = \frac{\sigma^2}{1 + \frac{1}{\beta} - \frac{N}{L}}.$$

For $N \leq L$, the optimal sequences for this problem is orthogonal sequences with

$$P^* = \sigma^2 \beta.$$

For the $N > L$ case, $0 < P^* < \infty$ implies

$$\frac{N}{L} < 1 + \frac{1}{\beta}.$$

This is the maximum number of users per degree of freedom the system can have provided the SIR requirements are satisfied. It is the user capacity for the downlink CDMA system using matched filter for the $N > L$ case. Recalling the results from the uplink section, we find that for both the uplink and the downlink $F=1$, $N > L$ case, the optimal sequences are the WBE sequences, the minimum power (of base station or any node) is $\sigma^2 / (1 + \frac{1}{\beta} - \frac{N}{L})$, and the user capacity is $1 + 1/\beta$ users per degree of freedom. Also for both the uplink and the downlink $N \leq L$ case, the optimal sequences are orthogonal, and the minimum power is $\sigma^2 \beta$.

3.3.2 Special Case of $N=1$

For $N=1$, both the downlink and the uplink are simple point-to-point links. Equation (3.14) becomes

$$\frac{\sigma^2}{P^*} = \min_f \left(1 + \frac{1}{\beta_f} - \alpha_f \right), \quad \alpha_f = \sum_g \rho_{gf}^2. \quad (3.18)$$

The feasible β_f should satisfy

$$\alpha_f < 1 + \frac{1}{\beta_f}, f=1,2,\dots,F. \quad (3.19)$$

If $F \leq L$, then orthogonal sequences is the optimal choice, with

$$P^* = \beta_f \sigma^2.$$

If $F > L$, we have $\alpha_f = \sum_s \rho_{fs}^2 = (\mathbf{R}^2)_{ff}$, and $\mathbf{R} = \mathbf{S}^T \mathbf{S} = \begin{bmatrix} 1 & \rho_{12} & \cdots & \rho_{1F} \\ \rho_{21} & 1 & \cdots & \rho_{2F} \\ \vdots & \vdots & \ddots & \vdots \\ \rho_{F1} & \rho_{F2} & \cdots & 1 \end{bmatrix}$.

Then the problem $\max_s \min_f (1 + 1/\beta_f - \alpha_f)$ becomes now

$$\max_s \min_f \left(1 + \frac{1}{\beta_f} - (\mathbf{S}^T \mathbf{S} \mathbf{S}^T \mathbf{S})_{ff} \right).$$

Again, $\mathbf{S} = [\mathbf{s}_1, \mathbf{s}_2, \dots, \mathbf{s}_F]$ is the matrix whose columns are the sequences.

It is difficult to get an exact analytic solution for this problem. Here we find some properties that the optimal sequences must satisfy. Let us start from $F=3$. If 3 codes are available with $\alpha_1 \geq \alpha_2 \geq \alpha_3$, then the question is how to assign these 3 codes to the 3 flow types so that $\min_{f=1,2,3} (1 + 1/\beta_f - \alpha_{i(f)})$ is maximized. The notation $i(f)$ used here implies that code $i(f)$ is assigned to flow type f . It is clear that we should assign the code with the least correlation (i.e., the code with $\min \alpha$) to the most demanding flow type (i.e., the flow type with $\max \beta$) and the code with highest correlation (i.e. the code with $\max \alpha$) to the least demanding flow type (i.e. the flow type with $\min \beta$). This assignment is always better or at least as good as other assignments. So, there is at least one optimal set of sequences that satisfies $\alpha_1 \geq \alpha_2 \geq \alpha_3$. Therefore, when we search for the optimal sequences, we can limit the search to the code sets that satisfy $\alpha_1 \geq \alpha_2 \geq \alpha_3$ without missing the minimum power. For $F > 3$, we can prove the following proposition.

Proposition 7: *The set of solutions for $\max_s \min_f (1+1/\beta_f - \alpha_f)$ with $\beta_1 \leq \beta_2 \leq \dots \leq \beta_F$ includes solutions that satisfy (Appendix J)*

$$\alpha_1 \geq \alpha_2 \geq \dots \geq \alpha_F.$$

(i.e., there is at least one optimal set of sequences that satisfies $\alpha_1 \geq \alpha_2 \geq \dots \geq \alpha_F$).

Using the definition of α_i , we can transform the condition for α into conditions that ρ_{ij} has to satisfy for small F . For $F=3$, this property implies $\rho_{12}^2 \geq \rho_{13}^2 \geq \rho_{23}^2$. For $F=4$, it implies $\rho_{12}^2 - \rho_{34}^2 \geq \rho_{13}^2 - \rho_{24}^2 \geq |\rho_{23}^2 - \rho_{14}^2| \geq 0$. For $F \geq 5$, we were not able to obtain similar analytic conditions.

3.3.3 General Case of $N>1$ and $F>1$

For the general case of $N>1$ and $F>1$, similarly to Proposition 7, we have the following property of the optimal sequences.

Proposition 8: *The set of optimal solutions of $\max_s \min_f (1+1/\beta_f - \max_i \alpha_{if})$ with $\beta_1 \leq \beta_2 \leq \dots \leq \beta_F$ includes solutions that satisfy*

$$\max_i (\alpha_{i1}) \geq \max_i (\alpha_{i2}) \geq \dots \geq \max_i (\alpha_{iF}).$$

We can use the same induction process as in the proof of Proposition 7 to prove this proposition, by changing α_f to $\min_i (\alpha_{if})$.

From this conclusion, we know that at least one optimal set of sequences assigns the N sequences with largest α to the flow type 1 at N nodes (permutation is fine within the N sequences), the next N sequences with largest α to flow type 2 at N nodes, and so on.

3.4 Effect of the One Power Level Constraint

The word “constraint” in this section means that all the flow types at one node has the same power level. On one hand, this constraint allows the usage of a simple and inexpensive transmitter structure; on the other hand, it degrades the performance. In this section, we inspect the performance degradation by comparing the systems with and without the constraint.

With the constraint, the problem is a synchronous CDMA system with one base station and N nodes. At each node, there are F flow types with SIR requirements $\beta_1 \leq \beta_2 \leq \dots \leq \beta_F$. For the uplink, the SIR requirements of flow type f at node i are given in (3.1) and (3.2). For the downlink, the minimum power level of the base station satisfies (3.14). Without the constraint, the problem is a synchronous CDMA system with one base station and NF nodes. For both the uplink and downlink, there are NF separate power levels for each of the flow types satisfying

$$P_{if} \geq \beta_f \sigma^2 + \beta_f \sum_{j=1}^N \sum_{g=1}^F (P_{jg} \cdot \rho_{if,jg}^2) - \beta_f P_{if}, \quad f=1,2,\dots,F, \quad i=1,2,\dots,N. \quad (3.20)$$

The problem with the constraint is a special case of the problem without the constraint. For the uplink if power vector $\mathbf{P} = [P_1, P_2, \dots, P_N]^T$ satisfies (3.1), then the power vector $\mathbf{P} \otimes \mathbf{1}_{1 \times F}$ is a solution of (3.20). (Notation $\mathbf{P} \otimes \mathbf{1}_{1 \times F}$ is the Kronecker product, which denotes the vector whose i th ($i=1,\dots,N$) element is replaced by $P_i \cdot [1, \dots, 1]_{1 \times F}^T$.) For the downlink, if power level P^* satisfies (3.14), then obviously, the power vector $P^* \cdot \mathbf{1}_{1 \times NF}$ satisfies (3.20). That is, it is more difficult for the power control problem with the constraint to have solutions.

If solutions exist, we suppose the optimum power vector of the uplink problem with the constraint is \mathbf{P}^* and the optimum power vector of the problem without the constraint

is $\tilde{\mathbf{P}}^*$. Since $\mathbf{P}^* \otimes \mathbf{1}_{1 \times F}$ is a solution of the problem without the constraint, from the property of the iterative algorithm, we have

$$\mathbf{P}^* \otimes \mathbf{1}_{1 \times F} \geq \tilde{\mathbf{P}}^*.$$

For the downlink, we suppose the minimum power level at the base station is P^* , then $P^* \cdot \mathbf{1}_{1 \times NF}$ is also the solution of the downlink power control problem without the constraint. From the component-wise minimum property of $\tilde{\mathbf{P}}^*$, we know that $P^* \cdot \mathbf{1}_{1 \times NF} \geq \tilde{\mathbf{P}}^*$ is true. Therefore the minimum total power needed to satisfy the same SIR requirements $(\beta_1, \beta_2, \dots, \beta_F)$ for the problem with the constraint is larger than or equal to the total power needed for the problem without the constraint.

In order to inspect the performance degradation more directly, we study some special cases and examples.

3.4.1 Special Case of $N=1$

The uplink and the downlink are the same for the $N=1$ case except the meaning of the variables. With the constraint, for fixed sequences, the condition to have solutions is that the SIR requirements satisfy (3.19) and the optimum power satisfies (3.18).

Without the constraint, we have

$$(\mathbf{I} - \mathbf{B} \cdot \mathbf{A}) \cdot \mathbf{P} \geq \sigma^2 \cdot \boldsymbol{\beta},$$

$$\text{with } \mathbf{A} = \begin{bmatrix} 0 & \rho_{12}^2 & \cdots & \rho_{1F}^2 \\ \rho_{21}^2 & 0 & \cdots & \rho_{2F}^2 \\ \vdots & \vdots & \ddots & \vdots \\ \rho_{F1}^2 & \rho_{F2}^2 & \cdots & 0 \end{bmatrix}, \quad \mathbf{B} = \begin{bmatrix} \beta_1 & 0 & \cdots & 0 \\ 0 & \beta_2 & \cdots & 0 \\ \vdots & \vdots & \ddots & \vdots \\ 0 & 0 & \cdots & \beta_F \end{bmatrix}, \quad \mathbf{P} = \begin{bmatrix} P_1 \\ P_2 \\ \vdots \\ P_F \end{bmatrix}, \quad \boldsymbol{\beta} = \begin{bmatrix} \beta_1 \\ \beta_2 \\ \vdots \\ \beta_F \end{bmatrix}.$$

For fixed sequences, from the property of nonnegative matrix $\mathbf{B} \cdot \mathbf{A}$, the condition to have solutions is that the SIR requirements satisfy

$$1 > \text{P-F eigenvalue of } (\mathbf{B} \cdot \mathbf{A}), \quad (3.21)$$

and the optimum power vector is

$$\tilde{\mathbf{P}}^* = \sigma^2 (\mathbf{I} - \mathbf{B}\mathbf{A})^{-1} \cdot \boldsymbol{\beta}. \quad (3.22)$$

Example of $N=1$ and $F=2$: We study this example to clearly compare the difference of the power with and without the constraint. We are comparing for fixed sequences, because the optimal sequences for this case are unknown, and might be different for the problems with and without the constraint.

For the problem with the constraint, Equations (3.19) and (3.18) give the conditions to have solutions and the minimum total power required as,

$$\beta_1 < \frac{1}{\rho^2} \quad \text{and} \quad \beta_2 < \frac{1}{\rho^2}, \quad (3.23)$$

$$\tilde{P}_{total} = \frac{2\sigma^2\beta_2}{1 - \rho^2\beta_2}. \quad (3.24)$$

For the problem without the constraint, now we have $\mathbf{B} \cdot \mathbf{A} = \begin{pmatrix} 0 & \rho^2\beta_1 \\ \rho^2\beta_2 & 0 \end{pmatrix}$, with eigenvalues $\lambda^2 = \rho^4\beta_1\beta_2$. After deriving $(\mathbf{I} - \mathbf{B} \cdot \mathbf{A})^{-1}$, equations (3.21) and (3.22) are simplified to

$$\beta_1\beta_2 < \frac{1}{\rho^4}, \quad (3.25)$$

$$P_{total} = \frac{\sigma^2}{1 - \rho^4\beta_1\beta_2} (\beta_1 + \beta_2 + \rho^2\beta_1^2 + \rho^2\beta_2^2). \quad (3.26)$$

Comparing (3.23) and (3.25), it is obviously that (3.25) defines a larger region for (β_1, β_2) than (3.23) does, i.e., it is easier for the power control problem without the constraint to have solutions.

From $\beta_1 \leq \beta_2$, we always have

$$\frac{\sigma^2}{1-\rho^4\beta_1\beta_2}(\beta_1 + \beta_2 + \rho^2\beta_1^2 + \rho^2\beta_2^2) \leq \frac{2\sigma^2}{1-\rho^4\beta_2^2}(\beta_2 + \rho^2\beta_2^2) = \frac{2\sigma^2\beta_2}{1-\rho^2\beta_2},$$

i.e., $\tilde{P}_{total} \leq P_{total}$, the problem with the constraint needs larger total power.

3.4.2 Special Case of $\beta_1 = \beta_2 = \dots = \beta_F$

With one power level constraint we have for the uplink the power vector satisfies

$$\mathbf{P} \geq \beta \mathbf{A}^{(f)} \cdot \mathbf{P} + \beta \sigma^2 \mathbf{1}, \quad f = 1, 2, \dots, F.$$

For the downlink, the minimum power needed at the base station is given by

$$P^* = \frac{\sigma^2}{1 + \frac{1}{\beta} - \min_f \left(\max_i \alpha_{if} \right)}.$$

Without the constraint, this is the same as the NF nodes, one flow type problem.

$$\tilde{\mathbf{P}}^* = \beta \sigma^2 (\mathbf{I} - \beta \mathbf{A})^{-1} \cdot \mathbf{1}.$$

Example of $N=1$ and $\beta_1 = \beta_2 = \dots = \beta_F$: We consider this example to clearly compare the performance difference. Now the uplink and downlink are the same except the meanings of the variables. This time we compare the minimum total power for optimal sequences.

For the problem with the constraint, it is actually the same as the one flow type, F nodes downlink case. Referring to Proposition 6, we know that the optimal sequences for $F \leq L$ are orthogonal sequences with minimum power at each of the flow type

$$P^{*F \leq L} = \beta \sigma^2,$$

and the optimal sequences for $F > L$ case are the WBE sequences with

$$P^{*F > L} = \frac{\sigma^2}{1 + \frac{1}{\beta} - \frac{F}{L}}.$$

For the problem without the constraint, this is actually same as the case of F nodes one flow type problem. Referring to Proposition 1, we know that the optimal sequences for $F \leq L$ are orthogonal sequences with minimum power at each of the flow type

$$\tilde{P}_{total}^{F \leq L} = \beta \sigma^2,$$

and the optimal sequences for the $F > L$ case are WBE sequences with

$$\tilde{P}_{total}^{F > L} = \frac{\sigma^2}{1 + \frac{1}{\beta} - \frac{F}{L}}.$$

In this example the constraint of one power level cost nothing for the optimal sequences. (Also agree with our conclusion.) The reason is that the optimum power vector for $N=1$ and $\beta_1 = \beta_2 = \dots = \beta_F$ case when optimal sequences are used has equal powers at different flow types; therefore the constraint is satisfied automatically without causing any performance degradation.

3.4.3 Numerical Example for General N And F

For general N and F , we don't have analytical expression of the power vector for the problem with the constraint. We study an example numerically to check the difference of the total power needed for the power control problem with and without the constraint. Basically, this difference depends on the SIR requirements and the level of correlations.

Example: $N=3$; $F=2$; $L=20$: Sequences are generated randomly as $\mathbf{s}_i = [V_{i1}, V_{i2}, \dots, V_{iL}]$, $i=1,2,\dots,NF$. Here $V_{ij} = \pm 1$ with equal probability. (The $L=20$ random sequences is just a way to introduce random correlations, this does not mean that the number of users has to be less than the number of degree of freedom.) Then we solve iteratively the power control problem with and without the constraint. Each time we run the program, a new set of sequences is generated, and power control problems are solved

and the results for both problems are compared. We define:

$$\text{Power ratio} = \frac{\text{Total power needed for the power control problem WITH constraint}}{\text{Total power needed for the power control problem WITHOUT constraint}}.$$

For SIR requirements $\beta_1 = 1.0$ and $\beta_2 = 1.5$, we run the program 100 times. Each time the solutions exist. The power ratio is between 1.0 and 1.4 most of the time (with about 80% probability). Please refer to Table 3.1 for details. For more strict SIR requirements $\beta_1 = 2.0$, $\beta_2 = 3.0$, we also run the program 100 times. There are 4 times no solution exists for either of the problems. There are 13 times only the problem without the constraint has solutions. For the remained 83 times, both problems have solutions. This again indicates that it is easier for the problem without the constraint to have solutions. When both of the problems have solutions, the power ratio distributed more widely than the $\beta_1 = 1.0$, $\beta_2 = 1.5$ case, with an obviously larger average.

Table 3.1: Comparison of the power for the power control problem with and without the constraint of one power level. $N=3$; $F=2$; $L=20$.

In 100 simulations, number of times that	$\beta_1 = 1.0, \beta_2 = 1.5$	$\beta_1 = 2.0, \beta_2 = 3.0$
Power ratio is in the region [1.0,1.2)	11	4
Power ratio is in the region [1.2,1.4)	69	23
Power ratio is in the region [1.4,2.0)	16	23
Power ratio is in the region [2.0,10)	2	21
Power ratio is in the region [10,∞)	2	12
Only problem w/o constraint has solutions	0	13
Neither problem has solutions	0	4

3.5 Summary

We study the problem of a power-controlled CDMA system with N nodes and F flow types with the constraint that each node uses the same power level for all flows that it multiplexes. Each flow type may have its own SIR requirement. For the $F=1$ case, we

find that for both the uplink and the downlink, if $N > L$, the optimal sequences are the WBE sequences, and the user capacity is $1 + 1/\beta$ users per degree of freedom. Also if $N \leq L$, the optimal sequences are orthogonal. For the uplink problem with $N=2$ and F arbitrary, the necessary and sufficient conditions to have solutions are found and proved. For the general $N > 1$ uplink problem, we provide an iterative algorithm to find the optimal solution and prove its convergence. For the downlink case with $F > 1$, the power assignment problem is solved and some properties of the optimal sequences are proved. Finally, the one power level constraint simplifies the transmitter structure, with the cost of performance degradation.

Chapter 4 Simple Rate Control for Fluctuating Channels in Ad Hoc Wireless Networks

4.1 Introduction

The link quality of a wireless connection may vary considerably due to noise burst, fades, and the mobility of transmitter and/or receiver nodes. Therefore a fixed modulation scheme and a fixed data rate will lead to variable link quality. When the Signal-to-Noise Ratio (SNR) of the received signal drops significantly, there are many ways to maintain the link quality. One way is to increase the transmission power [23]. Another way is to change the channel coding rate or choice of code, and therefore change the received data rate indirectly [24,25]. It can also be done by adapting the data rate directly [26,27,28], or some combination of the methods listed above [29,30,31].

Basically, there are two ways to control the bit rate transmitted over a channel. The first is to change the symbol transmission rate [26]. When the channel is poor, a longer pulse gives more energy per bit to mitigate the noise. Another method is to vary the size of the constellation of the modulation scheme (the number of points in the constellation) [27,28]. With this method, during a fade, the number of modulation levels is decreased accordingly. For the same transmission power, a smaller sized constellation creates a

larger Euclidean distance between the signal points, and hence it provides a better symbol error rate. For example, when a rectangular 16-QAM (QAM modulation with 16-point constellation) is used for a good channel, a 4-QAM could be used when the channel becomes poor.

However, all these methods require feedback channels from the receiver to the source. Some may require buffering of traffic at the source, which may cause longer delay and/or buffer overflows or underflows. Some methods may also require increased complexity in the transmitter design.

In this chapter we consider a passive rate adaptation scheme at the receiver in which only part of the transmitted bits are detected (i.e., some bits are intentionally dropped). For example, if the transmitter uses 8-PAM (PAM modulation with 8-point constellation), then when the channel is in poor condition, the receiver uses a detector with 4 output levels after the demodulator. We denote the procedure by 8-PAM->4. Figure 4.1 shows the signal space of 8-PAM and 8-PAM->4. As another example, the transmitter uses 16-QAM with rectangular constellation, while the receiver only decides which quadrant the signal is located in, i.e., uses a detector like the one used for 4-QAM to receive only 2 bits. We denote this by 16-QAM->4. Figure 4.2 shows the signal space of 16-QAM and 16-QAM->4.

This method is motivated by the need to have a quick and simple rate adaptation scheme when a link in an ad hoc wireless network fluctuates for very brief periods. To avoid declaring a link broken and, hence, necessitating a search for a new route, the link may be maintained at some loss of quality until the channel recovers. Of course if it does not, rerouting will be necessary. The intent of our method is to sacrifice moderately the

quality of the signal for a brief period in order to avoid costly frequent rerouting. The advantage of the proposed method is that no feedback is needed; and the receiver alone makes the decision according to the channel status. It is also fairly simple at the receiver, while there is no need for buffer or complicated design at the transmitter. One drawback of the proposed scheme is that it can only reduce, rather than also increase, the rate. However, for the intended use, rate reduction is what is required. Of course, since some bits are transmitted and then dropped, resources are wasted; and the overall performance of the link may be inferior to the alternative methods. But again, this scheme is motivated by the need for an emergency rate reduction scheme.

The proposed method is not meant as a replacement for more sophisticated rate adaptation schemes, but is intended as a simple additional capability that maintains the current connection when a link undergoes a temporary fluctuation. As an example, consider an ad hoc wireless network, in which a link is utilized to transmit data based on specific, given MAC and routing protocols. When the channel of that link degrades, what are the choices? One choice is to terminate the link and to reroute the traffic through an alternative route in the network; this method involves considerable delay and overhead. Another choice is to adapt the rate at the transmitter; this method requires feedback, complex transmitter design, and poses the risk of buffer overflow and disruption of real-time delivery. Our proposed scheme is a third choice that maintains the use of the link for a short time without engaging the higher layer protocols or the transmitter. Another example is the case of broadcasting. The channels from the transmitter to the receiving nodes can vary significantly and independently at each receiver. In this case it is pointless to involve the transmitter, since rate adaptation may be

required only at a subset of the receiving nodes.

With our method, when the receiver detects few of the transmitted bits (by using fewer levels at the detector), it decreases the symbol error probability by not distinguishing the precise position of the transmitted point on the signal space. At the same time, the dropped bits take away some signal information and cause additional quantization noise. In terms of the mean square distortion metric (defined in Section II), there is a trade-off between the error probability and the detected data rate. This trade-off is identified and illustrated in this chapter. In fact, it is the main focus of the chapter. The question is precisely whether the overall distortion, with fewer bits but with smaller symbol error probability, exceeds or not that achieved with more bits but with larger symbol error probability.

For some signals arising in multimedia applications, not all bits have the same importance in terms of signal representation accuracy. There are several ways to take advantage of this variation by exploiting it and providing unequal error protection. In [32], a non-uniform phase-shift-key (PSK) modulation is studied that allows a receiver to receive additional information in the multicast transmission without requiring additional network resources. By using non-uniform constellations, the Euclidean distance in detecting more significant bits increases. In [33], both more powerful conventional error-correction coding and non-uniform constellation are used to achieve unequal error protection and hence ensure the successful reception of the significant bits when channels fluctuate. Such methods involve special design at the transmitter. In this chapter, we do not consider source coding or error control coding, although the latter, at a cost of increased complexity and delay, is likely to result in improved performance.

In our proposed rate adaptation scheme by dropping bits at the receiver, the choice of which bits to drop is important. We assume real time analog traffic. For a digitized analog signal, the modulation scheme has the capability to decide which bits to retain and which bits to drop. Since we assume no source or channel coding, we may arrange the signal points in the constellation in such a way as to provide a measure of unequal error protection and favor the more significant bits. We consider in Section III-V the uniformly spaced constellation as an illustration, and do not change the basic transmitter structure at all. The only change is the mapping. For example, in the 16-QAM->4 case, instead of using a Gray code, we place all 4 points with the same first 2 bits in the same quadrant, and use a Gray code for the last 2 bits in each quadrant. In Section VI, we consider a simple non-uniform constellation and find that our scheme works for a larger range of SNR values since the important bits are given additional preferential treatment.

In this chapter we consider two examples of the modulation schemes, PAM and QAM, and study the performance of the rate adaptation in terms of symbol error probability and mean square distortion, in both a Gaussian channel and a Rayleigh fading channel. We compare the performance of the original modulation scheme (8-PAM or 16-QAM) with the rate adaptation at the source by using fewer levels of modulation (4-PAM or 4-QAM), and with the rate adaptation we proposed by using fewer levels at the detector (8-PAM->4 or 16-QAM->4). The reason we confine ourselves to rather simple modulation examples is to illustrate our method in a simple way. A preliminary and incomplete treatment of these ideas without substantial evaluation was presented in [34].

The organization of this chapter is as follows. In Section 4.2, we introduce the model used in the study, and define the criteria of symbol error probability and mean square

distortion. In Section 4.3 and 4.4, we compare the performance in a Gaussian channel for PAM and QAM examples separately. The comparisons are performed for fixed energy consumption and fixed symbol rate. In Section 4.5, the performance in a Rayleigh fading channel is given. In Section 4.6, we study a non-uniform constellation case. Finally we summarize our work in Section 4.7.

4.2 Model and Analysis

We now describe in detail our model. Suppose there are K independent samples generated per second, from a random variable X with probability density function (pdf) $f(x)$. These samples need to be transmitted from the source to the receiver. Each sample is first quantized into one of M levels (C_0, \dots, C_{M-1}) before the modulation. We call the quantized value \tilde{X} . Then quantity \tilde{X} is mapped to one of the signal points in the constellation of the modulation scheme. The modulated signal is transmitted over a channel with additive white Gaussian noise (AWGN), and/or Rayleigh fading. After transmission, the signal is demodulated and detected at the receiver. The receiver has a detector of N levels (D_0, \dots, D_{N-1}). We call the recovered sample after the demodulation and detection as \hat{X} . Therefore, the bit rate transmitted is $K \log_2 M$ bits/second; and the bit rate received is $K \log_2 N$ bits/second (possibly $M \geq N$).

For the 8-PAM and 8-PAM->4 examples shown in Figure 4.1, 8-PAM is used when the SNR is large enough and the performance requirement is satisfied. If this is the case, the correct recovery when C_0 is transmitted is still C_0 . When SNR is small, 8-PAM does not satisfy the requirement, and if 8-PAM->4 satisfies the requirement, we switch to the

8-PAM->4 and only detect the first 2 bits. In this case, when C_0 or C_1 is transmitted, the correct recovery is D_0 . We study the performance of both 8-PAM and 8-PAM->4 to find out when we should make this switch. In the 8-PAM->4 scheme, there is one bit per symbol that is transmitted but then dropped; to assess the effect of the elimination of this bit, it is fair to compare the result with the one obtained if that bit was dropped at the transmitter. Therefore, we also include the 4-PAM scheme for the purpose of this comparison.

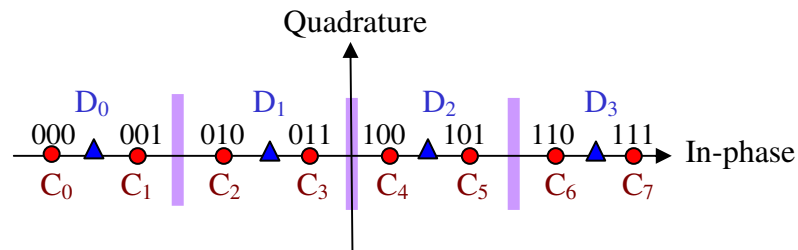


Figure 4.1: Signal space constellation of 8-PAM and 8-PAM->4.

For the 16-QAM->4 example shown in Figure 4.2, the first 2 bits are kept and the last 2 bits are dropped. In this case, when any one of the four points $C_0, C_1, C_2,$ and C_3 is transmitted, the correct recovery is D_0 . We study the performance of 16-QAM, 16-QAM->4, and 4-QAM scheme for the purpose of this comparison.

We define the correct recovery when C_i is transmitted as $g(C_i)$. If $N = M$, then $g(C_i) = C_i$. If $N < M$, $g(C_i)$ is a mapping from C_i to D_j . For the example of 8-PAM->4, we have $g(C_i) = D_{\lfloor i/2 \rfloor}$. For the example of 16-QAM->4, we have $g(C_i) = D_{\lfloor i/4 \rfloor}$. Here, the symbol $\lfloor x \rfloor$ denotes the maximum integer that is less than or equal to x .

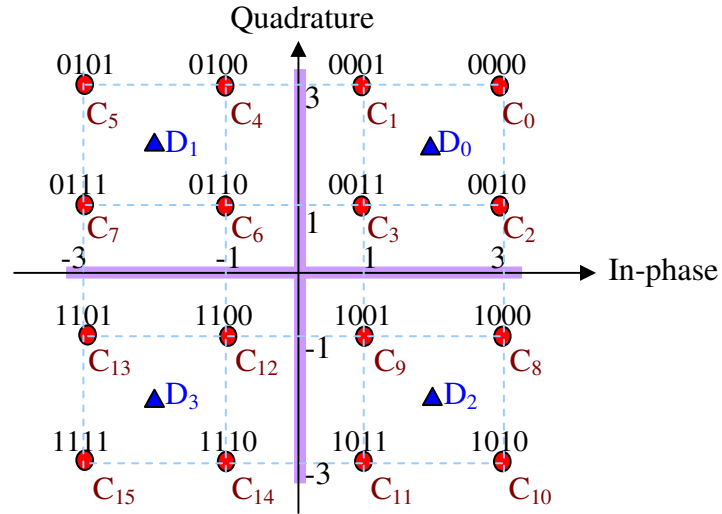


Figure 4.2: Signal space constellation of 16-QAM and 16-QAM->4.

In order to accurately compare the alternative modulation schemes, we need to define the criterion of overall performance. One criterion is simply the *Symbol Error Probability* (SEP), i.e., the probability of \hat{X} not being the correctly recovered symbol. If $N = M$, the SEP is the probability that $\hat{X} \neq \tilde{X}$. If $N < M$, the SEP is the probability that $\hat{X} \neq g(\tilde{X})$. For example, in 16-QAM->4, it is the probability that \hat{X} and \tilde{X} are in different quadrants. We focus here on the symbol error rate and not on the bit error rate, as the latter is less meaningful when bits are actually dropped. The drawback of this criterion is that it does not take into account the effect of the lost bits directly.

Consequently, it is more useful to consider a criterion that includes the effect of the dropped bits, namely the *Mean Square Distortion* (MSD), the mean value of the squared distortion between the original sample X , and the recovered sample \hat{X} . Although by reducing the number of bits transmitted or received we decrease the distortion caused by the detection error, the lost bits definitely induce additional quantization noise. The MSD is a combination of the quantization noise and the transmission error.

Define MSD from X to \hat{X} as

$$MSD = E\left\{\left(X - \hat{X}\right)^2\right\}. \quad (4.1)$$

Then, MSD of scheme $M \rightarrow N$ can be written as

$$MSD(M \rightarrow N) = E\left\{\int_{-\infty}^{\infty} f(x)\left(x - (\hat{X}|X=x)\right)^2 dx\right\} = \sum_{i=0}^{M-1} \int_{L_i}^{U_i} f(x) \left[\sum_{j=0}^{N-1} P(D_j|C_i)(x - D_j)^2 \right] dx.$$

That is,

$$MSD(M \rightarrow N) = \sum_{i=0}^{M-1} \sum_{j=0}^{N-1} P(D_j|C_i) \int_{L_i}^{U_i} f(x)(x - D_j)^2 dx. \quad (4.2)$$

Here $[L_i, U_i)$ and C_i , $i=0, \dots, M-1$, are the input ranges and their corresponding output levels of the quantizer; the quantity D_j is the output of the detector at the receiver side; and $P(D_j|C_i)$ is the probability of obtaining $\hat{X} = D_j$ given C_i is transmitted, which can be calculated from $P(C_k|C_i)$ as $P(D_j|C_i) = \sum_{\text{all } k \text{ s.t. } g(C_k)=D_j} P(C_k|C_i)$.

Assume C_i is chosen to be the centroid of the input range $[L_i, U_i)$ (as for example in the Lloyd-Max quantizer). Then we have $\int_{L_i}^{U_i} f(x)xdx = C_i P_i$. Here $P_i = \int_{L_i}^{U_i} f(x)dx$ is the probability that the sample X is in the range $[L_i, U_i)$. We also choose D_j to be the centroid of the corresponding region.

We can separate the distortion shown in (4.2) into two parts, one part with $D_j = g(C_i)$ (correct recovery), and the other part with $D_j \neq g(C_i)$ (detection error). Then we have

$$\begin{aligned} MSD(M \rightarrow N) &= \sum_{i=0}^{M-1} \left(1 - \sum_{\substack{j=0 \\ D_j \neq g(C_i)}}^{N-1} P(D_j|C_i) \right) \int_{L_i}^{U_i} f(x)(x - g(C_i))^2 dx + \sum_{i=0}^{M-1} \sum_{\substack{j=0 \\ D_j \neq g(C_i)}}^{N-1} P(D_j|C_i) \int_{L_i}^{U_i} f(x)(x - D_j)^2 dx, \\ &= \sum_{i=0}^{M-1} \int_{L_i}^{U_i} f(x)(x - g(C_i))^2 dx + \sum_{i=0}^{M-1} \sum_{\substack{j=0 \\ D_j \neq g(C_i)}}^{N-1} P(D_j|C_i) \int_{L_i}^{U_i} f(x) \left[(x - D_j)^2 - (x - g(C_i))^2 \right] dx. \end{aligned}$$

Therefore,

$$\begin{aligned}
MSD(M \rightarrow N) = & \left\{ E[X^2] + \sum_{i=0}^{M-1} P_i \cdot g(C_i)(g(C_i) - 2C_i) \right\} \\
& + \sum_{i=0}^{M-1} \sum_{\substack{j=0 \\ D_j \neq g(C_i)}}^{N-1} P_i \cdot P(D_j|C_i) \cdot (g(C_i) - D_j)(2C_i - D_j - g(C_i)). \quad (4.3)
\end{aligned}$$

The special case $M = N$ implies $g(C_i) = C_i$ and $D_j = C_j$. Then (4.3) becomes

$$MSD(M) = \left\{ E[X^2] - \sum_{i=0}^{M-1} P_i \cdot C_i^2 \right\} + \sum_{i=0}^{M-1} \sum_{\substack{j=0 \\ j \neq i}}^{M-1} P_i \cdot P(C_j|C_i) \cdot (C_i - C_j)^2. \quad (4.4)$$

In both (4.3) and (4.4), C_i and P_i are determined by the pdf of the random variable X and the quantizer used. For given noise, $P(C_j|C_i)$ is determined by the modulation scheme and the signal space constellation. The first terms of (4.3) and (4.4) are not related to the detection error; therefore they represent the quantization noise. The second terms are associated with SEP, and represent the distortion caused by the detection error.

In terms of the MSD of M -level modulation, there is a trade-off between the two terms. For larger M , the quantization noise is smaller, but the points in the signal space are more crowded (since we assume fixed average energy per symbol), and the SEP is larger, therefore the distortion caused by the detection error is larger. The total MSD depends on the modulation scheme, the signal, and the channel.

Comparing the $M \rightarrow N$ scheme and the M -level modulation scheme, there is also a trade-off between the quantization noise and the error probability. It is easy to verify that the quantization noise of $M \rightarrow N$ scheme is the same as that of an N -level quantizer with the same boundary and output levels $D_j, j=0, \dots, N-1$; therefore it is larger than that of the M -level modulation scheme. However, the SEP of the $M \rightarrow N$ scheme is smaller than that

of the M -level modulation scheme, which may cause smaller overall distortion. The exact MSD depends on the modulation scheme, the signal form, and the channel behavior.

Since we are considering only real time analog signals, we fix the symbol rate to K symbols/second, the rate at which the samples are generated. Then the bit rate depends on the modulation schemes. We also fix the average energy used to transmit a sample. Because the symbol rate is fixed, this is equivalent to fixing the average energy per symbol E_{av} .

4.3 PAM Example in a Gaussian Channel

In this section, we calculate and compare the SEP and MSD for the PAM example in a Gaussian channel. We assume the AWGN has power spectral density $N_0/2$. We consider two types of distribution for the source random variable X . One is uniform distribution $X \sim U[-\sqrt{3}, \sqrt{3}]$, and the other is Gaussian distribution $X \sim N(0,1)$. They all have $E[X] = 0$ and $E[X^2] = 1$ for the convenience of comparison.

4.3.1 Symbol Error Probability

In the $M \rightarrow N$ scheme, without distinguishing the detailed position of a transmitted point in the signal space, the probability of detection error decreases. So, we expect less SEP in the reduced-rate case compared to the original full-rate modulation scheme. However, by transmitting more bits than the detected bits, the signal points cannot be at their optimal position to minimize the error probability. Therefore the error probability will not be as small as in the case when the bits are dropped at the transmitter. This is the cost we have to pay for the simplicity of the scheme and the lack of feedback.

For M -ary PAM modulation, if X is uniformly distributed, we have $P_i = 1/M$; and the SEP, as a function of the average energy per symbol, is given [35] by

$$P(M - \text{PAM}) = 2(M - 1)/M \cdot Q\left(\sqrt{6/(M^2 - 1)} \cdot (E_{av}/N_0)\right). \quad (4.5)$$

The SEP of 8-PAM->4 can be easily obtained as

$$P(8 - \text{PAM} \rightarrow 4) = \frac{3}{4} \left\{ Q\left(\sqrt{(1/21)} \cdot (E_{av}/N_0)\right) + Q\left(3\sqrt{(1/21)} \cdot (E_{av}/N_0)\right) \right\} \quad (4.6)$$

The comparison of the SEP of 8-PAM, 8-PAM->4, and 4-PAM is shown in Figure 4.3. As expected, the SEP of 8-PAM->4 is less than that of 8-PAM, approximately half of the latter. Then we notice that the SEP of 8-PAM->4 is remarkably larger than that of 4-PAM. This is expected since the transmitted points of the 8-PAM->4 scheme in the signal space are closer to the detecting threshold than that of the 4-PAM scheme. For very small SNR, the SEP of 4-PAM and that of 8-PAM->4 are very close; they both approach 3/4.

The SEP for a Gaussian source is obtained through simulation, because it can not be expressed in a closed form. The result, shown in Figure 4.4, is almost the same as that for a uniform source.

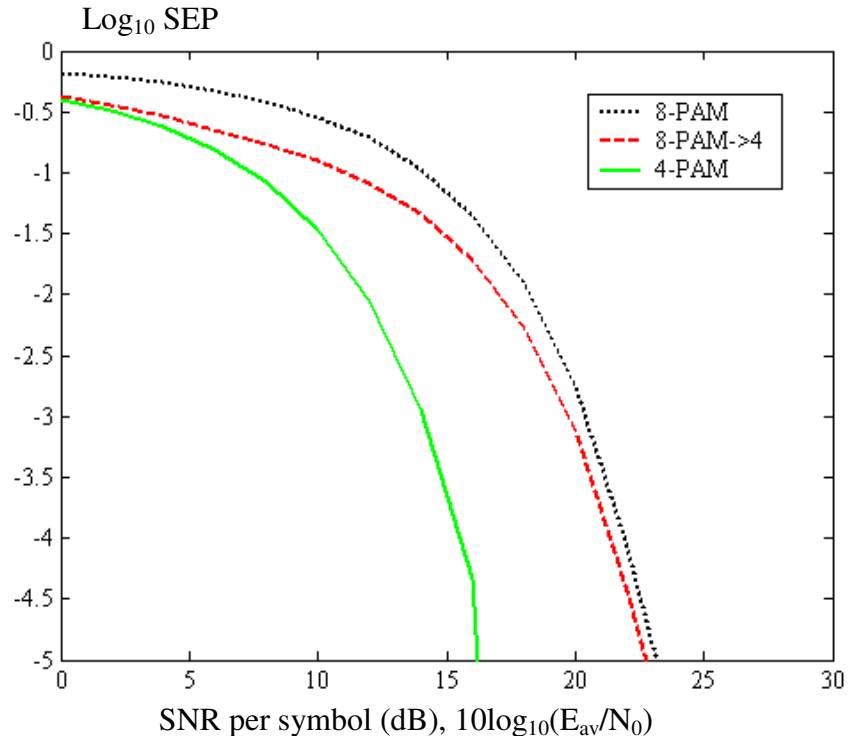


Figure 4.3: SEP of PAM example, for a uniform source, in a Gaussian channel.

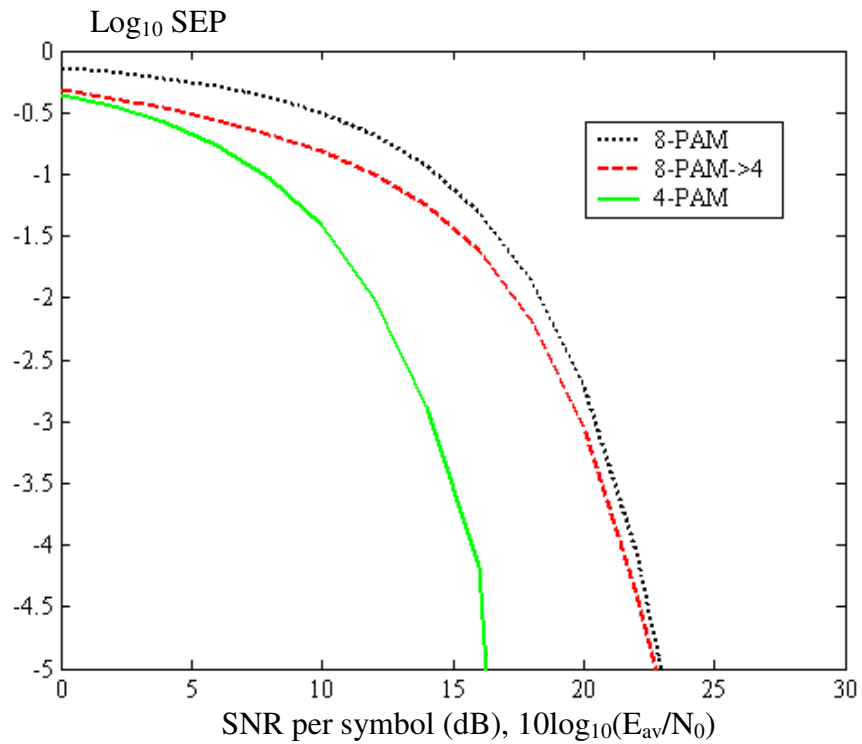


Figure 4.4: SEP of PAM example, for a Gaussian source, in a Gaussian channel.

4.3.2 Mean Square Distortion

We first assume a uniform source $X \sim U[-\sqrt{3}, \sqrt{3}]$. Then the uniform quantizer is the optimum quantizer among all quantizers with M levels. Using $C_i = (i - (M - 1)/2)2\sqrt{3}/M$ and $P_i = 1/M$, after some algebra, we obtain for general M (see Appendix K for details)

$$MSD(M - \text{PAM}) = M^{-2} + (24/M^3) \sum_{i=0}^{M-1} (M - i)(2i - 1)Q((2i - 1)z_M). \quad (4.7)$$

Here we let $z_M = \sqrt{6/(M^2 - 1) \cdot (E_{av}/N_0)}$ to simplify the error probability expression.

For strong signal ($SNR \gg 0$ dB), we have $Q((2i - 1)z_M) \rightarrow 0$, and, hence, only the quantization noise is left in the MSD expression, which is M^{-2} .

For very weak signal ($SNR \ll 0$ dB), we have $Q((2i - 1)z_M) \rightarrow 1/2$, and MSD approaches $[1 + 2(M - 1)(2M - 1)]/M^2$. Now, the quantization noise is almost negligible compared to the distortion caused by transmission error. For very large M , we can see clearly that the MSD approaches the value of 4. The explanation is as follows. As $SNR \ll 0$ dB, the signal is dominated by the noise; therefore the detection result is either $M-1$ or 0 with equal probability. When M is large, $C_{M-1} \rightarrow \sqrt{3}$, and $C_0 \rightarrow -\sqrt{3}$. The distortion is then given by

$$MSD(M - \text{PAM}) \xrightarrow{SNR \rightarrow -\infty, M \rightarrow \infty} \int_{-\sqrt{3}}^{\sqrt{3}} (2\sqrt{3})^{-1} \left[\frac{1}{2}(x - \sqrt{3})^2 + \frac{1}{2}(x + \sqrt{3})^2 \right] dx = 4.$$

Notice that the variance of the random variable X is only 1, but the MSD for $SNR \ll 0$ dB is much larger than 1. Therefore the transmission for very low SNR is not meaningful any more.

For 8-PAM $\rightarrow 4$, we recall (4.3), and we use $D_j = (2j - 3)\sqrt{3}/4$ and

$C_i = (i - 3.5)\sqrt{3}/4$, then obtain the numerical form of the MSD as

$$MSD(8 - \text{PAM} \rightarrow 4) = (1/16) + (3/128)\{12Q(z_{z_8}) + 36Q(3z_{z_8}) + 40Q(5z_{z_8}) + 56Q(7z_{z_8}) + 36Q(9z_{z_8}) + 44Q(11z_{z_8})\} \quad (4.8)$$

The comparison of the MSD of 8-PAM, 8-PAM->4, and 4-PAM is shown in Figure 4.5. First we notice that if $\text{SNR} < \sim -6$ dB, the distortion of the PAM transmission is larger than the variance of the random variable. Then we notice that the distortion of 8-PAM->4 is smaller than 8-PAM when $\text{SNR} < \sim 0$ dB, and larger in other regions of SNR values. This is the trade-off between the detection error and the quantization noise for different SNR values. There is not enough of a range of SNR values for which the switch from 8-PAM to 8-PAM->4 is meaningful for this example.

Comparing 8-PAM and 4-PAM, we notice that for not too small values of SNR, the larger the value of M , the smaller the distortion. And for other SNR values (< -3 dB), the order is reversed. Hence, when a strong signal is available, using larger M gives us better performance in terms of MSD. When the signal is very weak, smaller M gives smaller distortion. This behavior is another facet of the trade-off between the detection error and the quantization noise.

Comparing the distortion of 8-PAM->4 with that of 4-PAM, one might intuitively guess that 4-PAM should be better than 8-PAM->4, because by dropping one bit at the beginning, it is less likely to have detection error. This is true for the SEP, but not necessarily for the MSD. In this example, the MSD of 8-PAM->4 is slightly smaller than 4-PAM when $\text{SNR} < \sim 7$ dB, and larger in other regions of SNR values. Let us think through this more carefully. Since the quantization noise part is the same for both schemes, we only need to compare the distortion caused by the detection error. We can focus on the most likely detection error, i.e., the one that causes erroneous reception of a

symbol adjacent to the transmitted one (or adjacent range for the $M \rightarrow N$ scheme). Both 8-PAM- \rightarrow 4 and 4-PAM have 6 possible adjacent detection errors. But for a particular pair of adjacent symbol error, 8-PAM- \rightarrow 4 has larger error probability due to the fact that $Q(z_4) < Q(z_8)$; and the distortion of 8-PAM- \rightarrow 4, which is equal to $(g(C_i) - D_k)(2C_i - D_k - g(C_i))$, is half of that of 4-PAM, which is given by $(C_i - C_j)^2$, because the transmitted points are closer to the detected points. These effects are another trade-off for the MSD. Since the MSD is the mean value of all possible squared distortions, it is not a priori clear which scheme wins without exact numerical calculation.

Now we analyze again the distortion of the three schemes assuming a Gaussian random variable $X \sim N(0,1)$. The Lloyd-Max quantizer is used because it is the optimum quantizer for a Gaussian signal. We use a MATLAB file to calculate the quantization output levels, their input ranges, and the coefficients in the MSD expression. We omit the detailed calculation and only give the results in Figure 4.6.

Notice that if $\text{SNR} \sim -3$ dB, the distortion of PAM transmission is larger than the variance of the random variable. This time the distortion of 8-PAM- \rightarrow 4 is almost always larger than that of 4-PAM. We again observe the trade-off between the detection error and the quantization noise in the comparison of 8-PAM- \rightarrow 4 and 8-PAM. The distortion of 8-PAM- \rightarrow 4 is smaller than that of 8-PAM when $\text{SNR} \sim -4$ dB, and larger in other regions of the SNR. This means that we can switch to 8-PAM- \rightarrow 4 and get better performance when $\text{SNR} \sim -4$ dB.

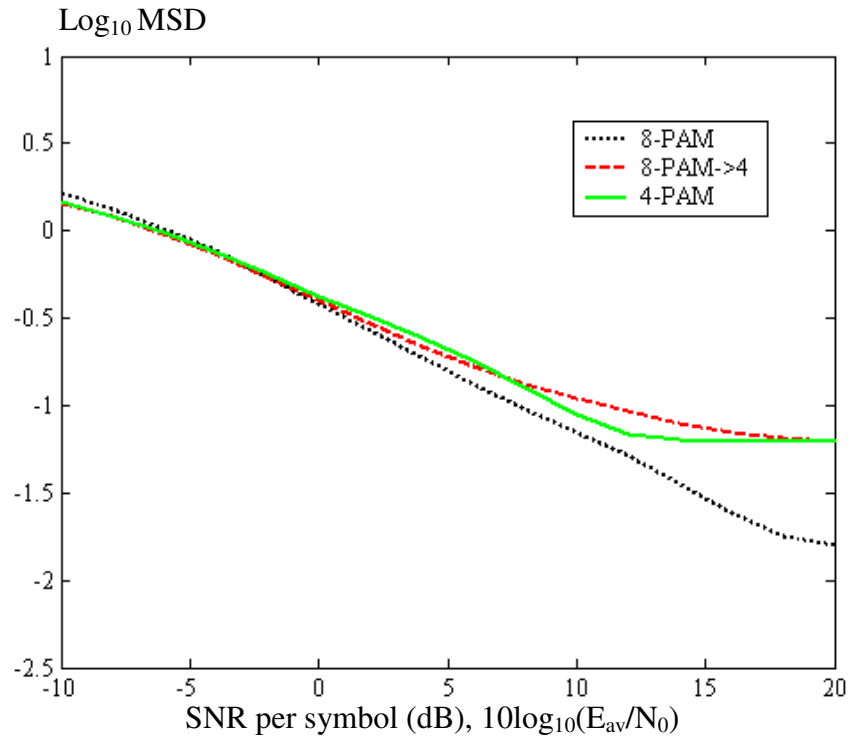


Figure 4.5: MSD of PAM example, for a uniform source, in a Gaussian channel.

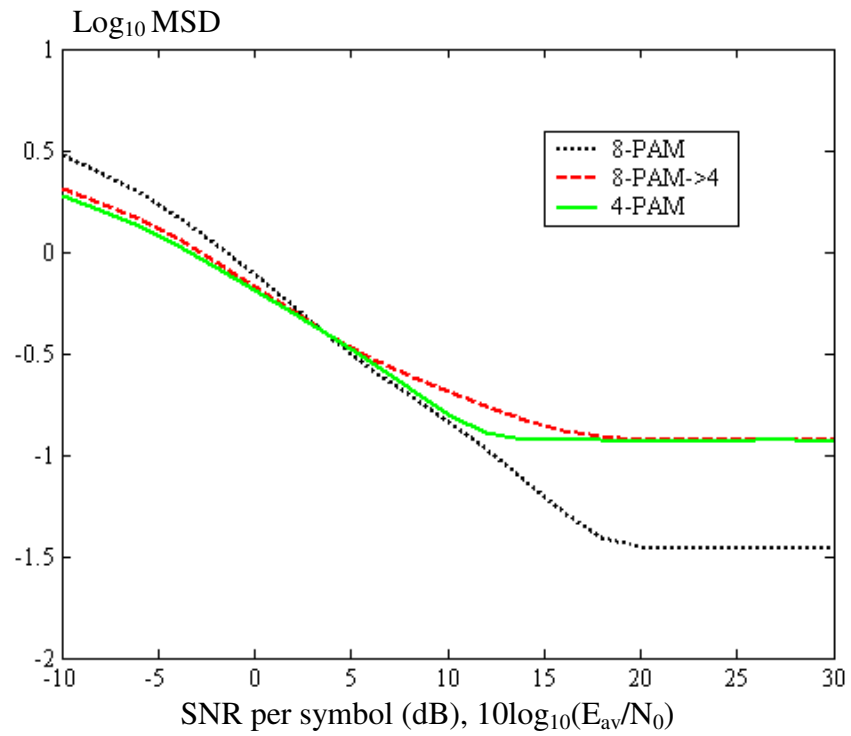


Figure 4.6: MSD of PAM example, for a Gaussian source, in a Gaussian channel.

4.4 QAM Example in a Gaussian Channel

In this section, we calculate and compare the SEP and MSD for the QAM method in a Gaussian channel.

4.4.1 Symbol Error Probability

Since the in-phase and quadrature components of the QAM signals can be perfectly separated at the demodulator for $M = 2^{2k}$, the probability of the symbol error for the M -QAM modulation scheme is easily determined from the formula of the \sqrt{M} -PAM modulation scheme with half the average energy per symbol [35]. That is,

$$P(M - \text{QAM}) = 1 - \left(1 - P(\sqrt{M} - \text{PAM})\right)^2. \quad (4.9)$$

For a uniform source X , using (4.5), we have

$$P(M - \text{QAM}) = 1 - \left(1 - (1 - M^{-1/2})2Q\left(\sqrt{3E_{av}/((M-1)N_0)}\right)\right)^2. \quad (4.10)$$

For 16-QAM->4, the in-phase and quadrature components of the signals can also be perfectly separated at the demodulator. Define P_x as the probability that the in-phase component of the detected symbol is in error; then,

$$P(16 - \text{QAM} \rightarrow 4) = 1 - (1 - P_x)^2 = 1 - \left(1 - \frac{1}{2}Q\left(\sqrt{E_{av}/5N_0}\right) - \frac{1}{2}Q\left(3\sqrt{E_{av}/5N_0}\right)\right)^2. \quad (4.11)$$

For $E_{av}/N_0 \gg 1$, we have $Q\left(\sqrt{E_{av}/5N_0}\right) \gg Q\left(3\sqrt{E_{av}/5N_0}\right)$. Therefore we have

$$P(16 - \text{QAM} \rightarrow 4) \approx \frac{1}{3}P(16 - \text{QAM}). \quad (4.12)$$

The comparison of the SEP of 16-QAM, 16-QAM->4, and 4-QAM is shown in Figure 4.7. The SEP of 16-QAM->4 is less than that of 16-QAM. For large SNR, the SEP of 16-QAM->4 is approximately 1/3 of that of 16-QAM. Another observation is that the

16-QAM->4 has significantly larger SEP than the 4-QAM. For very small SNR, the SEP of 16-QAM->4 and 4-QAM are very close, both approaching 3/4.

Again, same as for the PAM example, the SEP for a Gaussian X is also obtained from simulation, and is almost same as that of a uniform X . We omit the detailed result here.

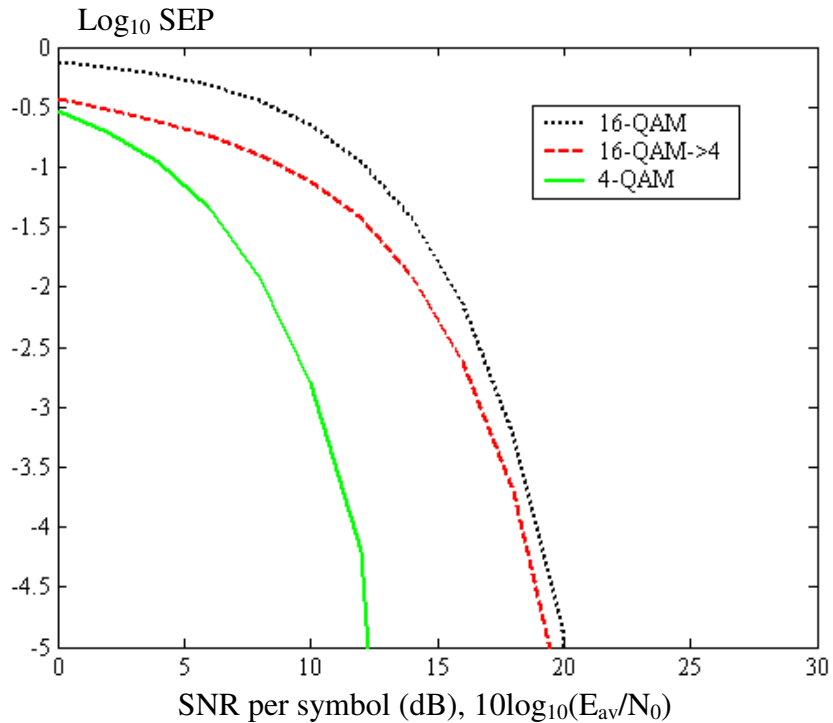


Figure 4.7: SEP of QAM example, for a uniform source, in a Gaussian channel.

4.4.2 Mean Square Distortion

We assume that a Gray code is used for 4-QAM. Gray code is also the one that minimizes the MSD for 4-QAM modulation. We use a 4×4 rectangular constellation for 16-QAM. Since we intend to use it as 16-QAM->4 when the channel is poor, we want the symbols with the same first two bits to be located in the same quadrant. Thus we can recover the first 2 bits of the signal with smaller SEP and can know the approximate range of the transmitted signal. Define the 4×4 signal space matrix as shown in Figure

4.2. This is the optimal rectangular constellation that minimizes MSD among all the matrices that locate the symbols with the same first two bits in the same quadrant. This constellation is not the optimal one among all rectangular constellations, but its distortion is only slightly worse than the optimum. Notice that this is not the Gray code.

For a uniform signal, the uniform quantizer is the optimum quantizer, and a MATLAB file was written to calculate the MSD. For a Gaussian signal, the optimum quantizer is the Lloyd-Max quantizer. MATLAB files were written to calculate the quantization output levels and their input ranges, and to calculate the numerical results of MSD. We obtain results for both a uniform signal and a Gaussian signal, shown in Figure 4.8 and 4.9. At the range of low SNR values, the difference between the MSD of 16-QAM and 16-QAM- \rightarrow 4 for a uniform signal is smaller than that for a Gaussian signal. This is very similar to the PAM example shown in Figure 4.5 and 4.6.

The comparison for a Gaussian signal is shown in Figure 4.9. In this case, if $\text{SNR} < \sim 0.3$ dB, the distortion of QAM transmission is larger than the variance of the random variable. We notice that, the MSD of 16-QAM- \rightarrow 4 is always larger than that of 4-QAM in this example. Also, the MSD of 16-QAM- \rightarrow 4 is smaller than 16-QAM for $\text{SNR} < \sim 3$ dB, and larger in other regions of SNR values. This means there is not enough of a range of SNR values in which the switch from 16-QAM to 16-QAM- \rightarrow 4 is very meaningful.

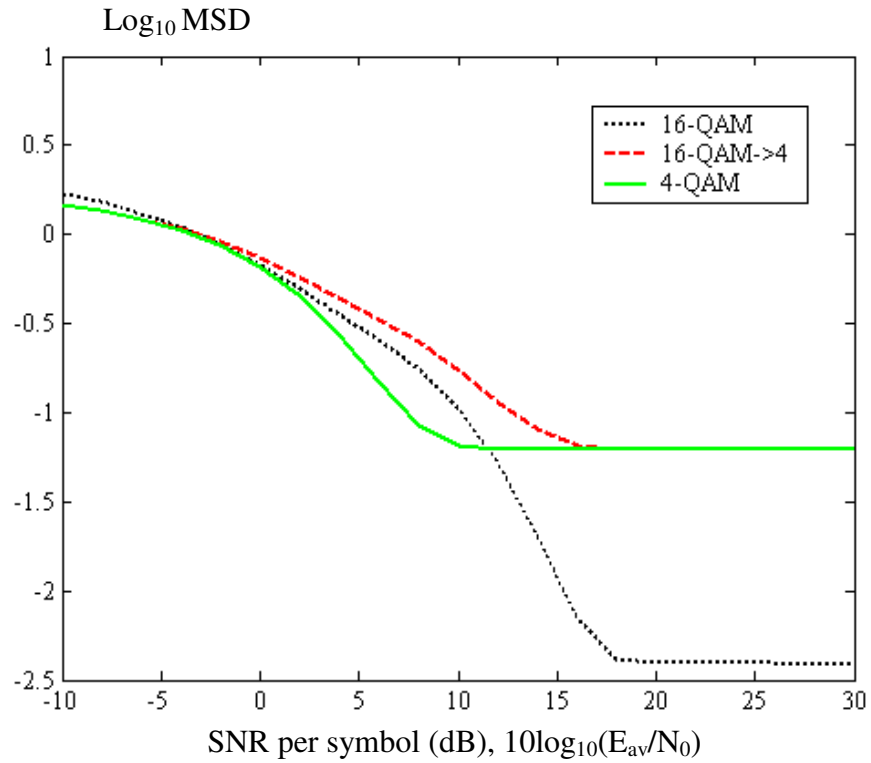


Figure 4.8: MSD of QAM example, for a uniform source, in a Gaussian channel.

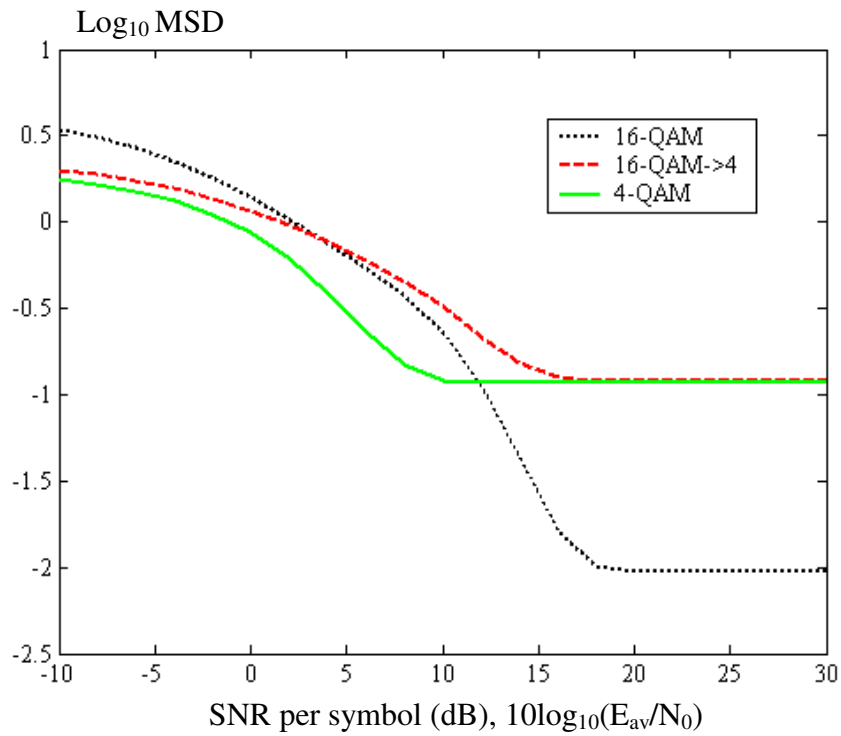


Figure 4.9: MSD of QAM example, for a Gaussian source, in a Gaussian channel.

4.5 Rayleigh Fading Channel

In order to study the effect of fading on the system performance, we assume a frequency-nonselective, slow fading channel, where the attenuation α has Rayleigh distribution and the phase shift φ has uniform distribution. Modulation schemes PAM and QAM are not suitable for a fading channel, unless the amplitude attenuation can be compensated, since the detection depends on the amplitude of the received signal. We assume that the channel fades sufficiently slowly, so that perfect measurement and compensation of both attenuation and phase shift are possible at the receiver. The AWGN with power spectral density $N_0/2$ is added on top of the fading.

For a fixed attenuation α , the SEP of both PAM and QAM examples for a uniform source are derived in the previous sections; and they can be used by replacing E_{av}/N_0 with $\gamma_s = \alpha^2 E_{av}/N_0$ in (4.5), (4.6), (4.10), and (4.11). To obtain the error probability of M -PAM when α is random, we must average $P(M - \text{PAM}|\gamma_s)$ over the pdf of γ_s . The pdf of α with parameter $\Omega = E[\alpha^2]$ is given by

$$f(\alpha) = (2\alpha/\Omega) \cdot e^{-\alpha^2/\Omega} . \quad (4.13)$$

Then the pdf of γ_s is exponential with parameter $\bar{\gamma}_s = \Omega E_{av}/N_0$,

$$f(\gamma_s) = (1/\bar{\gamma}_s) \cdot e^{-\gamma_s/\bar{\gamma}_s} . \quad (4.14)$$

For the PAM example, the integral can be computed, and we obtain

$$P(M - \text{PAM}) = (M - 1)/M \cdot \left(1 - \sqrt{3\bar{\gamma}_s / (3\bar{\gamma}_s + (M^2 - 1))}\right), \quad (4.15)$$

$$P(8 - \text{PAM} \rightarrow 4) = \frac{3}{8} \left\{ 2 - \sqrt{\bar{\gamma}_s / (\bar{\gamma}_s + 21)} - \sqrt{3\bar{\gamma}_s / (3\bar{\gamma}_s + 7)} \right\} \quad (4.16)$$

The integral for the QAM example does not have a closed-form expression. In [36]

and [37], the SEP of 16-QAM in a fading channel is studied and numerical results are given. What we show here are results from our simulation. Figures 4.10 and 4.11 show the comparison of a Rayleigh fading channel with $\Omega=1$ and a Gaussian channel.

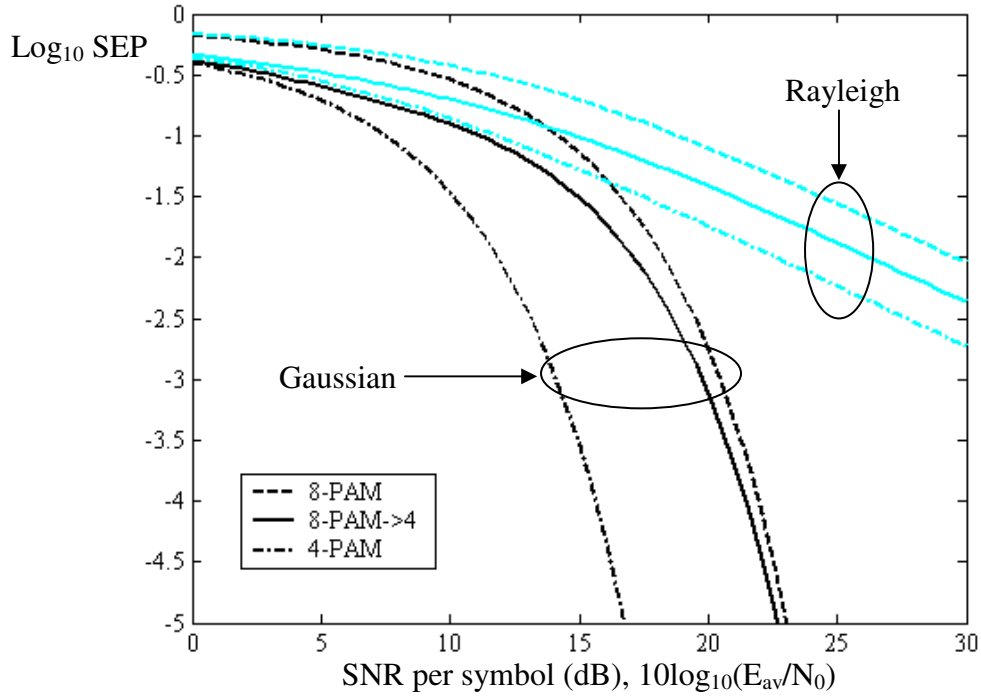


Figure 4.10: SEP of PAM example, for a uniform source, in a Gaussian channel and a Rayleigh fading channel with $\Omega=1$.

In a Rayleigh fading channel, the SEP of any modulation scheme is worse than that of the same scheme in an equivalent Gaussian channel. At high SNR, SEP in a Gaussian channel decreases exponentially, while in a fading channel it only decreases linearly. Also, the comparison of the three schemes in a Rayleigh fading channel is very different. In a Gaussian channel the rate reduction at the receiver diminishes the SEP only slightly (to about 1/2 for PAM and 1/3 for QAM). However, the rate reduction at the transmitter significantly diminishes the error probability. By contrast, in a Rayleigh fading channel, although the rate reduction at the transmitter still has the advantage over the rate

reduction at the receiver, that advantage is NOT as significant as in a Gaussian channel.

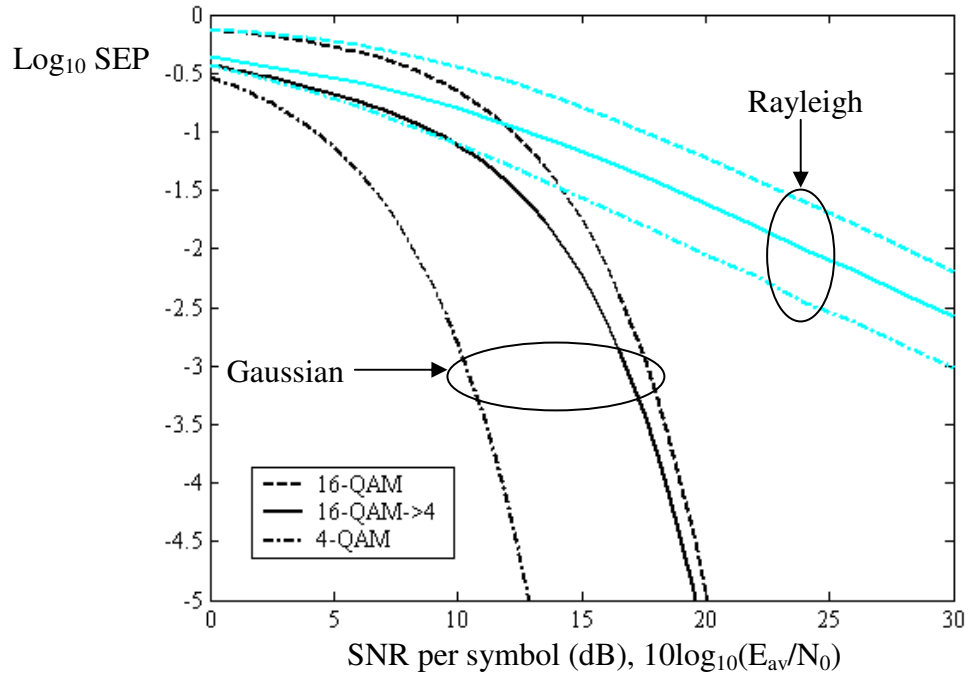


Figure 4.11: SEP of QAM example for a uniform source, in a Gaussian channel and a Rayleigh fading channel with $\Omega=1$.

The MSD is obtained from a simulation program written in C. Figures 4.12 and 4.13 show the MSD of PAM and QAM for a Gaussian source in a Rayleigh fading channel with $\Omega=1$, as well as the results in a Gaussian Channel. The MSD of any scheme in a Rayleigh fading channel is worse than that of the same scheme in a Gaussian channel. In a Rayleigh fading channel, the rate reduction at the transmitter only has slight advantage over the rate reduction at the receiver. Also we notice that in a Rayleigh fading channel, there is a larger range of SNR values where the switch to our scheme is meaningful. For example in the PAM case, our scheme achieves smaller MSD for $\text{SNR} < \sim 10\text{dB}$ in a Rayleigh channel, while only for $\text{SNR} < \sim 3\text{dB}$ in a Gaussian channel.

From both the SEP and MSD comparisons, we conclude that our scheme is more suitable for use in fading channel environments.

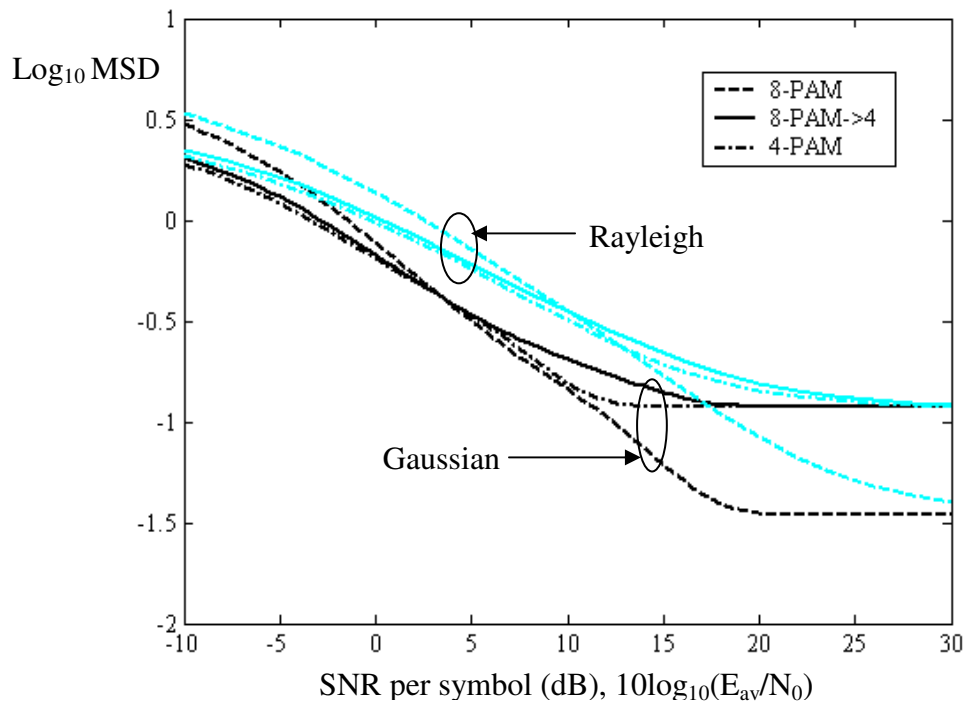


Figure 4.12: MSD of PAM example, for a Gaussian source, in a Gaussian channel and a Rayleigh fading channel with $\Omega=1$.

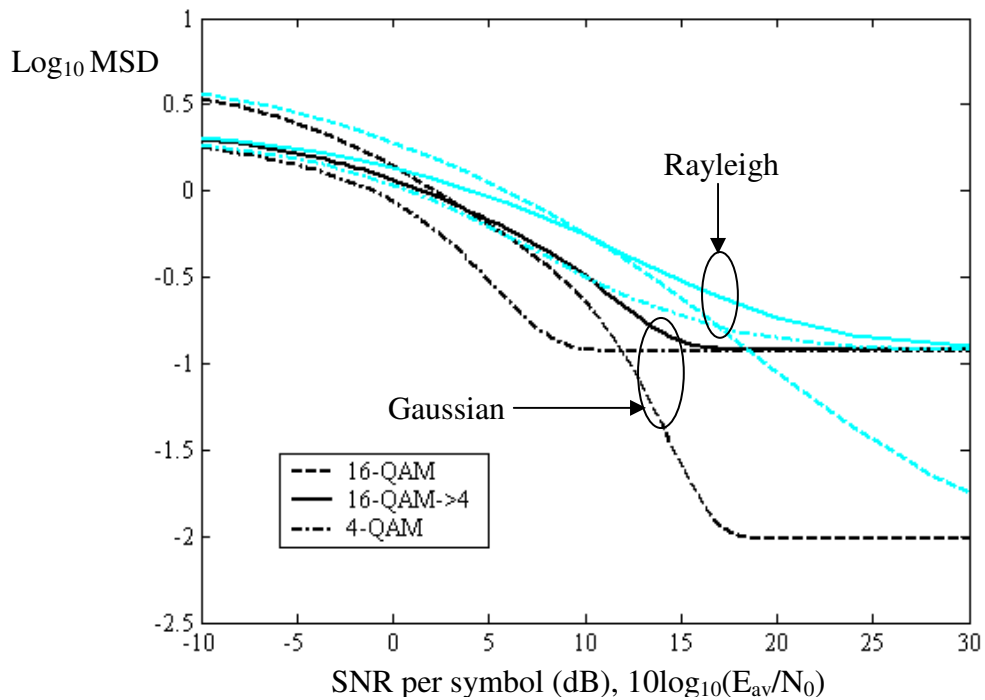


Figure 4.13: MSD of QAM example, for a Gaussian source, in a Gaussian channel

and a Rayleigh fading channel with $\Omega=1$.

4.6 Non-uniform Constellation

In our scheme of rate reduction, the choice of bits to be dropped is important. So far, for the case of uniform constellation, we do not offer any special treatment to the important bits, except that we map the more important bits to a certain subset of the constellation. In this section, we study a simple example of non-uniform constellation. This example is a non-uniform 4-QAM shown in Figure 4.14. It is also the non-uniform 4-PSK studied in [32]. The angle θ indicates the level of the non-uniformity. When $\theta=\pi/4$, the scheme reduces to the uniform 4-QAM. We only need to consider $\theta\leq\pi/4$ because of symmetry.

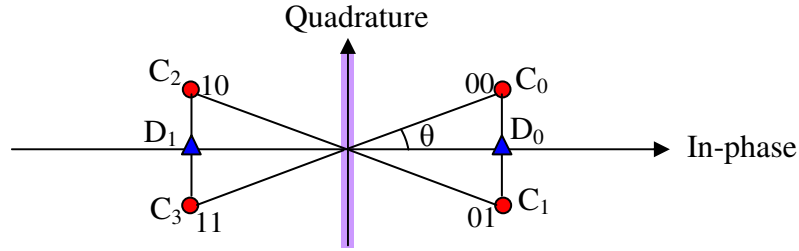


Figure 4.14: Signal space constellation of non-uniform 4-QAM and 4-QAM->2.

The SEP for a uniform source in a Gaussian channel is given by

$$P(4\text{-QAM}, \theta) = Q\left(\sqrt{2} \sin \theta \sqrt{E_{av}/N_0}\right) + Q\left(\sqrt{2} \cos \theta \sqrt{E_{av}/N_0}\right) - Q\left(\sqrt{2} \sin \theta \sqrt{E_{av}/N_0}\right) \cdot Q\left(\sqrt{2} \cos \theta \sqrt{E_{av}/N_0}\right) \quad (4.17)$$

$$P(4\text{-QAM} \rightarrow 2, \theta) = Q\left(\sqrt{2} \cos \theta \sqrt{E_{av}/N_0}\right) \quad (4.18)$$

The comparison of SEP is shown in Figure 4.15 for two values of θ , namely $\pi/4$ (uniform) and $\pi/16$ (non-uniform). Because of the implied extra protection for the first bit and the reduced protection for the second bit, the SEP of 4-QAM increases significantly

as θ decreases, while the SEP for 4-QAM->2 decreases as θ decreases. This results in remarkable gain for 4-QAM->2 over 4-QAM in terms of SEP.

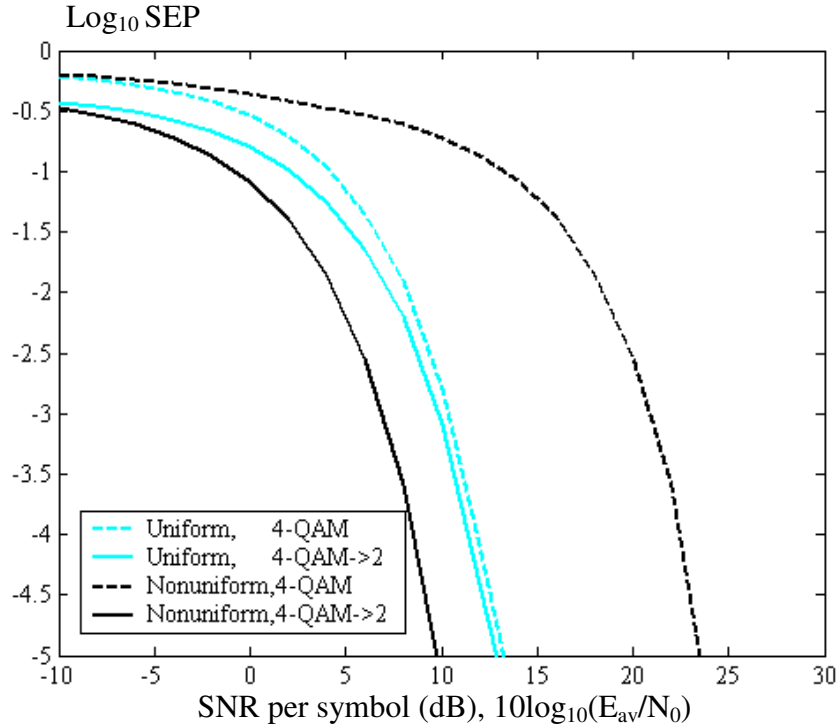


Figure 4.15: SEP of uniform and non-uniform 4-QAM and 4-QAM->2, for a uniform source in a Gaussian channel.

We simulated the MSD for a Gaussian source in a Gaussian channel for two values of θ , $\pi/4$ (uniform) and $\pi/16$ (non-uniform). The results are shown in Figure 4.16. We find that as θ decreases, the MSD of 4-QAM->2 decreases for any SNR value, and the MSD of 4-QAM increases for the region $\text{SNR} > \sim 0\text{dB}$. This results in a larger range of SNR values in which 4-QAM->2 has smaller MSD than 4-QAM. For $\theta = \pi/16$, this range is $\text{SNR} < \sim 9\text{dB}$, comparing to $\text{SNR} < \sim 3\text{dB}$ for $\theta = \pi/4$. We also notice that at $\theta = \pi/16$, for $\text{SNR} < \sim 5\text{dB}$, the scheme 4-QAM->2 has the smallest MSD among all four schemes considered.

Our scheme outperforms the original scheme without rate adaptation over a larger

range of SNR values in the non-uniform constellation case. But the cost we incur is the complexity associated with the transmitter design, and the worse performance of the original 4-QAM scheme at medium values of SNR.

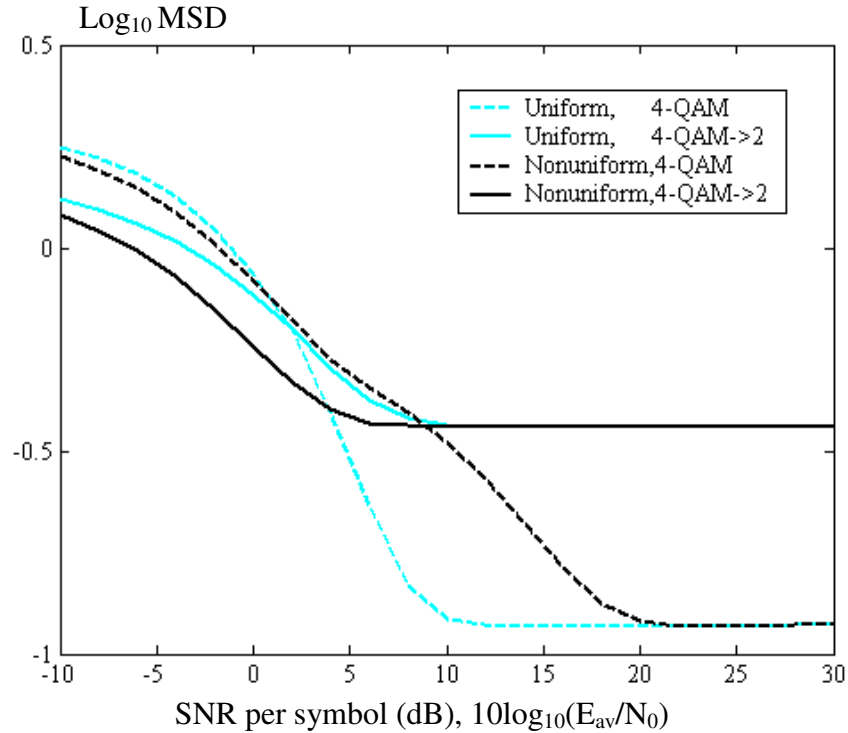


Figure 4.16: MSD of uniform and non-uniform 4-QAM and 4-QAM->2, for a Gaussian source in a Gaussian channel.

4.7 Summary and Conclusions

From the examples of PAM and QAM that we have considered, we notice that the performance depends significantly on the distribution of the signal, on the modulation scheme, and on the channel behavior. In a Gaussian channel, the rate reduction scheme at the transmitter reduces the SEP significantly, while the rate reduction scheme at the receiver reduces SEP only slightly. In terms of MSD, our scheme achieves smaller MSD for a certain region of SNR values when compared to the original scheme without rate

adaptation. However, the rate reduction scheme at the transmitter has significant advantage over our rate reduction scheme which only operates at the receiver. In a Rayleigh fading channel, the rate reduction scheme at the transmitter still has advantage over the rate reduction scheme at the receiver, but that advantage is NOT significant anymore. Our scheme achieves smaller MSD for a much larger region of SNR values. Therefore, our scheme is more suitable for use in a fading channel rather than in a Gaussian channel. The study of an example with non-uniform constellation verifies that our scheme has a larger applicable region of SNR values if the important bits are given additional protection.

The trade-off between compression and detection is identified and illustrated in this chapter. More elaborate quantization and/or modulation schemes will lead to similar, and perhaps more meaningful, trade-offs. Also, the incorporation of error control coding will alter the identified trade-offs in possibly significant ways.

Nevertheless, we believe that the proposed rate control technique represents a practical choice that can augment the arsenal of tools for the quality control of wireless communications. The simplicity of our method makes it especially attractive for the wireless links in an ad hoc wireless network, where link failures can be “softened” without rerouting and other drastic measures.

Chapter 5 Joint Scheduling, Power Control, and Routing

Algorithm for Ad-Hoc Wireless Networks

5.1 Introduction

An ad-hoc wireless network is a collection of wireless mobile hosts forming a temporary network. Connections of mobile hosts are via multihop wireless connection without the support from a fixed infrastructure (“Base Station”). Its classical applications are battlefield communications, disaster recovery, search and rescue, and so on. Due to the mobility of nodes, the status of a communication link is a function of the location and transmission power of the source and destination nodes, and the channel interference from other links.

The traditional layered structure of networks simplifies the design and implementation, and allows end systems manufactured by different vendors to share the information seamlessly. Recently, more and more people realize that in wireless networking there is strong coupling among the traditional layers of the OSI (open systems interconnection) architecture and that these interactions can not be ignored. These couplings are most obvious in the ad hoc networks. Cross-layer design is able to improve the network performance [38,39,40].

One example of the coupling is between the routing in the network layer and the access control in the MAC (medium access control) sublayer. The selection of routes clearly affects the flows and, hence, the requirement of bandwidth allocation at each wireless link. On the other hand, the choice of bandwidth allocation and access control affects the accumulation of queuing at links, and therefore changes the distance of each link and the route selection. Many works on routing in such networks (see, e.g., [41,42]) assume a fixed underlying protocol for access control, and most of the researches on multiple access assume fixed routes and flow requirements [43]. In the past several years, the problem of coupling routing with access control in ad-hoc wireless networks has been addressed [44,45,46].

In TDMA-based structure, the bandwidth is partitioned by nodes (or links) in terms of time slots; and the access control is achieved by scheduling time slots for links to activate. If the system has multiple flow types of traffic in the network, (each flow type can be thought of as a distinct application with its own QoS requirement,) then in each link, different flow types also share the bandwidth in terms of time slots. Another example of the coupling between layers is the coupling of power control in the physical layer and the scheduling in the MAC layer. The power assignment of links changes the link status, and the topology of the network, and hence the scheduling result. On the other hand, the scheduling decides the link activation and the interference generated, and therefore changes the power required at each link to achieve the QoS. Joint scheduling and power control algorithm are studied in [47,48].

In this chapter, we assume a TDMA-based wireless ad-hoc network, where each node has one receiver and one transmitter. All nodes share the bandwidth by occupying

different time slots. In the scheduling, links are assigned slots depending on their link metrics. Our algorithm gives priority to the links which have large queue and blocks less traffic from neighboring links. We study both algorithms with joint power control and without joint power control, and conclude that with joint power control, the network achieves significantly larger throughput and less delay in the cost of calculation complexity, and slightly higher energy consumption. We also compare our algorithm with the one based on [48], and conclude that our algorithm achieves better throughput and delay with less complexity, with the cost of slightly higher energy consumption.

In the route selection, the least energy route could be selected at the beginning of the network operation to save energy. But for some unbalanced topology, bandwidth requirements can not be satisfied by scheduling only, rerouting is needed periodically to lead some packets to go through alternative route and release the congestion. Routes are then selected periodically according to both the energy consumption and the traffic accumulation. The simulation results show that there is a trade-off between the energy consumption and the network performance. There is an optimal weight factor of energy consumption and queue accumulation in the routing distance such that the performance is best. The optimal point depends on the specific topology of the network.

The organization of this chapter is as follows. The network model is given in Section 5.2. We introduce our joint scheduling and power control algorithm in Section 5.3. The centralized algorithm and simulation results are also given. In Section 5.4, we discuss our joint scheduling and routing algorithm with simulation results. The distributed implementation is discussed in Section 5.5. Finally, the future work and extension of the research is discussed in Section 5.6, and conclusions are given in Section 5.7.

5.2 Network Model

For a wireless ad-hoc network, there is no support from a fixed infrastructure, and the network is connected by wireless channels. In TDMA-based structure, all nodes share the same frequency band, and time is slotted. We assume there is a good global time known to all users. We assume same waveform for all users and there is no multiuser detection available. A separate low data rate channel is used for network control, exchange of various information, scheduling, and routing. Power decay law is assumed to be inversely proportional to the γ -th order of the distance between the transmitter and the receiver. That is, the attenuation factor from node i to node j is given by

$$G_{ij} = (R_{ij}/R_0)^{-\gamma}. \quad (5.1)$$

Here R_{ij} is the distance between node i and j , and R_0 is a normalization constant.

Each node is supported by one omni-directional antenna; and has one receiver and one transmitter, which cannot work simultaneously. Due to the property of the receiver and the transmitter, a node cannot transmit and receive at the same time; it can not receive from more than one node at the same time; and cannot transmit to more than one node at the same time either. We assign time slots to directed links, for example, link (i,j) . Each link has two possible statuses, active or idle; and each node has three possible modes: transmission mode, receiving mode, and idle mode.

Node i can adjust the power of transmission P_i within the range $0 < P_i \leq P_{\max} < \infty$; here P_{\max} is the maximal available power. We assume each successful transmission has to satisfy SIR (Signal-to-interference and noise-ratio) requirement β , then the maximal transmission distance can be defined as:

$$R_{\max} = \left(P_{\max} / (\beta \sigma^2) \right)^{\frac{1}{\gamma}} \cdot R_0, \quad (5.2)$$

with σ^2 the power spectral density of the noise.

We assume that each node generates data packets of fixed length to all other nodes, according to Poisson distribution. Each packet needs a slot to transmit. The number of nodes is N . We assume that the rates from node i to each of the $(N-1)$ destinations are the same, and equal to λ_e packets per second. After routing, local rate of traffic from node i to j is $\Lambda_i(j) = \sum_{(m,n)} \lambda_e$. Here (m,n) are source destination pairs whose route include link (i,j) .

5.3 Jointly Scheduling and Power Control

We assign time slots to directed links according to their priority defined by their link metric.

5.3.1 Scheduling Metric

The definition of metric is as follows:

$$L(i, j) = a \cdot \frac{1}{1 + Q_{ij}} + b \cdot \frac{\sum_{\text{Links blocked by } (i,j)} Q_{kl}}{1 + \sum_{\text{Links blocked by } (i,j)} Q_{kl}}. \quad (5.3)$$

a and b : Weight factors between 0 and 1, $a + b = 1$.

Q_{ij} : Queue size of link (i,j) at node i .

Q_{kl} : Queue size at blocked link (k,l) . Blocked links (k,l) are links such that $k = i$ or j , or, $l = i$ or j , excluding the link (i,j) itself.

The first term takes into account the delay by giving large queue the higher priority.

The second term takes care of the possible blocked links. We prefer assigning slot to links which block less other links. Both terms are between 0 and 1. Therefore the metric of link (i,j) is also between 0 and 1.

The choice of the weight factors affects the performance of the network. We have run simulations to compare the performance of the network for different values of a and b , and choose $a = 0.5, b = 0.5$ for later use.

Originally we have a third term in the link metric definition. However, we tried $(R_{ij}/R_{\max})^\gamma$ (to encourage the links to use less power), and $\left(1 - \Lambda_i(j)/\max_{i,j}(\Lambda_i(j))\right)$ (to encourage the link with large average rate), and find out that the best performance always has a zero weight factor for the third term. Therefore, we now use two terms.

5.3.2 Scheduling Rules

The scheduling rules include three parts. First, the link with lower link metric has higher priority in the scheduling to occupy the time slot. Next, when link (i,j) is active, node i and node j can not transmit to other nodes or receive from other nodes. Finally, the SIR requirements are satisfied. That is,

$$\frac{P_i G_{ij}}{\sigma^2 + \sum_{k \neq i} P_k G_{kj}} \geq \beta, \quad \forall \text{ link } (i, j) \text{ activated.} \quad (5.4)$$

The scheduling rules require that one node can only be associated with one active link, and then the first order collision is avoided. We then need each activated link satisfy the SIR requirement, which means, the interference from all other nodes is small enough to guarantee the SIR threshold β .

5.3.3 Scheduling Algorithms and Power Control

Scheduling and power control are coupled. The power assignment decides the network topology, and therefore, affects the scheduling result. The scheduling decides the link activation and interference generated, and hence the power requirement at each link to achieve the SIR requirement. There are two alternative methods for scheduling. One is the simplified method without power control. Power is preset to each link before scheduling. The other is finding the maximal possible allowable links to transmit at the same time, with the joint power control and scheduling. The algorithm provided in [48] belongs to the second category. Here we propose one simplified algorithm without power control, and one joint scheduling and power control algorithm.

Simplified scheduling: The power of link (i,j) is calculated before scheduling according to the attenuation factor G_{ij} , so that the SIR of link (i,j) is satisfied if there is no interference from other links. Then the power is preset by (5.5). Here α ($\alpha > 1$) is the marginal protection to allow some interference from other links.

$$P_i = \beta \cdot \alpha \cdot \frac{\sigma^2}{G_{ij}} \quad (5.5)$$

The first link scheduled is the lowest metric one. Then links are tried one by one according to their metric. If the new link does not introduce excessive interference to the prescheduled links, and its own SIR requirement can be satisfied, then it is added. Otherwise it is rejected. Each time when a new link is added, the links this link blocked are out of future consideration. Since there is no iterative power control, this method can be extent to distributed algorithm easily.

Our joint algorithm: We add link one by one from the lowest metric. Each time a

new link is tried, run the iterative power control algorithm (5.6) to calculate the required power to satisfy the SIR requirement.

$$P_i^{(n+1)} = \beta \left(\sigma^2 + \sum_{k \neq i} P_k^{(n)} G_{kj} \right) / G_{ij}, \quad \forall \text{ link } (i, j) \quad (5.6)$$

If there is a solution, the power control algorithm converges fast to the minimum power vector [12]. There are two possible cases that the SIR requirements can not be satisfied. One is when some of the elements in the converged minimum power vector are larger than P_{\max} . The other is when there is no solution. In this case the algorithm diverges, and the elements in the power vector will grow beyond P_{\max} very fast. In either case, power elements exceed P_{\max} . In the simulation, we have limited number of iterations N_i , “Iterative power control algorithm succeed” is replaced by “Power does not exceed P_{\max} within N_i iterations”. There is a chance of non-satisfactory of SIR requirement after N_i iterations even if the power vector does not exceed P_{\max} . If this happens, the transmission is considered failed.

The selection of parameter N_i is important. Due to the inherent characteristics of the converging process of the power control algorithm, some marginal protection (that is, using $\beta\alpha$ ($\alpha > 1$) instead of β as the SIR requirement.) significantly reduces the number of iterations to achieve acceptable level of failure. The algorithm is as follows:

1. Calculate metrics of links, define link set as all links that have traffic, and define activation set as an empty set.
2. Select the lowest metric link and add it into the activation set. Remove this link and the links blocked by this link from the link set.

3. Select the lowest metric link from the link set and try iterative power control algorithm with this link added to the activation set.
4. If not succeed, remove this link from the link set, and go back to step 3. Otherwise, continue to step 5.
5. If succeed, add this link to activation set, and update power of scheduled links. Remove this link and the links blocked by this link from the link set.
6. Repeat step 3 to 5 until the link set is empty.

This method has to run the iterative power allocation each time a new link is tried. But it can achieve optimal throughput because all the links are tried. And since the links are added one by one, it is easier for the power control iterations to satisfy SIR requirement in less number of iterations.

Algorithm based on [48]: Reference [48] provided a joint power control and scheduling algorithm working in two phases. It calls a transmission scenario *Valid* if one node can only be associated with one active link at a time, and any receiver is spatially separated from other transmitter by at least a distance D . This algorithm first finds the valid scenario with maximum number of links by a *centralized* scheduling algorithm. Then, power control algorithm is executed in a distributed fashion. If there is no power vector can be found to satisfy the SIR requirements, the link with the smallest SIR is removed from the valid scenario. Then, power control algorithm is executed again, until the SIR requirements are satisfied.

An alternative way of joint power control and scheduling is using the centralized version of the algorithm from [48], with $D=0$. We consider this algorithm based on [48] in our simulation, and compare it to our joint power control and scheduling algorithm.

This method gives suboptimal throughput; and the number of power control algorithm is limited to number of links in the valid scenario. However, it needs more iterations for the power control algorithm to satisfy SIR requirement, therefore has the problem of high failure rate or high complexity.

5.3.4 Simulation Results

We study centralized algorithm first to evaluate the performance gain of the joint algorithm, and to provide a reference point for the distributed algorithm. It is also applicable to some networks with a base station.

A 10-node network and a 20-node network are generated by random points in a 10×10 area. We assume that the maximal transmission distance is 4 for both networks. The topologies of these networks are shown in Figure 5.1. Packets are generated by Poisson process at each node pair. We assume that λ_e is the average number of packets generated per slot for any source destination pair, and then the traffic rate at node i is $\lambda_i = (N - 1)\lambda_e$. We assume large buffer size Q_{\max} at nodes. Packets are discarded if the buffer is full. Packets are failed if the SIR is not satisfied due to the inaccurate power calculation because of the finite number of iterations.

Simulation parameters are listed as the follows:

Maximal transmission distance $R_{\max} = 4$,

Buffer size $Q_{\max} = 10000$.

SIR requirement $\beta = 1$.

Power decay factor $\gamma = 4$.

Simulation time 100000 slots.

Link metric $a=0.5, b=0.5$.

Simplified scheduling, $\alpha = 1.3$.

Our joint algorithm, $\alpha = 1.05, N_i = 10$.

Algorithm based on [48], $\alpha = 1.05, N_i = 15$.

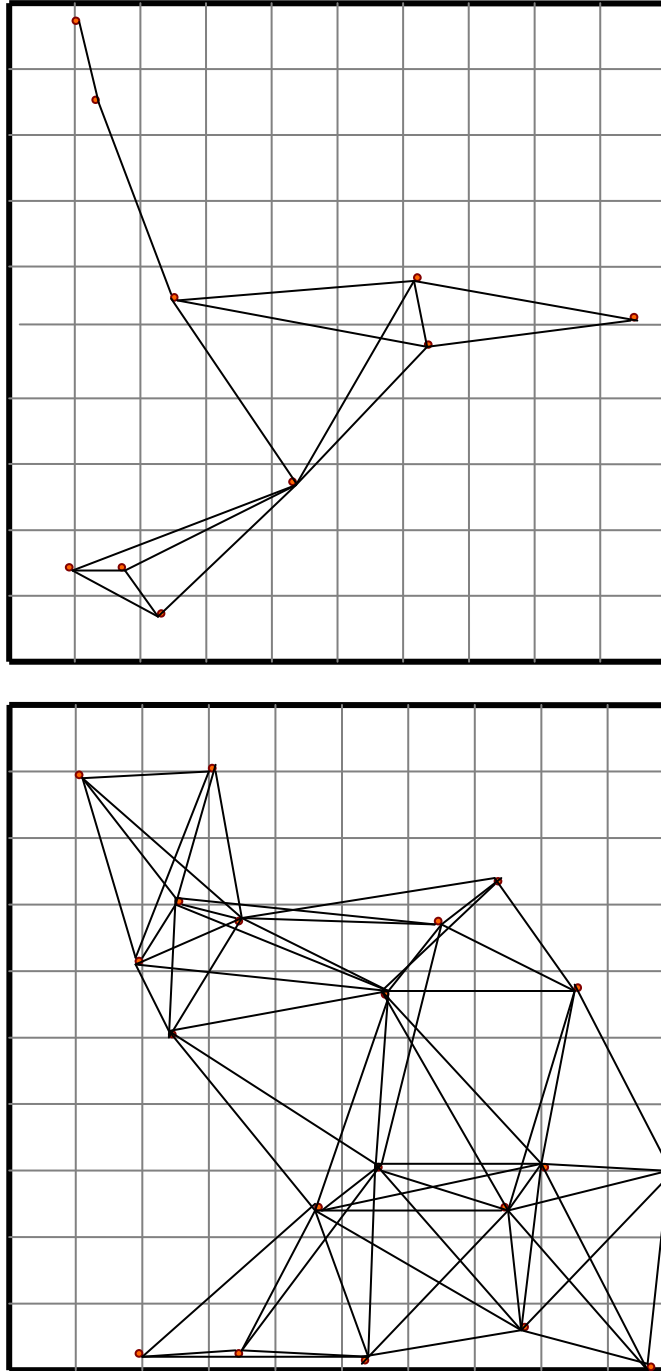


Figure 5.1: The 10-node network and 20-node network used in simulation.

The three scheduling algorithms we have just discussed are simulated. The

performance of the 10-node network and the 20-node network in terms of throughput, delay, and power versus λ_e is shown in Figure 5.2 and 5.3. There is no joint routing and scheduling at this point, the route is selected to be the least power route. The results are discussed as the follows.

Effect of α in simplified scheduling: The performance of the 10-node network for different values of α is listed in Table 5.1. Obviously, transmission power increases with α . The throughput also increases with α , and achieves the maximum throughput when $\alpha \geq 1.1$ in the 10-node example. However, there is an optimal α to maximize the throughput/Power, which is around 1.1 for the 10-node example. Although the optimal value of α depends on the SIR requirement, the traffic rate, and the network topology, the great news is that the extra 10~30% power can improve the network performance significantly. In the following comparison with other scheduling algorithms, we use $\alpha=1.3$ for the simplified scheduling to achieve the maximum throughput and small delay, with the cost of 30% more energy consumption.

Table 5.1: The throughput, delay, and power of the 10-node network with simplified scheduling for different values of α .*

α	Throughput	Delay	Power	Throughput/Power
1.0	0.339	11852.	61.5	5.51e-3
1.1	0.449	12.88	67.8	6.62e-3
1.2	0.449	9.76	73.9	6.07e-3
1.3	0.449	7.10	80.1	5.60e-3
1.5	0.449	6.37	92.5	4.85e-3
2.0	0.449	5.69	118.0	3.80e-3
5.0	0.449	4.12	163.9	2.74e-3
10.0	0.449	3.98	165.8	2.71e-3

*: These results are for $\lambda_e=0.005$. Throughput is the number of packets transmitted from the source to the destination per slot. Delay is in slots. The unit of power is σ^2 .

Convergence of the power control: The choice of N_i and α are coupled. Usage of $\alpha > 1$ reduces number of iterations to reach SIR satisfaction. For the 10-node example with $\lambda_e = 0.01$, and the 20-node example with $\lambda_e = 0.002$, the minimum N_i needed to have less than 0.1% failure rate is listed in Table 5.2. We choose $\alpha = 1.05$ in the following simulation. To reach the same $\leq 0.1\%$ failure rate in both the 10-node and 20-node examples, we use $N_i = 10$ for our algorithm, and $N_i = 15$ for the algorithm based on [48].

Table 5.2: Minimum number of iteration needed for joint scheduling and power control algorithms with 0.1% failure rate.

α		1.10	1.05	1.02	1.01
10 nodes $\lambda_e = 0.01$	Our algorithm	7	9	12	14
	Algorithm based on [48]	10	12	18	21
20 nodes $\lambda_e = 0.002$	Our algorithm	7	10	14	16
	Algorithm based on [48]	12	16	21	26

Threshold rate and throughput: There is a threshold rate for each of the scheduling algorithm. If the rate is larger than the threshold rate, then the number of waiting packets keeps increasing until the buffer is full and packets are dropped. The delay also increases rapidly if the rate exceeds the threshold. Table 5.3 shows the threshold rates (packets/slot/source destination pair) for the three scheduling algorithms for the 10-node network and the 20-node network we simulated.

As we can see from Figure 5.2 and 5.3, when the rate is larger than the threshold, the throughput no longer increases as the rate in the same slope. We find that both joint algorithms achieve larger throughput and threshold rate than the simplified algorithm; and our algorithm has larger throughput than the algorithm based on [48].

Table 5.3: Threshold rates for scheduling algorithms

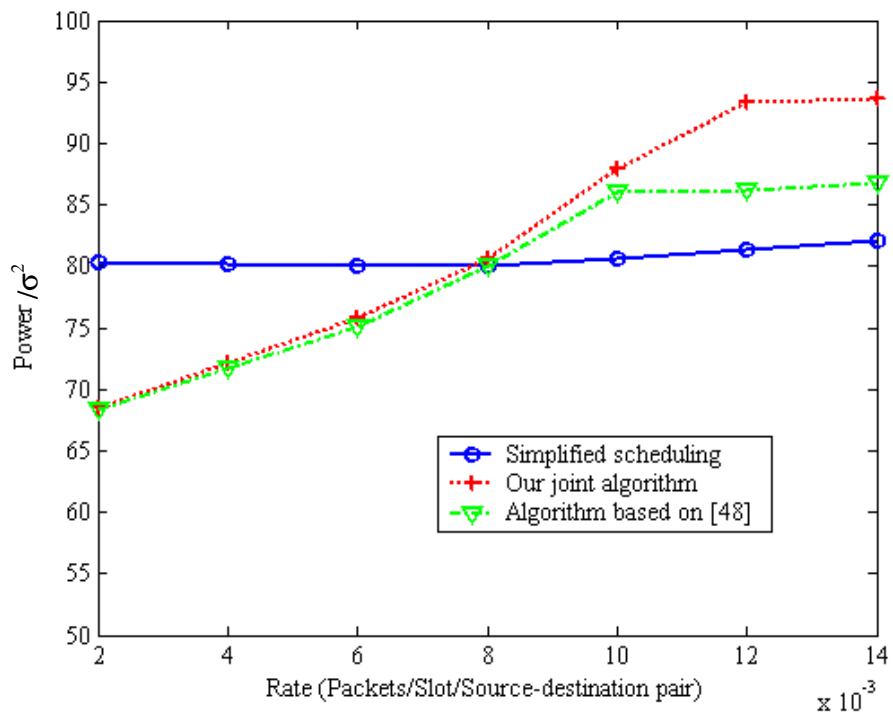
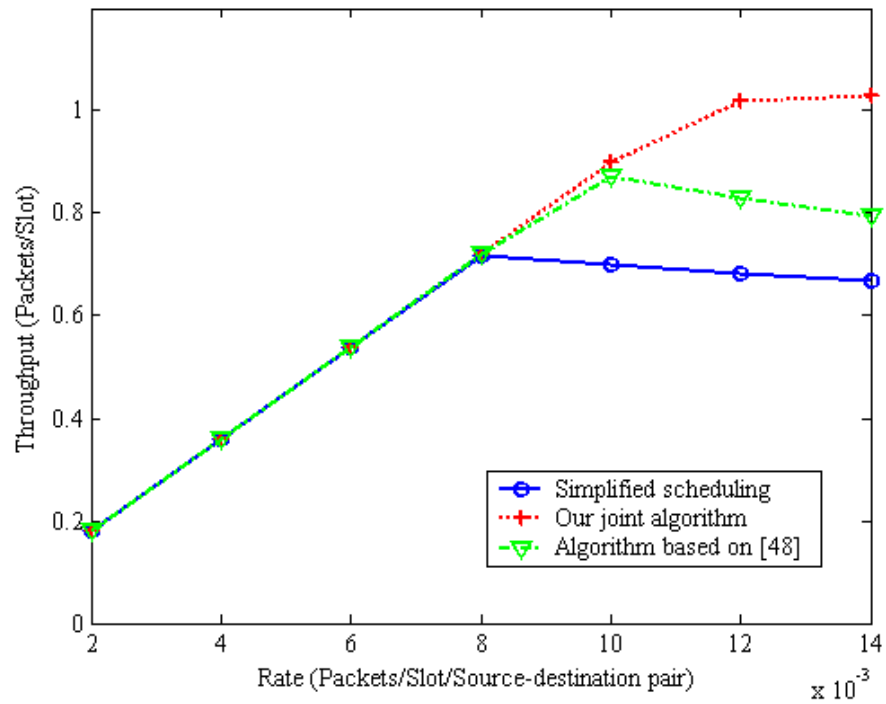
	10-node	20-node
Simplified scheduling, $\alpha=1.3$	0.0078	0.00175
Our joint algorithm, $\alpha=1.05, N_i=10$	0.0109	0.00215
Algorithm based on [48], $\alpha=1.05, N_i=15$	0.0096	0.00210

Power: The average power of the simplified algorithm does not change significantly as the rate increases, because the power is preset, and is not related to the interference caused by higher rate. On the contrary, the joint scheduling and power control algorithms use more power for larger rate. The reason is that more interference is generated by more links, and therefore more power is needed to overcome the interference and satisfy the SIR requirement. Our algorithm has slight larger power than the algorithm based on [48], due to the larger throughput it achieves.

Delay: Delay depends significantly on the rate. If the rate is larger than the threshold rate, the queues keep growing, and the delay also increases very fast as the rate increase, as shown in Figure 5.2 and 5.3. Our joint scheduling and power control algorithm achieve best delay among the three scheduling algorithms compared.

Complexity: We count the number of calculations (comparison and updating) to compare the complexity of the three scheduling algorithms. The number of calculations per packet transmission is shown in Figure 5.2 and 5.3.

Because the algorithm based on [48] needs more iterations to converge, it has more complexity than our joint algorithm. The simplified scheduling has smallest complexity at the low rate. However, at high rate, its number of calculations is not smaller than that of our joint algorithm. Actually, it has the highest complexity when normalized by its smallest throughput.



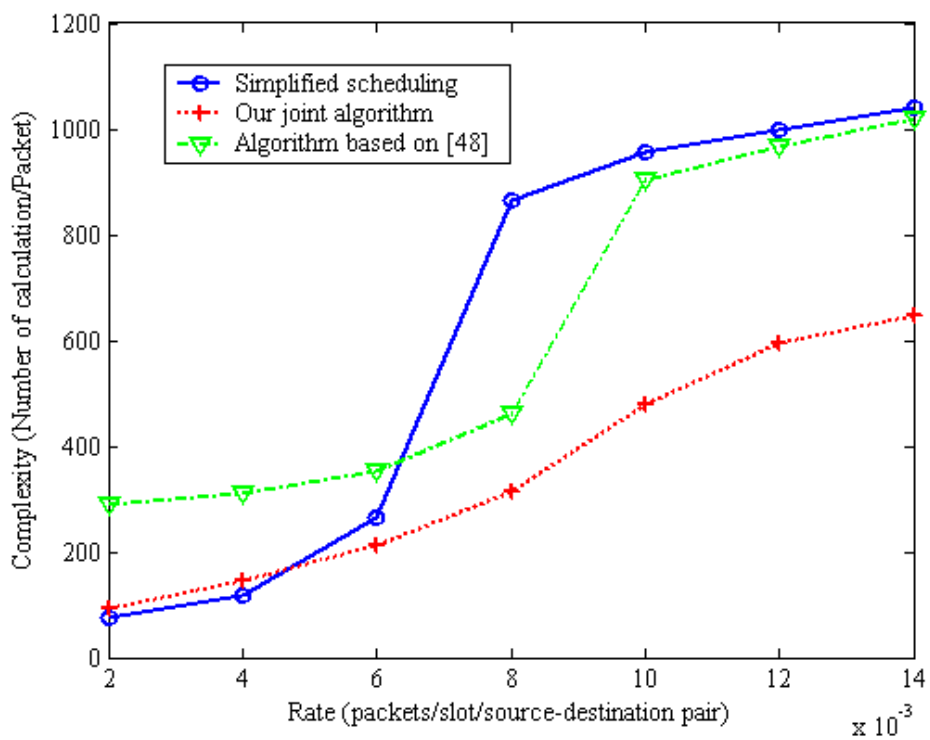
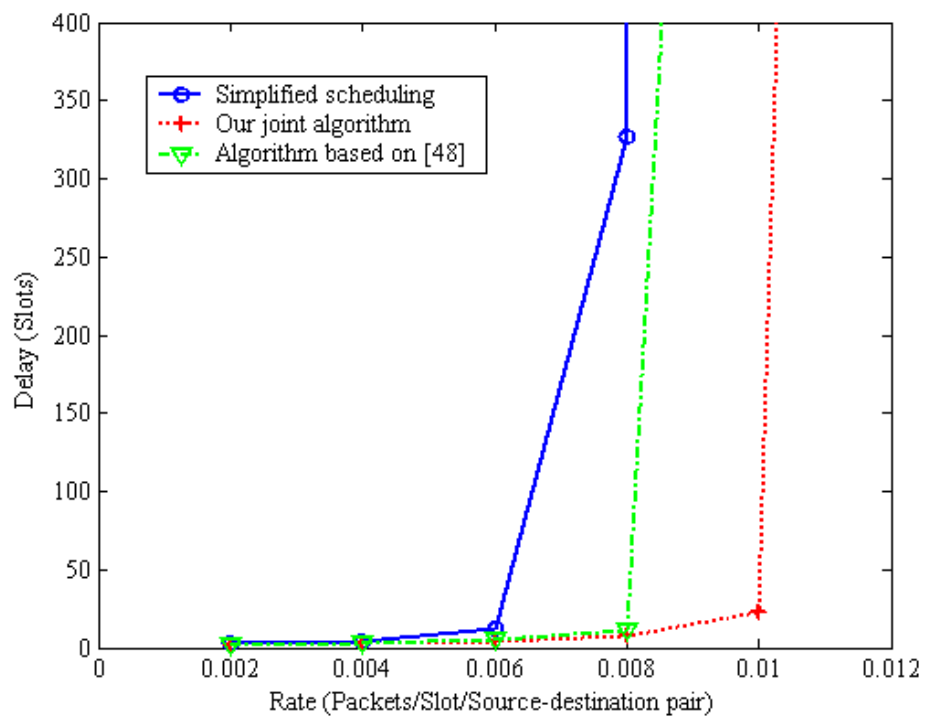
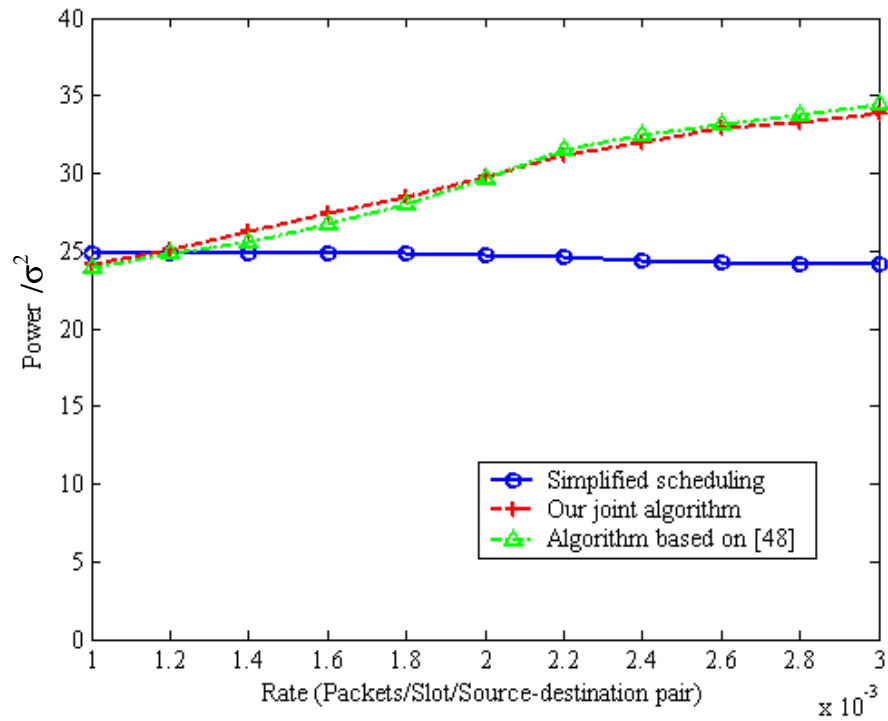
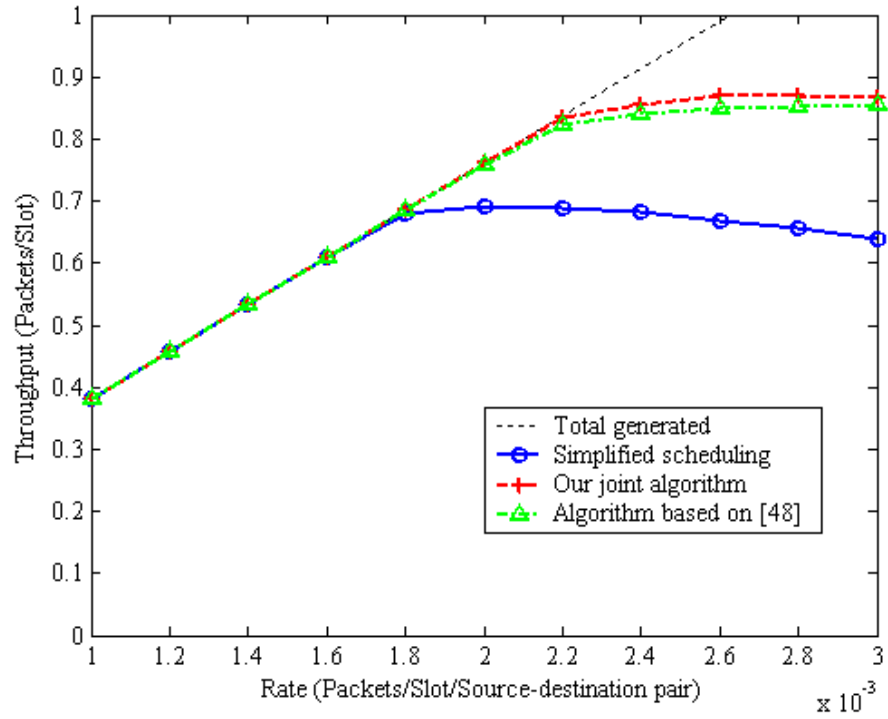


Figure 5.2: Throughput, power, delay, and complexity of scheduling algorithms, for the 10-node network.



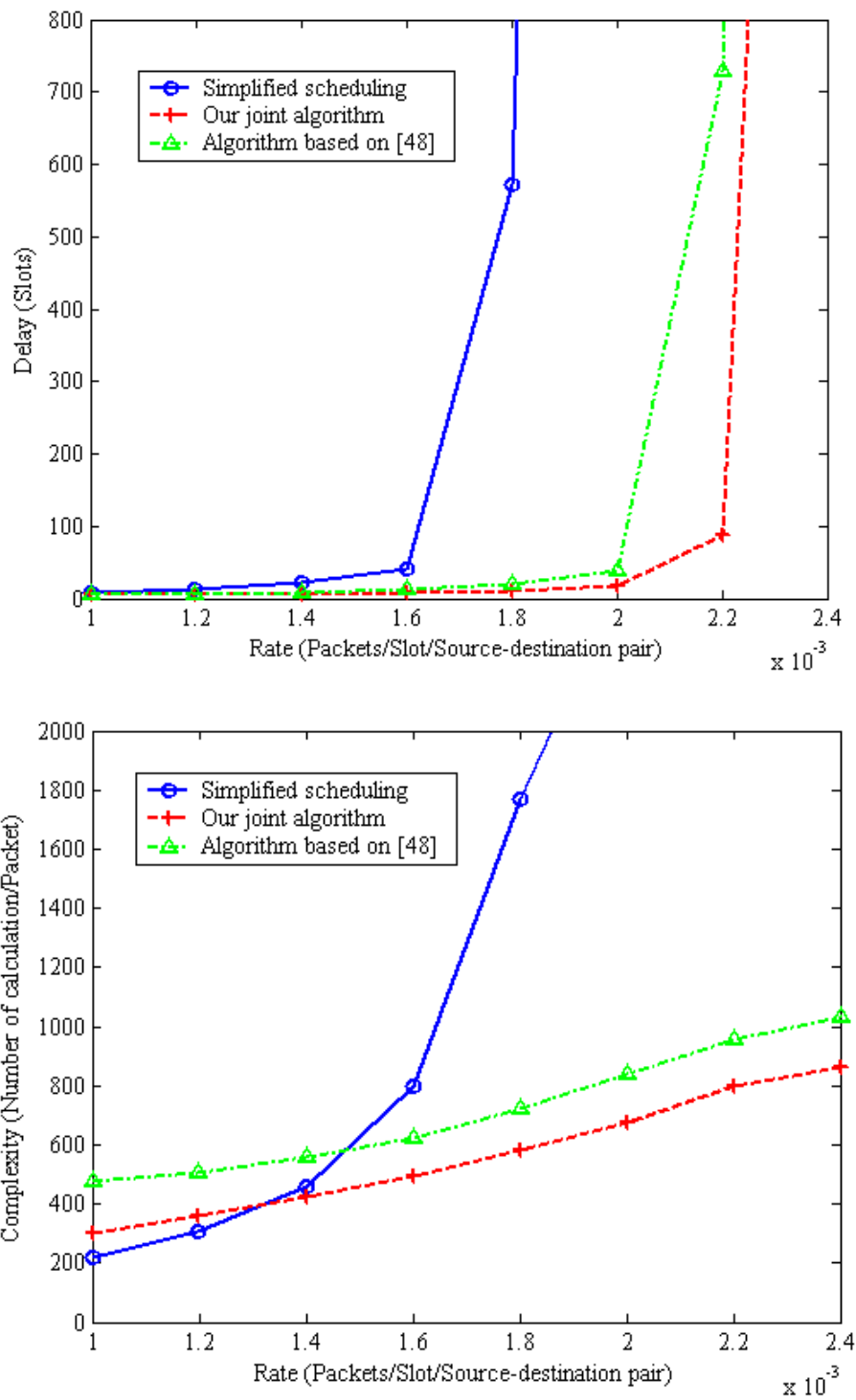


Figure 5.3: Throughput, power, delay, and complexity of scheduling algorithms, for the 20-node network.

Comparison: The simplified scheduling is the simplest one because there is no

power control. But the amount of calculation is not less than that of the joint scheduling and power control algorithms, and the delay and throughput are significantly worse than other schemes for the roughly same level of power consumption.

Our joint scheduling and power control algorithm gives the maximum use of the channel (i.e., maximum throughput and smallest delay). It is easy to prove that, whatever scheduling result algorithm based on [48] found will also be accepted by our algorithm at a certain step. Our algorithm also has smaller complexity compare to the algorithm based on [48], and only slightly larger power.

5.4 Jointly Scheduling and Routing

The actually assigned bandwidth by the scheduling algorithm may be different from the required bandwidth, which is $\Lambda_i(j)$ in average. As time goes on, queues start building up at the buffers of some links. These queues do not build up uniformly among all nodes. The link distance is changed by the building up of the queues. A least distance routing algorithm can re-compute routes using the updated information about the queues at links. The recomputed routes provide new values of the average rates on each link that the scheduling aims to satisfy. This is the problem of joint solving the access control and the routing problem in ad-hoc networks.

This successive interaction from frame to frame, between the route selection, (that determines the required bandwidth,) and the bandwidth allocation, (that determines the actually assigned bandwidth,) is the heart of the joint routing/access resolution.

5.4.1 Routing Distance

Bellman-Ford algorithm is chosen because it can be operated distributedly. The

distance is defined as:

$$D(i, j) = d \cdot \left(\frac{Q_{ij}}{Q_{\max}} \right) + e \cdot \left(\frac{R_{ij}}{R_{\max}} \right)^\gamma. \quad (5.7)$$

d and e : Weight factor, $d + e = 1$.

Q_{ij} : Queue at the buffer of link (i, j) .

Q_{\max} : Maximum buffer size.

The first term is the queue size, to encourage the usage of less congested links and avoid congestion. The second term is related to power consumption, or physical distance of the link, to encourage transmission over short distance. The link between two nodes in close distance not only spends less power in transmission, therefore prolong the lifetime of nodes and network, it also causes less interference to all other link in the network. At the beginning of the network operation, we have $Q_{ij} = 0$. As long as $e > 0$, routes are optimized by energy consumption. After that, routes are calculated periodically by the Bellman-Ford algorithm based on the defined link distance in (5.7).

5.4.2 Rerouting

Although the scheduling algorithm takes into account the average bandwidth requirement and the queue, there are still cases where the bandwidth requirement can not be satisfied by scheduling only. For example, in an unbalanced topology, if a node is close to many nodes, and is on the route of many source destination pairs, the bandwidth requirement to that node may just exceed the maximal possible value, even if it is assigned slots all the time. As time goes on, the difference between the bandwidth requirement and the bandwidth assignment at some links may stay positive for a number

of slots, and queues start building up at the buffers. These queues do not build up uniformly among all nodes and flows. Thus the packets which are encountering long delay in their current route need to be rerouted. The rerouting helps in balancing the traffic throughout the links and nodes in the network. Rerouting periodically may increase the throughput and stable rate, and decrease the number of discarded packets and the delay.

The route is rerouted periodically by Bellman-Ford algorithm. It may not be possible to redefine routes across the network at the rate of every frame. Then the time constant of route adjustment can be made greater to encompass multiple frames and react only to the aggregate queue size fluctuations over a sufficiently large number of frames. We compare the performance of the network with and without periodic rerouting.

5.4.3 Simulation Results

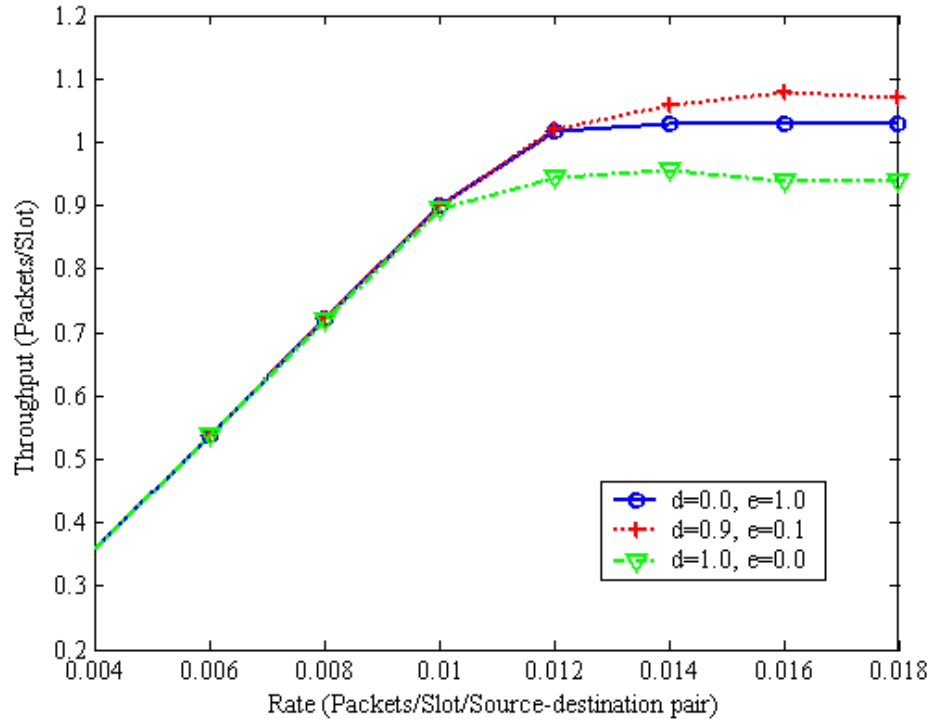
In order to study the effect of joint routing and scheduling algorithm, we simulated the two networks shown in Figure 5.1. The performance of the 10-node network, in terms of throughput, delay, and power, is shown in Figure 5.4, and the performance of the 20-node network is shown in Figure 5.5. Since the maximum transmission power P_{\max} , and the maximum transmission distance R_{\max} , are the same for the two networks, the 20-node network is a denser network than the 10-node one.

For the joint scheduling and routing algorithm, we use our joint scheduling and power control algorithm (with $\alpha = 1.05, N_i = 10$) to do the scheduling, and the routes are updated every 1000 slots.

In Figure 5.4 and 5.5, the curves for $d=0, e=1$ is the least power route without

rerouting; and the curves for $d=1, e=0$ is the least congestion route without the consideration of power. We found that for both 10-node example and 20-node example, the power consumption of $d=0, e=1$ is the smallest, and the power of $d=1, e=0$ is the largest. All the other curves are in between. The reason for this is straight forward.

From Figure 5.4, we find that rerouting only improves the throughput and delay slightly compare to the least energy route. It shows that the link metric and the scheduling algorithm assigns bandwidth to links in a way that the queues are built up evenly in average; therefore the adding of queuing term in the routing distance does not improve the performance significantly for this particular 10-node network.



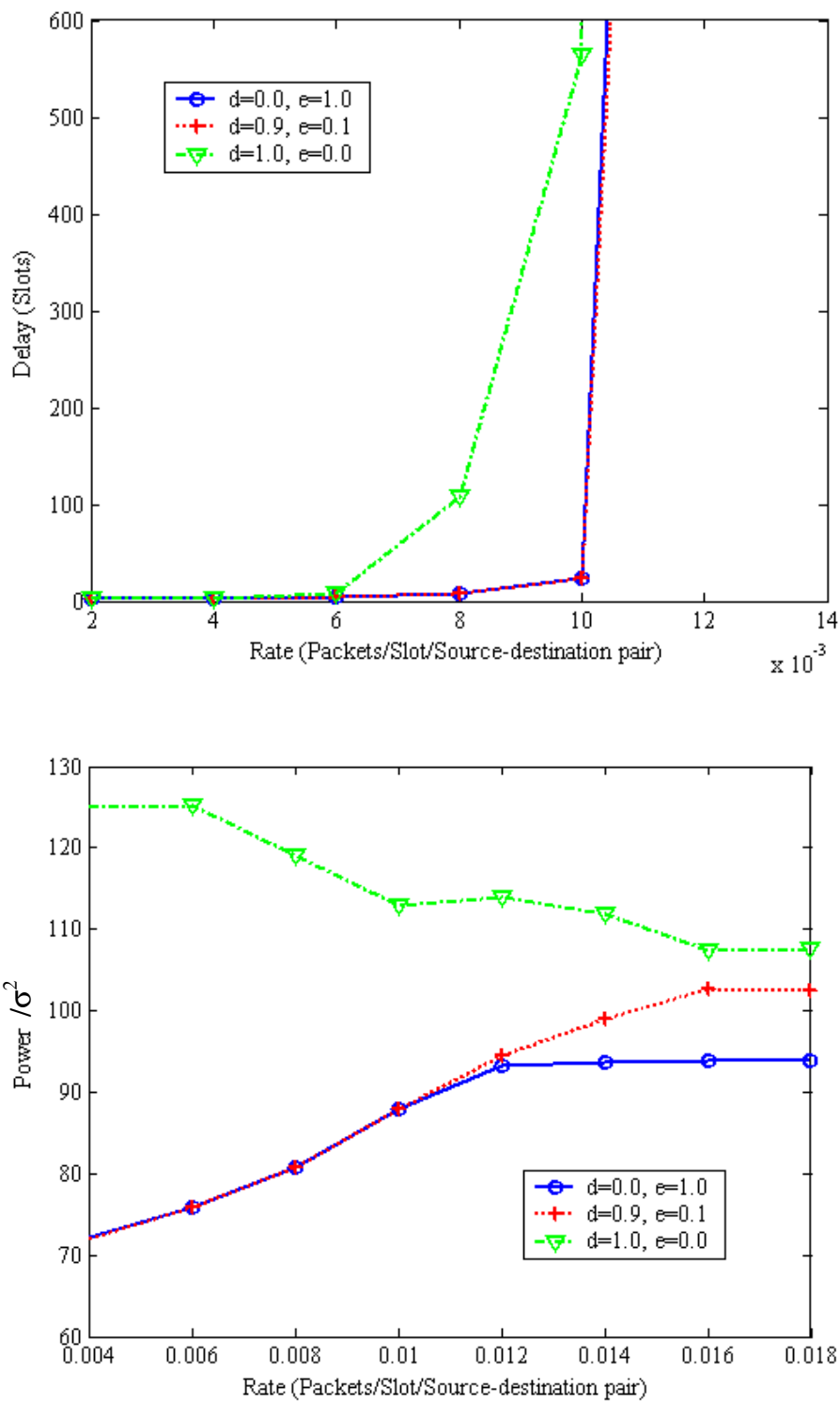
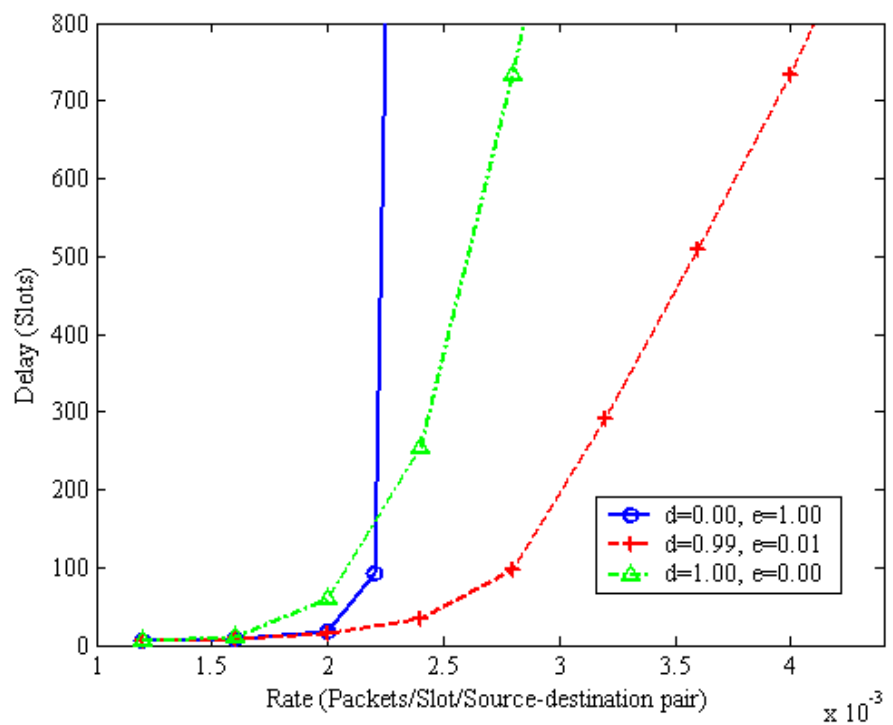
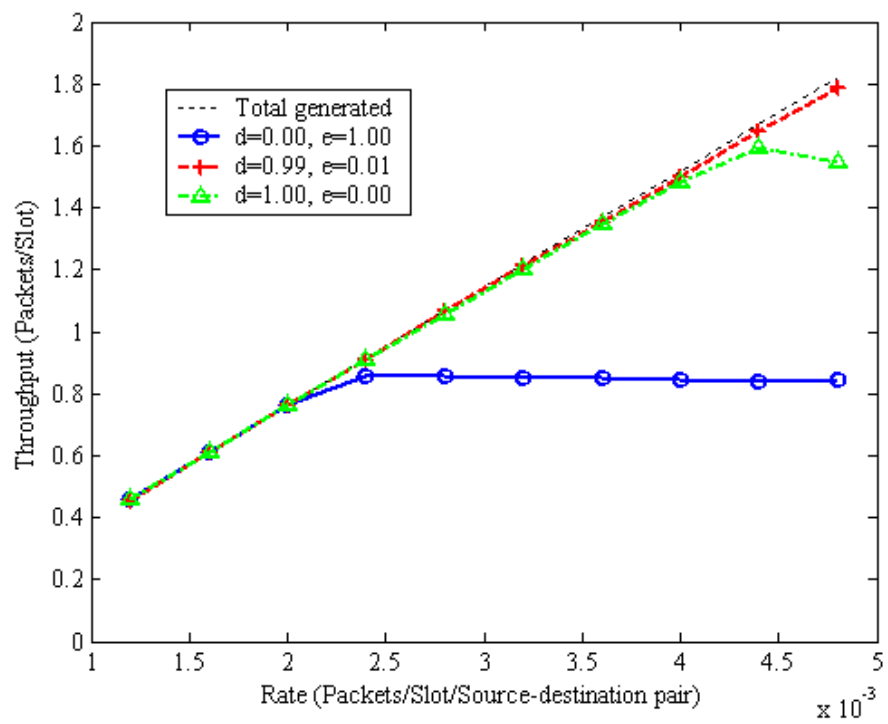


Figure 5.4: Throughput, delay, and power for different routing parameters,

10-node example.



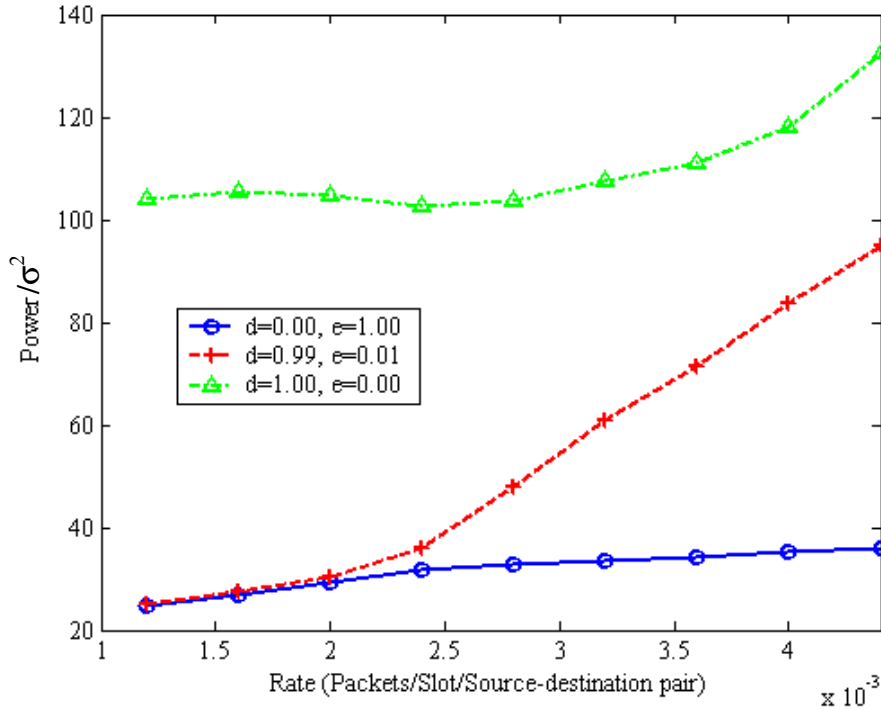


Figure 5.5: Throughput, delay, and power for different routing parameters, 20-node example.

However, from Figure 5.5, we find that the least power route performs very badly in both throughput and delay; and rerouting improves the performance significantly. This is because that the 20-node example has some busy nodes and is easy to be congested without the help of rerouting. It is more likely for a larger and denser network to have unbalanced topology, so that rerouting is important to balance the traffic through links.

For both examples, the optimal values of (d, e) in terms of throughput and delay are somewhere between $(1, 0)$ and $(0, 1)$. For the 10-node example, it is around $(0.9, 0.1)$, and for the 20-node example, it is around $(0.99, 0.01)$.

5.5 Distributed Algorithm

Since ad hoc networks do not have a central controller, distributed implementation is

very important for the routing and scheduling algorithms. The distributed routing based on Bellman-Ford algorithm converges and is well studied [49]. We now need to focus on the distributed scheduling and power control algorithm.

We assume there is a separate channel for scheduling, routing, and information exchange. In each frame of this channel, there are M iterations for the scheduling. In each iteration, each node has its own time slot to send its request or information to its neighbors. A node i knows its neighbor j about its attenuation factor G_{ji} and the link metric of the requesting link from it, $L(j, k)$.

One problem of distributed algorithm is how to relate allocated slots to the metric of links. We let a node send request at a random time of the M iterations, and that random time is related to the link metric. That is, the link with lower link metric is more likely to request earlier than the link with higher link metric. Another possibility would be let links with lower metric replace the existing higher metric one.

Another problem is the iterative power control. The distributed power control algorithm with P_{\max} uses the measured SNR to update power, and its convergence is proved [50]. However, it is possible that the power vector converges to the vector whose elements are all P_{\max} , that is, the SIR requirements are not satisfied. We now hope to run power control along with scheduling. Each link should update its power according to the power levels of its neighbors. Methods to reduce the number of iteration include using discrete power levels and set margin protection. The complexity of asynchronous power control algorithm and the information needs to be exchanged between neighbors are other possible problems.

We do not have exactly distributed algorithm in detail for the joint scheduling and

power control algorithm at this moment. For the simplified scheduling, we have an outline of the distributed algorithm, and plan to finalize it and simulate it in the near future. For the joint scheduling and power control algorithm, we have some thoughts and wish to finish the distributed algorithm in the future. We discuss these in the following subsections.

5.5.1 With Simplified Scheduling

We first discuss the distributed simplified scheduling where the power is preset before scheduling, as in Section 3.3.1. We define *Tolerable Interference (TI)* of link (m,n) as

$$TI(m,n) = P_m G_{mn} - \beta \sigma^2 - \beta \sum_{k \neq m} P_k G_{km}. \quad (5.8)$$

If the SIR requirement of link (m,n) is satisfied, then $TI(m,n) \geq 0$. For a new link (i,j) to be added without destroying link (m,n) , the power P_i must satisfy

$$\beta \cdot P_i \cdot G_{in} \leq TI(m,n). \quad (5.9)$$

Assume each node knows the TI of all of nodes it can hear. In order to check whether (5.9) is satisfied; each node keeps tracking the scheduling information of its neighbors.

When node i (which is idle) want to request a slot to transmit to node j , it first presets power according to (5.5), then goes through the following process.

1. Node i first check whether (5.9) is satisfied for all its neighbor n who is the receiver of a scheduled link.
2. Then node i sends request message RQS to node j .
3. Node j checks whether it is in idle mode, and the SIR is satisfied, i.e., (5.4) is satisfied.

4. If yes, it send accepting reply message RPL to node i . If no, it sends rejecting reply message RJT back to node i .
5. When node i receives the message RPL, it sends confirm message CNF to node j and all its neighbors and then changes the database. Its neighbors update their information.
6. Upon receive the message CNF from node i , node j broadcast its new TI to all its neighbors and change the database.
7. If node i receives RJT, it stops requesting for the current slot.

In order to avoid the change of TI during the RQS-RPL-CNF process, the nodes who hear the RQS message should stop scheduling until the finish of the current link scheduling.

5.5.2 With Joint Scheduling and Power Control

To reduce the number of iteration for the power control algorithm to converge, we use multiple power levels instead of continuous power.

When a new link (i,j) wants to be added, the transmitter i first checks the TI of neighboring receivers, and find out the Max power level it could use. Then it sends a RQS to its receiver j . The receiver checks whether this Max power level can satisfy the SIR requirement. If not, it sends RJT message, and the power level needed. If yes, it sends RPL along with the actual power level needed. Upon getting RPL from node j , node i sends out CNF message to receiver, and all its neighbors for them to update their database. If the transmitter gets RJT message, it send out request to the neighbor k (whose TI limited node i 's Max power level) to increase its power, so that the Max power level of node i can be the power level needed for link (i,j) . If neighbor k can do this, then

node i can resend RQS to node j . If for some reason, (for example, node k already at highest power level) node k can not improve its power, it reject node i 's request of increasing power, and node i give up the scheduling of link (i,j) .

In order to leave some TI for the later links, we should leave some marginal protection when decide power level, like using $\alpha\beta$ instead of β .

5.6 Future Work and Extension

We plan to finish the distributed joint scheduling and power control algorithm and simulate it in the near future.

The algorithms above can be easily modified to have multiple flow types. The only modification is using $\beta_f, f = 1, 2, \dots, F$, instead of β when checking SIR requirement. For some applications, it may not be possible to do the scheduling for each slot; we can also do scheduling for a frame consists of many slots. The basic ideas are the same. This study can also be extended to CDMA-based systems by slightly changing the scheduling rules.

5.7 Conclusions

In this chapter, we provide a centralized algorithm of joint power control, scheduling, and routing. Simulation results show that the joint scheduling and power control algorithm improve the throughput and delay significantly, and the joint scheduling and routing algorithm also improves the network performance. Our simulation shows that there is a trade-off between the energy consumption and the network performance, such as throughput and delay. Algorithm for distributed implementation is also discussed.

Chapter 6 Summary

For the CDMA system with symmetric sequences, we found the user capacity and the effective bandwidth for the $(K,0)$ and the (M,N) matched filter and decorrelator detectors, by assuming fixed total power from unknown users. By making the equal power assumption for all known users, we obtained the user capacity for the $(K,0)$ and the (M,N) MMSE detectors. For symmetric sequences, the effective bandwidth can not be expressed by a scalar, because two constraints have to be satisfied simultaneously to satisfy the SIR requirement. We introduce a 2-D vector notion of effective bandwidth with and without unknown users. For both the decorrelator and the MMSE detector, the user capacity is one when all users are known to the receivers and is reduced to $(1-N/L)$ when N users are unknown (with L the processing gain).

We study the problem of a power-controlled CDMA system with N nodes and F flow types with the constraint that each node uses the same power level for all flows that it multiplexes. For the $F=1$ case with SIR requirement β , we find that for both the uplink and the downlink, if $N>L$, the optimal sequences are the WBE sequences, and the user capacity is $1+1/\beta$ users per degree of freedom. Also if $N \leq L$, the optimal sequences are orthogonal. For the uplink problem with $N=2$ and F arbitrary, the necessary and sufficient conditions to have solutions are found and proved. For the general $N>1$ uplink problem, we provide an iterative algorithm to find the optimal solution and prove its convergence. For the downlink case with $F>1$, the power assignment problem is solved

and some properties of the optimal sequences are proved. Finally, the one power level constraint simplifies the transmitter structure, with the cost of performance degradation.

We study an unusual method of passive rate adaptation in which some bits are dropped at the receiver end of a link. From the examples of PAM and QAM, we notice that the performance depends significantly on the distribution of the signal, on the modulation scheme, and on the channel property. In Gaussian channels, the rate reduction scheme at the transmitter has significant advantage over our rate reduction scheme at the receiver, in terms of both SEP and MSD. In Rayleigh fading channels, the rate reduction scheme at the transmitter still has advantage over the rate reduction scheme at the receiver, but that advantage is NOT significant anymore. Our scheme achieves smaller MSD for a much larger region of SNR values. Therefore, our scheme is more suitable to use in fading channels than in Gaussian channels. The study of an example with non-uniform constellation verifies that our scheme has a larger applicable region of SNR values if the important bits are given additional protection.

We study the cross-layer coupling in a wireless ad hoc network. We assume a TDMA-based wireless ad-hoc network, and provide a centralized algorithm of joint power control, scheduling, and routing. Energy efficiency is another very important topic for ad hoc networks, and is considered in our algorithm. Simulation results show that the joint scheduling and power control algorithm improve the throughput and delay significantly, and the joint scheduling and routing algorithm also improves the network performance substantially. Our simulation shows that there is a trade-off between the energy consumption and the network performance, such as throughput and delay. Algorithm for distributed implementation is also discussed.

Appendices

A. Proof of Restriction 1

Any two symmetric vectors, \mathbf{s}_i and \mathbf{s}_j , satisfy $\|\mathbf{s}_i\| = \|\mathbf{s}_j\| = 1$ and $\mathbf{s}_i \cdot \mathbf{s}_j = \rho$. Then, by the Schwarz inequality we have $|\mathbf{s}_i \cdot \mathbf{s}_j| \leq \|\mathbf{s}_i\| \cdot \|\mathbf{s}_j\|$, which implies $-1 \leq \rho \leq 1$.

First we prove the sufficiency by giving a construction scheme.

Assume (2.1) is true. Then K symmetric $1 \times K$ vectors can be constructed one by one starting from $\mathbf{s}_1 = [1 \ 0 \ \dots \ 0]$ in the following way. When adding \mathbf{s}_i , we guarantee that $\|\mathbf{s}_i\| = 1$ and $\mathbf{s}_i \cdot \mathbf{s}_j = \rho$ for all $j < i$, by setting $s_{i,1} = s_{i-1,1}$, \dots , $s_{i,i-2} = s_{i-1,i-2}$, $s_{i,i-1} = (\rho - \sum_{j=1}^{i-2} s_{i-1,j} s_{i,j}) / s_{i-1,i-1}$, and $s_{i,i} = (1 - \sum_{j=1}^{i-1} s_{i,j}^2)^{\frac{1}{2}}$. The resulting vectors are given by:

$$\begin{aligned} \mathbf{s}_1 &= [1 \quad 0 \quad 0 \quad 0 \quad 0 \quad \dots] , \\ \mathbf{s}_2 &= \left[\rho \quad \sqrt{1-\rho^2} \quad 0 \quad 0 \quad 0 \quad \dots \right] , \\ \mathbf{s}_3 &= \left[\rho \quad \rho \sqrt{\frac{1-\rho}{1+\rho}} \quad \sqrt{\frac{(1-\rho)(1+2\rho)}{1+\rho}} \quad 0 \quad 0 \quad \dots \right] , \\ \mathbf{s}_4 &= \left[\rho \quad \rho \sqrt{\frac{1-\rho}{1+\rho}} \quad \rho \sqrt{\frac{(1-\rho)}{(1+\rho)(1+2\rho)}} \quad \sqrt{\frac{(1-\rho)(1+3\rho)}{1+2\rho}} \quad 0 \quad \dots \right] , \\ &\dots\dots \\ \mathbf{s}_K &= \left[\rho \quad \rho \sqrt{\frac{1-\rho}{1+\rho}} \quad \rho \sqrt{\frac{(1-\rho)}{(1+\rho)(1+2\rho)}} \quad \dots \right. \\ &\quad \left. \rho \sqrt{\frac{(1-\rho)}{[1+\rho(K-3)][1+\rho(K-2)]}} \quad \sqrt{\frac{(1-\rho)[1+\rho(K-1)]}{1+\rho(K-2)}} \right] . \end{aligned}$$

The condition of (2.1) guarantees that all the factors inside the square root are positive. It is easy to check that the K vectors constructed above have unit length and pair-wise crosscorrelation ρ .

We prove the necessity by induction. Because $-1 \leq \rho \leq 1$ is true, (2.1) is satisfied for $K=2$.

Now assume that, if $K-1$ symmetric vectors with unit length and crosscorrelation ρ exist, then $[(K-1)-1]^{-1} \leq \rho \leq 1$ is satisfied. The K symmetric vectors with unit length and crosscorrelation ρ can always be rotated to:

$$\begin{aligned} \mathbf{s}_1 &= [1 \quad 0 \quad 0 \quad \cdots], \\ \mathbf{s}_2 &= [\rho \quad s_{22} \quad s_{23} \quad \cdots], \\ &\cdots, \\ \mathbf{s}_K &= [\rho \quad s_{32} \quad s_{33} \quad \cdots] . \end{aligned}$$

Define

$$\mathbf{s}'_i = (1 - \rho^2)^{-\frac{1}{2}} [s_{i2} \quad s_{i3} \quad \cdots], \quad i=1, \dots, K.$$

Then $\|\mathbf{s}'_2\| = \cdots = \|\mathbf{s}'_K\| = 1$ is true from $\|\mathbf{s}_2\| = \cdots = \|\mathbf{s}_K\| = 1$; and $\mathbf{s}'_i \cdot \mathbf{s}'_j = \rho/(1+\rho)$ is true from $\mathbf{s}_i \cdot \mathbf{s}_j = \rho$ for all $i, j \neq 1$. Therefore, $\mathbf{s}'_2, \dots, \mathbf{s}'_K$ are $K-1$ symmetric vectors with unit length and crosscorrelation $\rho/(1+\rho)$. From our hypothesis, we have $-(K-2)^{-1} \leq \rho/(1+\rho) \leq 1$, and hence for K symmetric vectors with unit length and crosscorrelation ρ , the inequality $-(K-1)^{-1} \leq \rho \leq 1$ is satisfied.

B. Proof of Restriction 2

First we look at the example of $L=2$.

Obviously there are at most 3 symmetric vectors from the origin to the unit circle. They can be $\mathbf{s}_1 = [1 \quad 0]$, $\mathbf{s}_2 = [\cos \frac{2\pi}{3} \quad \sin \frac{2\pi}{3}]$, $\mathbf{s}_3 = [\cos \frac{4\pi}{3} \quad \sin \frac{2\pi}{3}]$, and $\rho = -\frac{1}{2}$. The 3 vectors are separated by 120° in the plane; they are the 3 vertices of an equal-side triangle

inscribed in the unit circle.

For $L \geq 3$, we want to find the largest possible number of vectors $\mathbf{s}_i = [s_{i1} \ s_{i2} \ \dots \ s_{iL}]$, $i=1,2,\dots, K$, such that $|\mathbf{s}_i|^2 = 1$, and $\mathbf{s}_i \cdot \mathbf{s}_j = \rho$ for all $j \neq i$.

Without loss of generality, we can let $\mathbf{s}_1 = [1 \ 0 \ \dots \ 0]$. Then, $\mathbf{s}_1 \cdot \mathbf{s}_j = \rho$ implies $s_{j1} = \rho$, and $\|\mathbf{s}_j\|^2 = 1$ implies $s_{i2}^2 + \dots + s_{iL}^2 = 1 - \rho^2$, and finally $\mathbf{s}_i \cdot \mathbf{s}_j = \rho$ implies $s_{i2}s_{j2} + \dots + s_{iL}s_{jL} = \rho - \rho^2$, for all $i,j=2,\dots,K$ and $j \neq i$. Define now

$$\mathbf{s}_i^{(1)} = (1 - \rho^2)^{-\frac{1}{2}} \cdot [s_{i2} \ s_{i3} \ \dots \ s_{iL}], \quad i = 2, \dots, K.$$

Then in $(L-1)$ dimension space, we want to have the largest K such that the $K-1$ vectors $\mathbf{s}_i^{(1)}$ satisfy

$$\begin{aligned} |\mathbf{s}_i^{(1)}|^2 &= s_{i2}^{(1)2} + \dots + s_{iL}^{(1)2} = 1, \quad \text{for } i = 2, \dots, K, \\ \mathbf{s}_i^{(1)} \cdot \mathbf{s}_j^{(1)} &= s_{i2}^{(1)}s_{j2}^{(1)} + \dots + s_{iL}^{(1)}s_{jL}^{(1)} = \frac{\rho}{1 + \rho}, \\ &\text{for all } i, j = 2, \dots, K \text{ and } j \neq i. \end{aligned}$$

This is the same problem as the original one, except the L -dimensional space is reduced to an $(L-1)$ -dimension, and the crosscorrelation changes to $\rho_{L-1} = \rho_L / (1 + \rho_L)$. Similarly, we can rotate the vectors such that $\mathbf{s}_i^{(1)} = [1 \ 0 \ \dots \ 0]$, and then define $\mathbf{s}_i^{(2)}$ similarly and reduce to $(L-2)$ dimension. After J times of reduction, the problem reduces to a search for $K-J$ symmetric vectors in $(L-J)$ dimensional space. But we know that in the 2-dimensional space, there are at most 3 symmetric vectors with $\rho_2 = -\frac{1}{2}$, therefore $K \leq L+1$.

From the induction, we know that in order to get the maximal number of symmetric vectors, we must have $\rho_{L-1} = \rho_L / (1 + \rho_L)$, i.e., $\rho_L^{-1} = \rho_{L-1}^{-1} - 1$. Thus,

$$\frac{1}{\rho_L} = \frac{1}{\rho_{L-1}} - 1 = \dots = \frac{1}{\rho_{L-(L-2)}} - (L-2) = \frac{1}{-\frac{1}{2}} - L + 2 = -L.$$

Therefore, to have $L+1$ symmetric vectors in L -dimensional space, we must have $\rho = -L^{-1}$.

C. Derivation of (2.5)

Let us first obtain \mathbf{R}_M^{-1} . Consider the symmetric Hermitian matrix \mathbf{D} with $(\mathbf{D})_{ij} = 0$, if $i = j$, and $(\mathbf{D})_{ij} = 1$, if $i \neq j$. Then \mathbf{D} can be diagonalized as $\mathbf{U} \cdot \mathbf{\Lambda}_D \cdot \mathbf{U}^T$, where $\mathbf{\Lambda}_D$ is the diagonal eigenvalue matrix $\text{diag}\{M-1, -1, \dots, -1\}$. The unitary matrix $\mathbf{U} = [\mathbf{v}_1 \ \mathbf{v}_2 \ \dots \ \mathbf{v}_M]$ consists of normalized eigenvectors of \mathbf{D} . Define the $(M \times 1)$ vector $\mathbf{u}_M = [1 \ 1 \ \dots \ 1]^T$; then $\mathbf{v}_1 = M^{-\frac{1}{2}} \mathbf{u}_M$, and the other eigenvectors satisfy $\mathbf{u}_M^T \cdot \mathbf{v}_i = 0$ and $\mathbf{v}_i^T \cdot \mathbf{v}_i = 1$, for all $i=2, 3, \dots, M$.

Since

$$\mathbf{I}_{ij} = (\mathbf{U}\mathbf{U}^T)_{ij} = (\mathbf{v}_1 \cdot \mathbf{v}_1^T)_{ij} + \sum_{k=2}^M (\mathbf{v}_k \cdot \mathbf{v}_k^T)_{ij} = \begin{cases} 1, & i = j \\ 0, & i \neq j \end{cases}$$

the following are true and will be used later:

$$(\mathbf{v}_1 \cdot \mathbf{v}_1^T)_{ii} = \frac{1}{M}, \quad \sum_{k=2}^M (\mathbf{v}_k \cdot \mathbf{v}_k^T)_{ii} = \frac{M-1}{M},$$

$$(\mathbf{v}_1 \cdot \mathbf{v}_1^T)_{ij} = \frac{1}{M}, \quad i \neq j, \quad \sum_{k=2}^M (\mathbf{v}_k \cdot \mathbf{v}_k^T)_{ij} = \frac{-1}{M}, \quad i \neq j.$$

It is well known [14] that the matrix $\mathbf{R}_M^{-1} = (\mathbf{I} + \rho \mathbf{D})^{-1}$ has the same eigenvectors as \mathbf{D} and eigenvalues $\lambda_{\mathbf{R}} = (1 + \rho \lambda_{\mathbf{D}})^{-1}$, where $\lambda_{\mathbf{D}}$ are the eigenvalues of \mathbf{D} . Then,

$$\Lambda_{\mathbf{R}^{-1}} = \text{diag} \left\{ \frac{1}{1+\rho(M-1)}, \frac{1}{1-\rho}, \dots, \frac{1}{1-\rho} \right\}.$$

We have

$$\mathbf{R}_M^{-1} = \mathbf{U} \Lambda_{\mathbf{R}^{-1}} \mathbf{U}^T = \frac{1}{1+\rho(M-1)} \mathbf{v}_1 \cdot \mathbf{v}_1^T + \frac{1}{1-\rho} \sum_{j=2}^M \mathbf{v}_j \cdot \mathbf{v}_j^T,$$

$$\begin{aligned} (\mathbf{R}_M^{-1})_{ii} &= \frac{1}{1+\rho(M-1)} \cdot \frac{1}{M} + \frac{1}{1-\rho} \cdot \frac{M-1}{M} \\ &= \frac{1+\rho(M-2)}{[1+\rho(M-1)](1-\rho)}, \quad i=1,2,\dots,M, \end{aligned}$$

$$\begin{aligned} \mathbf{R}_M^{-1} \mathbf{u}_M &= \mathbf{U} \Lambda_{\mathbf{R}^{-1}} \cdot \begin{bmatrix} \mathbf{v}_1^T & \mathbf{v}_2^T & \dots & \mathbf{v}_M^T \end{bmatrix}^T \cdot \mathbf{u}_M \\ &= \mathbf{U} \Lambda_{\mathbf{R}^{-1}} \begin{bmatrix} \sqrt{M} & 0 & \dots & 0 \end{bmatrix}^T = \frac{1}{1+\rho(M-1)} \mathbf{u}_M, \end{aligned}$$

$$\begin{aligned} \mathbf{R}_M^{-1} \Delta \mathbf{A}_N \mathbf{b}_N &= \mathbf{R}_M^{-1} \cdot \mathbf{u}_M \cdot \rho \sum_{j=M+1}^{M+N} \sqrt{P_j} b_j \\ &= \mathbf{u}_M \cdot \frac{\rho}{1+\rho(M-1)} \sum_{j=M+1}^{M+N} \sqrt{P_j} b_j. \end{aligned}$$

Therefore we obtain

$$\begin{aligned} SIR_{\text{dec},i}^{(M,N)} &= \frac{P_i}{\sigma^2 (\mathbf{R}_M^{-1}) + E \left\{ \left(\mathbf{R}_M^{-1} \Delta \mathbf{A}_N \mathbf{b}_N \right)_i^2 \right\}} \\ &= \frac{P_i}{\frac{\sigma^2}{1-\rho} \cdot \frac{1+\rho(M-2)}{1+\rho(M-1)} + \left[\frac{\rho}{1+\rho(M-1)} \right]^2 \sum_{j=M+1}^{M+N} P_j}. \end{aligned} \tag{2.5}$$

D. Derivation of (2.15) and (2.16)

Define the same Hermitian matrix \mathbf{D} and unitary matrix \mathbf{U} as in Appendix C. Define $\varepsilon = P/\sigma^2$, $\delta = 1+\rho(M-1)$, and $\gamma = 1-\rho$. Then the matrix $\mathbf{R}_M = \mathbf{I} + \rho \mathbf{D}$ and $\mathbf{G} = ((1+\varepsilon^{-1}) \cdot \mathbf{I} + \rho \cdot \mathbf{D})^{-1}$ can be written as:

$$\mathbf{G} = \mathbf{U} \Lambda_{\mathbf{G}} \mathbf{U}^T, \text{ with } \Lambda_{\mathbf{G}} = \text{diag} \left\{ \varepsilon / (\delta \varepsilon + 1), \varepsilon / \gamma \varepsilon + 1, \dots, \varepsilon / \gamma \varepsilon + 1 \right\}.$$

and $\mathbf{R}_M = \mathbf{U}\mathbf{\Lambda}_R\mathbf{U}^T$, with $\mathbf{\Lambda}_R = \text{diag}\{\delta, \gamma, \dots, \gamma\}$.

Similarly as in Appendix C, we have $(\mathbf{G} \cdot \mathbf{u}_M)_i = \frac{\mathcal{E}}{\delta\mathcal{E} + 1}$.

From

$$\begin{aligned} \mathbf{G}\mathbf{R}_M &= \mathbf{U}\mathbf{\Lambda}_G\mathbf{U}^T \cdot \mathbf{U}\mathbf{\Lambda}_R\mathbf{U}^T = \mathbf{U}(\mathbf{\Lambda}_G\mathbf{\Lambda}_R)\mathbf{U}^T \\ &= \frac{\delta\mathcal{E}}{\delta\mathcal{E} + 1}(\mathbf{v}_1 \cdot \mathbf{v}_1^T) + \frac{\gamma\mathcal{E}}{\gamma\mathcal{E} + 1} \sum_{k=2}^M (\mathbf{v}_k \cdot \mathbf{v}_k^T), \end{aligned}$$

we have

$$(\mathbf{G}\mathbf{R}_M)_{ii} = \frac{\delta\mathcal{E}}{\delta\mathcal{E} + 1} \frac{1}{M} + \frac{\gamma\mathcal{E}}{\gamma\mathcal{E} + 1} \frac{M-1}{M},$$

$$(\mathbf{G}\mathbf{R}_M)_{ij} = \frac{1}{M} \left(\frac{\delta\mathcal{E}}{\delta\mathcal{E} + 1} - \frac{\gamma\mathcal{E}}{\gamma\mathcal{E} + 1} \right), \quad i \neq j.$$

Then, from

$$\begin{aligned} \mathbf{G}\mathbf{R}_M\mathbf{G} &= \mathbf{U}(\mathbf{\Lambda}_G\mathbf{\Lambda}_R\mathbf{\Lambda}_G)\mathbf{U}^T \\ &= \frac{\delta\mathcal{E}^2}{(\delta\mathcal{E} + 1)^2}(\mathbf{v}_1 \cdot \mathbf{v}_1^T) + \frac{\gamma\mathcal{E}^2}{(\gamma\mathcal{E} + 1)^2} \sum_{k=2}^M (\mathbf{v}_k \cdot \mathbf{v}_k^T), \end{aligned}$$

we have

$$(\mathbf{G}\mathbf{R}_M\mathbf{G})_{ii} = \frac{\delta\mathcal{E}^2}{(\delta\mathcal{E} + 1)^2} \frac{1}{M} + \frac{\gamma\mathcal{E}^2}{(\gamma\mathcal{E} + 1)^2} \frac{M-1}{M}.$$

Therefore,

$$\begin{aligned} SIR_{\text{mmse}}^{(M,N)} &= (\mathbf{G}\mathbf{R}_M)_{ii}^2 P / \left\{ (M-1)(\mathbf{G}\mathbf{R}_M)_{ij}^2 P \right. \\ &\quad \left. + \left(\sum_{j=M+1}^{M+N} P_j \right) \rho^2 (\mathbf{G}\mathbf{u}_M)^2 + \sigma^2 (\mathbf{G}\mathbf{R}_M\mathbf{G})_{ii} \right\} \\ &= \left(\frac{\delta\mathcal{E}}{\delta\mathcal{E} + 1} \cdot \frac{1}{M} + \frac{\gamma\mathcal{E}}{\gamma\mathcal{E} + 1} \frac{M-1}{M} \right)^2 P / \left\{ \frac{M-1}{M^2} \left(\frac{\delta\mathcal{E}}{\delta\mathcal{E} + 1} - \frac{\gamma\mathcal{E}}{\gamma\mathcal{E} + 1} \right)^2 P + \right. \\ &\quad \left. \left(\sum_{j=M+1}^{M+N} P_j \right) \left(\frac{\rho\mathcal{E}}{\delta\mathcal{E} + 1} \right)^2 + \sigma^2 \left(\frac{\delta\mathcal{E}^2}{(\delta\mathcal{E} + 1)^2} \cdot \frac{1}{M} + \frac{\gamma\mathcal{E}^2}{(\gamma\mathcal{E} + 1)^2} \frac{M-1}{M} \right) \right\} \end{aligned}$$

$$\begin{aligned}
&= \frac{\varepsilon(\delta\gamma\varepsilon+1)^2}{(M-1)\rho^2\varepsilon+(1+2\delta\gamma\varepsilon+\delta\gamma(\delta-\rho)\varepsilon^2)+(P_u/\sigma^2)\rho^2(\gamma\varepsilon+1)^2} \\
&= \frac{P(\delta\gamma P+\sigma^2)^2}{(\delta-1)\rho P\sigma^4+\sigma^2(\sigma^4+2\delta\gamma\sigma^2 P+\delta\gamma(\delta-\rho)P^2)+P_u\rho^2(\gamma P+\sigma^2)^2}.
\end{aligned} \tag{2.15}$$

Let $P_u=0$, then $\delta=1+\rho(K-1)$ and, hence, we obtain

$$\begin{aligned}
SIR_{\text{mmse}}^{(K,0)} &= \frac{\varepsilon(\delta\gamma\varepsilon+1)^2}{(M-1)\rho^2\varepsilon+1+2\delta\gamma\varepsilon+\delta\gamma(\delta-\rho)\varepsilon^2} = \frac{\varepsilon(\delta\gamma\varepsilon+1)}{(\delta-\rho)\varepsilon+1} \\
&= \frac{P(\delta\gamma P+\sigma^2)}{(\delta-\rho)P\sigma^2+\sigma^4} = \frac{P((1+\rho(K-1))(1-\rho)P+\sigma^2)}{\sigma^2((1+\rho(K-2))P+\sigma^2)}.
\end{aligned} \tag{2.16}$$

E. Monotonicity of $SIR_{\text{mmse}}^{(K,0)}(P, K)$ and $SIR_{\text{mmse}}^{(M,N)}(P, M)$

In the simplification, the following constraints are used:

$$K \geq 1, \delta \geq 1, \delta - 1 \geq 0, 0 \leq \rho < 1, 0 < \gamma \leq 1, \delta\gamma > 0, \varepsilon > 0, \delta\gamma\varepsilon + 1 > 0.$$

Rewrite (2.16) as

$$SIR_{\text{mmse}}^{(K,0)} \stackrel{(a)}{=} \frac{\varepsilon}{1 + \frac{\rho}{\gamma} \cdot \left(1 - \frac{1 + \gamma\varepsilon}{1 + \delta\gamma\varepsilon}\right)} \stackrel{(b)}{=} \frac{\delta\gamma\varepsilon + 1}{(\delta - \rho) + \frac{1}{\varepsilon}}.$$

From (a), SIR is a decreasing function of $\delta (=1+\rho(K-1))$ when P is fixed ($\varepsilon = P/\sigma^2$ is fixed), and therefore it is a decreasing function of K from P/σ^2 for $K=1$ to $(1-\rho)P/\sigma^2$ for $K=\infty$. From (b), the SIR is an increasing function of ε when K is fixed, and therefore it is an increasing function of P from 0 to ∞ as P goes from 0 to ∞ .

We rewrite (2.15) as

$$\begin{aligned}
SIR_{\text{mmse}}^{(M,N)} &= \frac{\varepsilon(\delta\gamma\varepsilon+1)^2}{(\delta-1)\rho\varepsilon+(1+2\delta\gamma\varepsilon+\delta\gamma(\delta-\rho)\varepsilon^2)+\theta\rho^2(\gamma\varepsilon+1)^2} \\
&= \frac{\varepsilon}{1+\frac{\varepsilon\rho(\delta-1)-\delta^2\gamma^2\varepsilon^2+\delta\gamma(\delta-\rho)\varepsilon^2}{(\delta\gamma\varepsilon+1)^2}+\theta\rho^2\frac{(\gamma\varepsilon+1)^2}{(\delta\gamma\varepsilon+1)^2}} \\
&= \frac{\varepsilon}{1+\frac{\varepsilon\rho(\delta-1)}{\delta\gamma\varepsilon+1}+\theta\frac{\rho^2}{\delta^2}\left(1+\frac{\delta-1}{\delta\gamma\varepsilon+1}\right)^2} \\
&= \left[\frac{1}{\varepsilon}+\frac{\rho(\delta-1)}{\delta\gamma\varepsilon+1}+\theta\frac{\rho^2}{\varepsilon\delta^2}\left(1+\frac{\delta-1}{\delta\gamma\varepsilon+1}\right)^2\right]^{-1}.
\end{aligned}$$

Hence, SIR is an increasing function of P from 0 to ∞ .

F. Proof of Proposition 1

Matrix \mathbf{A} is real and symmetric, so it can be diagonalized to $\mathbf{A}=\mathbf{U}\cdot\mathbf{\Lambda}_A\cdot\mathbf{U}^T$. Here \mathbf{U} is a unitary matrix (i.e., $\mathbf{U}\mathbf{U}^T=\mathbf{U}^T\mathbf{U}=\mathbf{I}$), and $\mathbf{\Lambda}_A$ is a diagonal matrix, whose diagonal elements are equal to the real eigenvalues of \mathbf{A} . Define $\mathbf{G}=\mathbf{I}-\beta\mathbf{A}$. Then \mathbf{G} can be diagonalized to $\mathbf{G}=\mathbf{U}\cdot\mathbf{\Lambda}\cdot\mathbf{U}^T$, with $\mathbf{\Lambda}=\mathbf{I}-\beta\mathbf{\Lambda}_A$. From the feasibility assumption on β , (i.e. $\beta < 1/\rho_A$), the diagonal elements of $\mathbf{\Lambda}$ (eigenvalues of \mathbf{G}) are all positive. So \mathbf{G} and \mathbf{G}^{-1} are positive definite, and they can be written as $\mathbf{G}=\mathbf{U}\cdot\mathbf{\Lambda}^{\frac{1}{2}}\cdot\mathbf{\Lambda}^{\frac{1}{2}}\cdot\mathbf{U}^T$, and $\mathbf{G}^{-1}=\mathbf{U}\cdot\mathbf{\Lambda}^{-\frac{1}{2}}\cdot\mathbf{\Lambda}^{-\frac{1}{2}}\cdot\mathbf{U}^T$. Then, by the Cauchy-Schwartz inequality, we have

$$\begin{aligned}
(\mathbf{1}^T\mathbf{G}\mathbf{1})(\mathbf{1}^T\mathbf{G}^{-1}\mathbf{1}) &= (\mathbf{1}^T\cdot\mathbf{U}\mathbf{\Lambda}^{\frac{1}{2}}\mathbf{\Lambda}^{\frac{1}{2}}\mathbf{U}\cdot\mathbf{1})(\mathbf{1}^T\cdot\mathbf{U}\mathbf{\Lambda}^{-\frac{1}{2}}\mathbf{\Lambda}^{-\frac{1}{2}}\mathbf{U}\cdot\mathbf{1}) = \|\mathbf{\Lambda}^{\frac{1}{2}}\mathbf{U}^T\mathbf{1}\|^2 \cdot \|\mathbf{\Lambda}^{-\frac{1}{2}}\mathbf{U}^T\mathbf{1}\|^2 \\
&\geq \left| \left(\mathbf{\Lambda}^{\frac{1}{2}}\mathbf{U}^T\mathbf{1} \right)^T \cdot \left(\mathbf{\Lambda}^{-\frac{1}{2}}\mathbf{U}^T\mathbf{1} \right) \right|^2 = |\mathbf{1}^T\mathbf{1}|^2 = N^2.
\end{aligned} \tag{a}$$

The condition to have equality in (a) is $\mathbf{\Lambda}^{\frac{1}{2}}\mathbf{U}^T\mathbf{1}=\gamma\mathbf{\Lambda}^{-\frac{1}{2}}\mathbf{U}^T\mathbf{1}$, for some constant γ . This means $\mathbf{G}\cdot\mathbf{1}=\gamma\cdot\mathbf{1}$ and $\mathbf{A}\cdot\mathbf{1}=\left[\frac{1-\gamma}{\beta}\right]\cdot\mathbf{1}$; i.e., the row summation of matrix \mathbf{A} should be a constant. Then,

$$\left(\sum_{j=1}^N \rho_{ij}^2 \right) - 1 = (1 - \gamma) / \beta, \quad i = 1, 2, \dots, N, \quad \text{for some constant } \gamma. \quad (\text{b})$$

For $N > L$, apply the Welch bound [20] that yields $\sum_{i=1}^N \sum_{j=1}^N \rho_{ij}^2 \geq N^2/L$. So, we have

$$\mathbf{1}^T \cdot \mathbf{G} \cdot \mathbf{1} = N - \beta \left(\sum_{i=1}^N \sum_{j=1}^N \rho_{ij}^2 - N \right) \leq (1 + \beta)N - \beta \frac{N^2}{L} = N \left(1 + \beta - \beta \frac{N}{L} \right). \quad (\text{c})$$

The sequences that satisfy the equality in (c) are the WBE sequences, which obey $\mathbf{S}\mathbf{S}^T = (N/L)\mathbf{I}$, and $\sum_{j=1}^N \rho_{ij}^2 = N/L, i = 1, 2, \dots, N$. Notice that the WBE sequences also satisfy

(b) with $\gamma = 1 + \beta - \beta N/L$. Therefore WBE sequences also achieve equality in (a).

Since $P_{total} = \beta \sigma^2 \mathbf{1} \cdot \mathbf{G}^{-1} \cdot \mathbf{1}$, using (a) and (c) in succession yields

$$P_{total} \geq \frac{N\sigma^2}{1 + \frac{1}{\beta} - \frac{N}{L}}. \quad (\text{d})$$

Therefore, the minimum value in (d) is achieved by the WBE sequence, and the assigned power vector should be

$$\mathbf{P} = \beta \sigma^2 \mathbf{G}^{-1} \mathbf{1} = \frac{\beta \sigma^2}{\gamma} \mathbf{1} = \frac{\sigma^2}{1 + \frac{1}{\beta} - \frac{N}{L}} \mathbf{1}.$$

For $N \leq L$, orthogonal sequences are available for $N \leq L$ to achieve the lowest total crosscorrelation, and $\sum_{i=1}^N \sum_{j=1}^N \rho_{ij}^2 \geq N$. Thus,

$$\mathbf{1}^T \cdot \mathbf{G} \cdot \mathbf{1} = N - \beta \left(\sum_{i=1}^N \sum_{j=1}^N \rho_{ij}^2 - N \right) \leq N. \quad (\text{e})$$

Orthogonal sequences also achieve equality in (a) with $\gamma = 1$. Therefore, the minimum total power can be obtained from (a) and (e) as

$$P_{total} \geq N\beta\sigma^2,$$

and the assigned power vector is given by

$$\mathbf{P} = \beta \sigma^2 \mathbf{1}.$$

G. Proof of (3.10)

Suppose the power control problem has solutions; then there exist some $P_1 > 0$ and $P_2 > 0$, which satisfy

$$P_1 \geq \beta_{1f} \sigma^2 + \beta_{1f} P_1 (\alpha_{11}^f - 1) + \beta_{1f} P_2 \alpha_{12}^f, \quad f = 1, 2, \dots, F_1,$$

$$\text{and } P_2 \geq \beta_{2f} \sigma^2 + \beta_{2f} P_1 \alpha_{21}^f + \beta_{2f} P_2 (\alpha_{22}^f - 1), \quad f = 1, 2, \dots, F_2.$$

Because $\alpha_{12}^f \geq 0$, $\beta_{1f} > 0$, and $P_2 > 0$, we obtain for node 1 that

$$P_1 [1 - \beta_{1f} (\alpha_{11}^f - 1)] \geq \beta_{1f} \sigma^2 + \beta_{1f} P_2 \alpha_{12}^f > 0.$$

Therefore from $P_1 > 0$, we have $\alpha_{11}^f < 1 + 1/\beta_{1f}$, $f = 1, 2, \dots, F_1$,

Also, because $\alpha_{21}^f \geq 0$, $\beta_{2f} > 0$, and $P_1 > 0$, we obtain for nodes 2

$$P_2 [1 - \beta_{2f} (\alpha_{22}^f - 1)] \geq \beta_{2f} \sigma^2 + \beta_{2f} P_1 \alpha_{21}^f > 0.$$

Therefore from $P_2 > 0$, we have $\alpha_{22}^f < 1 + 1/\beta_{2f}$, $f = 1, 2, \dots, F_2$.

Then from the definition of the parameters a , b , c , and d , and because $\alpha_{12}^f \geq 0$, $f = 1, 2, \dots, F_1$, and $\alpha_{21}^f \geq 0$, $f = 1, 2, \dots, F_2$, we have

$$a_f > 0, \quad b_f \geq 0, \quad f = 1, 2, \dots, F_1;$$

$$c_f > 0, \quad d_f \geq 0, \quad f = 1, 2, \dots, F_2.$$

Notice that, if we start from $P_i \geq \beta_{if} \sigma^2 + \beta_{if} P_i (\alpha_{ii}^f - 1) + \beta_{if} \sum_{j \neq i} P_j \alpha_{ij}^f$, $f = 1, 2, \dots, F_i$, and

go through the same steps, we can prove Proposition 5 for the case of N nodes.

H. Proof of Proposition 3

The solution set can be described as

$$\{(P_1, P_2) > 0 \mid P_2 \geq c_f + d_f P_1, f = 1, 2, \dots, F_2 \text{ and } P_1 \geq a_f + b_f P_2, f = 1, 2, \dots, F_1\}.$$

The necessity: Suppose $\alpha_{11}^f \leq 1 + 1/\beta_{1f}$ and $\alpha_{22}^f \leq 1 + 1/\beta_{2f}$ are not satisfied; then there is no solution. Suppose $\alpha_{11}^f \leq 1 + 1/\beta_{1f}$ and $\alpha_{22}^f \leq 1 + 1/\beta_{2f}$ are satisfied, but

$\max_{f=1,2,\dots,F_1} (b_f) \cdot \max_{f=1,2,\dots,F_2} (d_f) < 1$ is not satisfied; then, there exist at least one pair of h and g

($h \neq g$) such that $0 < 1/b_h \leq d_g$. From the non-negative property of the coefficients, for any

$P_1 > 0$, we have $c_g + d_g P_1 > -a_h/b_h + P_1/b_h$. So,

$$\begin{aligned} & \{(P_1, P_2) > 0 \mid P_2 \geq c_g + d_g P_1 \text{ and } P_1 \geq a_h + b_h P_2\} \\ &= \left\{ (P_1, P_2) > 0 \mid P_2 \geq c_g + d_g P_1 \text{ and } P_2 \leq -\frac{a_h}{b_h} + \frac{1}{b_h} P_1 \right\} \\ &= \emptyset. \end{aligned}$$

Since the solution set is a subset of $\{(P_1, P_2) > 0 \mid P_2 \geq c_g + d_g P_1 \text{ and } P_1 \geq a_h + b_h P_2\}$, it is also an empty set, i.e., no solution exists.

The sufficiency: Suppose $\alpha_{11}^f \leq 1 + 1/\beta_{1f}$, $\alpha_{22}^f \leq 1 + 1/\beta_{2f}$, and $\max_{f=1,2,\dots,F_1} (b_f) \cdot \max_{f=1,2,\dots,F_2} (d_f) < 1$ are satisfied. From

$$\begin{aligned} & \max_{f=1,2,\dots,F_2} (c_f) + \max_{f=1,2,\dots,F_2} (d_f) P_1 \geq c_f + d_f P_1, f = 1, 2, \dots, F_2, \\ & \max_{f=1,2,\dots,F_1} (a_f) + \max_{f=1,2,\dots,F_1} (b_f) P_2 \geq a_f + b_f P_2, f = 1, 2, \dots, F_1, \end{aligned}$$

we have

$$\begin{aligned} & \{(P_1, P_2) > 0 \mid P_2 > c_f + d_f P_1, f = 1, 2, \dots, F_2 \text{ and } P_1 > a_f + b_f P_2, f = 1, 2, \dots, F_1\} \\ &= \{(P_1, P_2) > 0 \mid P_2 > c_f + d_f P_1, f = 1, 2, \dots, F_2\} \cap \{(P_1, P_2) > 0 \mid P_1 > a_f + b_f P_2, f = 1, 2, \dots, F_1\} \end{aligned}$$

$$\begin{aligned}
&\supseteq \left\{ (P_1, P_2) > 0 \left| P_2 > \max_{f=1,2,\dots,F_2} (c_f) + \max_{f=1,2,\dots,F_2} (d_f) P_1 \right. \right\} \cap \left\{ (P_1, P_2) > 0 \left| P_1 > \max_{f=1,2,\dots,F_1} (a_f) + \max_{f=1,2,\dots,F_1} (b_f) P_2 \right. \right\} \\
&= \left\{ (P_1, P_2) > 0 \left| \max_{f=1,2,\dots,F_2} (c_f) + \max_{f=1,2,\dots,F_2} (d_f) P_1 < P_2 < \frac{P_1 - \max_{f=1,2,\dots,F_1} (a_f)}{\max_{f=1,2,\dots,F_1} (b_f)} \right. \right\} \\
&\neq \emptyset.
\end{aligned}$$

The last step is justified because $\max_{f=1,2,\dots,F_2} (c_f) + \max_{f=1,2,\dots,F_2} (d_f) P_1 < \left(P_1 - \max_{f=1,2,\dots,F_1} (a_f) \right) / \max_{f=1,2,\dots,F_1} (b_f)$

is guaranteed when P_1 is large enough, specifically, when

$$P_1 > \left(\max_{f=1,2,\dots,F_2} c_f + \max_{f=1,2,\dots,F_1} a_f / \max_{f=1,2,\dots,F_1} b_f \right) / \left(1 / \max_{f=1,2,\dots,F_1} b_f - \max_{f=1,2,\dots,F_2} d_f \right) > 0.$$

The last part “>0” is from the non-negative properties of the coefficients and

$$\max_{f=1,2,\dots,F_1} (b_f) \cdot \max_{f=1,2,\dots,F_2} (d_f) < 1.$$

Notice that the proof of Proposition 2 can be obtained from the proof of Proposition 3 by changing F_1 and F_2 into F , and β_{1f} and β_{2f} into β_f .

Furthermore, by specifying $F=2$ in the proof of Proposition 2, we obtain the necessary and sufficient conditions for the $N=2, F=2$ uplink problem to have solutions is:

$$\alpha_{11}^f < 1 + \frac{1}{\beta_f}, \quad \alpha_{22}^f < 1 + \frac{1}{\beta_f}, \quad f=1,2, \quad \text{and} \quad \max_{f=1,2} (b_f) \cdot \max_{f=1,2} (d_f) < 1.$$

I. Proof of Proposition 4

First we prove that $\mathbf{I}(\mathbf{P})$ defined in (3.12) is standard.

The positivity property follows directly from the non-negativeness of matrix $\mathbf{A}^{(f)}$.

For the monotonicity property, assume $\mathbf{P} \geq \mathbf{P}'$; then we have

$$\mathbf{I}(\mathbf{P}) = \max_f \left\{ \beta_f \mathbf{A}^{(f)} \cdot \mathbf{P} + \beta_f \sigma^2 \mathbf{1} \right\} \geq \max_f \left\{ \beta_f \mathbf{A}^{(f)} \cdot \mathbf{P}' + \beta_f \sigma^2 \mathbf{1} \right\} = \mathbf{I}(\mathbf{P}').$$

For scalability, assume $\alpha > 1$, then

$$\alpha \mathbf{I}(\mathbf{P}) = \max_f \left\{ \alpha \beta_f \mathbf{A}^{(f)} \mathbf{P} + \alpha \beta_f \sigma^2 \mathbf{1} \right\} > \max_f \left\{ \beta_f \mathbf{A}^{(f)} (\alpha \mathbf{P}) + \beta_f \sigma^2 \mathbf{1} \right\} = \mathbf{I}(\alpha \mathbf{P}).$$

Therefore, $\mathbf{I}(\mathbf{P})$ defined in (3.12) is standard. Using the main theorem from [22], the iterative algorithm $\mathbf{P}^{(i+1)} = \mathbf{I}(\mathbf{P}^{(i)})$ converges to the optimum power vector \mathbf{P}^* .

Then we prove that $\mathbf{I}(\mathbf{P})$ defined in (3.13) is standard.

The positivity property follows directly from $\alpha_{ii}^f \geq 1, \alpha_{ij}^f \geq 0$.

For the monotonic property, assume $\mathbf{P} \geq \mathbf{P}'$; then we have

$$\begin{aligned} \mathbf{I}_i(\mathbf{P}) &= \max_{f=1,2,\dots,F_i} \left\{ \beta_{if} \sigma^2 + \beta_{if} P_i (\alpha_{ii}^f - 1) + \beta_{if} \sum_{j \neq i} P_j \alpha_{ij}^f \right\} \\ &\geq \max_{f=1,2,\dots,F_i} \left\{ \beta_{if} \sigma^2 + \beta_{if} P'_i (\alpha_{ii}^f - 1) + \beta_{if} \sum_{j \neq i} P'_j \alpha_{ij}^f \right\} \\ &= I_i(\mathbf{P}'), \quad i=1,2,\dots,N. \end{aligned}$$

For the scalability property, assume $\alpha > 1$; then

$$\begin{aligned} \alpha I_i(\mathbf{P}) &= \max_{f=1,2,\dots,F_i} \left\{ \alpha \beta_{if} \sigma^2 + \alpha \beta_{if} P_i (\alpha_{ii}^f - 1) + \alpha \beta_{if} \sum_{j \neq i} P_j \alpha_{ij}^f \right\} \\ &> \max_{f=1,2,\dots,F_i} \left\{ \beta_{if} \sigma^2 + \beta_{if} (\alpha P_i) (\alpha_{ii}^f - 1) + \beta_{if} \sum_{j \neq i} (\alpha P_j) \alpha_{ij}^f \right\} \\ &= I_i(\alpha \mathbf{P}). \end{aligned}$$

In conclusion, the iterative algorithm $\mathbf{P}^{(i+1)} = \mathbf{I}(\mathbf{P}^{(i)})$ with $\mathbf{I}(\mathbf{P})$ defined by (3.13) converges to the optimum power vector \mathbf{P}^* .

J. Proof of Proposition 7

We start from $F=3$. Suppose there are 3 codes, with $\alpha_1 \geq \alpha_2 \geq \alpha_3$, ($\alpha_i = \sum_{j \neq i} \rho_{ij}^2$), and 3 flow types with SIR requirements $\beta_1 \leq \beta_2 \leq \beta_3$. We use notation (i,j,k) to imply that code i is assigned to flow type β_1 , code j is assigned to flow type β_2 , and code k is assigned to

flow type β_3 . We want to maximize $f(i, j, k) = \min(1/\beta_1 - \alpha_i, 1/\beta_2 - \alpha_j, 1/\beta_3 - \alpha_k)$.

Suppose $\beta_i \leq \beta_j$, and $\alpha_i \geq \alpha_j$; then $1/\beta_i - \alpha_i \geq 1/\beta_j - \alpha_i$, $1/\beta_j - \alpha_j \geq 1/\beta_j - \alpha_i$,
 $1/\beta_i - \alpha_j \geq 1/\beta_j - \alpha_i$.

Therefore, $\min(1/\beta_i - \alpha_i, 1/\beta_j - \alpha_j) \geq 1/\beta_j - \alpha_i = \min(1/\beta_i - \alpha_j, 1/\beta_j - \alpha_i)$.

Consequently,

$$\begin{aligned} f(1,2,3) &= \min(1/\beta_1 - \alpha_1, 1/\beta_2 - \alpha_2, 1/\beta_3 - \alpha_3) = \min(1/\beta_1 - \alpha_1, \min(1/\beta_2 - \alpha_2, 1/\beta_3 - \alpha_3)) \\ &\geq \min(1/\beta_1 - \alpha_1, \min(1/\beta_2 - \alpha_3, 1/\beta_3 - \alpha_2)) = f(1,3,2). \end{aligned}$$

Similarly, we show $f(1,2,3) \geq f(2,1,3) \geq f(2,3,1)$, and $f(1,3,2) \geq f(3,1,2) \geq f(3,2,1)$.

Therefore, $f(1,2,3)$ is the maximal assignment among all 6 possible ones, i.e., for any code set, the best assignment should always assign the code with minimum α to the flow with maximum β , and the code with maximum α to the flow with minimum β . So, the problem of $\min_f(1/\beta_f - \alpha_f)$ should have solutions that satisfy $\alpha_1 \geq \alpha_2 \geq \alpha_3$. i.e., Proposition 7 is true for $F=3$.

Now consider $F=4$ with $\alpha_1 \geq \alpha_2 \geq \alpha_3 \geq \alpha_4$. From the conclusion for $F=3$, since $\alpha_2 \geq \alpha_3 \geq \alpha_4$, and $\beta_2 \leq \beta_3 \leq \beta_4$, we have

$$f(1,2,3,4) \geq f(1,i,j,k), \text{ where } (i,j,k) \text{ is any permutation of } (2,3,4).$$

Similarly,

$$f(2,1,3,4) \geq f(2,i,j,k), \text{ where } (i,j,k) \text{ is any permutation of } (1,3,4).$$

$$f(3,1,2,4) \geq f(3,i,j,k), \text{ where } (i,j,k) \text{ is any permutation of } (1,2,4).$$

$$f(4,1,2,3) \geq f(4,i,j,k), \text{ where } (i,j,k) \text{ is any permutation of } (1,2,3).$$

We can also show $f(1,2,3,4) \geq f(2,1,3,4) \geq f(4,1,2,3)$, and $f(1,2,3,4) \geq f(3,1,2,4)$.

Altogether, $f(1, 2, 3, 4) \geq f(i, j, k, m)$, where (i, j, k, m) is any permutation of $(1, 2, 3, 4)$.

Then assume that for $F=n$ the proposition is true, that is,

$$f(1, 2, \dots, n) \geq f(i_1, i_2, \dots, i_n), \text{ with } (i_1, i_2, \dots, i_n) \text{ any permutation of } (1, 2, \dots, n).$$

Then using the same procedure as above, we prove that the proposition is true for $F=n+1$.

Hence, the induction process implies that for any F flow types with $\beta_1 \leq \beta_2 \leq \dots \leq \beta_F$, the optimal codes should always include the sequences that satisfy $\alpha_1 \geq \alpha_2 \geq \dots \geq \alpha_F$.

K. Derivation of (4.7)

Using $C_i = (i - (M - 1)/2)2\sqrt{3}/M$ and $P_i = 1/M$, from (4.4) we have

$$MSD(M - \text{PAM}) = M^{-2} + (12/M^3) \sum_{i=0}^{M-1} \sum_{j \neq i} P(C_j | C_i) \cdot (i - j)^2,$$

$$\text{with } P(C_j | C_i) = \begin{cases} Q((2|i - j| - 1)z_M) - Q((2|i - j| + 1)z_M), & j = 1, \dots, M - 2. \\ Q((2|i - j| - 1)z_M), & j = 0 \text{ or } M - 1. \end{cases}$$

Here $z_M = \sqrt{6/(M^2 - 1) \cdot (E_{av}/N_0)}$. Therefore,

$$\begin{aligned} MSD(M - \text{PAM}) &= M^{-2} + (24/M^3) \sum_{i=0}^{M-1} \sum_{|i-j|=1}^{M-1} P(C_j | C_i) \cdot |i - j|^2 \\ &= M^{-2} + (24/M^3) \sum_{k=1}^{M-1} k^2 \{ (M - k)Q((2k - 1)z_M) - (M - k - 1)Q((2k + 1)z_M) \} \quad (k = |i - j|) \\ &= M^{-2} + (24/M^3) \sum_{k=1}^{M-1} k^2 (M - k)Q((2k - 1)z_M) - (24/M^3) \sum_{i=2}^M (i - 1)^2 (M - i)Q((2i - 1)z_M) \\ & \quad (i = k + 1) \\ &= M^{-2} + (24/M^3) \sum_{i=1}^{M-1} i^2 (M - i)Q((2i - 1)z_M) - (24/M^3) \sum_{i=1}^{M-1} (i - 1)^2 (M - i)Q((2i - 1)z_M) \\ &= M^{-2} + (24/M^3) \sum_{i=1}^{M-1} (2i - 1)(M - i)Q((2i - 1)z_M) \end{aligned}$$

References

- [1]. F. Adachi, M. Sawahashi, and H. Suda, "Wideband DS-CDMA for next-generation mobile communications systems," *IEEE Commun. Mag.*, vol. 36, pp. 56-69, Sept. 1998.
- [2]. G. W. Wornell, "Spread-signature CDMA: efficient multiuser communication in the presence of fading," *IEEE Trans. Inform. Theory*, vol. 41, no. 5, pp 1418-1438, Sept. 1995.
- [3]. S. Verdú, *Multiuser Detection*, Cambridge Univ. Press, 1998.
- [4]. R. Lupas and S. Verdú, "Linear multiuser detectors for synchronous code-division multiple access," *IEEE Trans. Inform. Theory*, vol. 35, pp. 126-136, Jan. 1989.
- [5]. U. Madhow and M. Honig, "MMSE interference suppression for direct sequence spread-spectrum CDMA," *IEEE Trans. Commun.*, vol. 42, pp. 3178-3188, Dec. 1994.
- [6]. S. Verdú, "Optimum multiuser asymptotic efficiency," *IEEE Trans. Commun.*, vol. 34, pp. 890-897, Sept. 1996.
- [7]. U. Madhow and M. Honig, "On the average near-far resistance for MMSE detection of direct sequence CDMA signals with random spreading," *IEEE Trans. Inform. Theory*, vol. 45, pp. 2039-2045, Sept. 1999.
- [8]. R. Guérin, H. Ahmadi, and M. Naghshineh, "Equivalent capacity and its application to bandwidth allocation in high-speed networks," *IEEE J. Select. Areas Commun.*, vol. 9, no. 7, pp. 968-981, Sept. 1991.
- [9]. D. N. C. Tse and S. V. Hanly, "Linear multiuser receivers: effective interference, effective bandwidth, and user capacity," *IEEE Trans. Inform. Theory*, vol. 45, no. 2, pp. 641-657, Mar. 1999.
- [10]. P. Viswanath, V. Anantharam, and D. N. C. Tse, "Optimal sequence, power control, and user capacity of synchronous CDMA systems with linear MMSE multiuser receivers," *IEEE Trans. Inform. Theory*, vol. 45, no. 6, pp. 1968-1983, Sept. 1999.
- [11]. J. Zhang and E. K. P. Chong, "CDMA systems in fading channels: admissibility, network capacity, and power control," *IEEE Trans. Inform. Theory*, vol. 46, no. 3, pp. 962-981, May 2000.

- [12]. X. Wang, and A. Host-Madsen, "Group-blind multiuser detection for uplink CDMA," *IEEE J. Select. Areas Commun.*, vol. 17, no. 11, pp. 1971-1984, Nov. 1999.
- [13]. G. Ricci, M. K. Varanasi, and A. D. Maio, "Blind multiuser detection via interference identification," *IEEE Trans. Commun.*, vol. 50, no. 7, pp. 1172-1181, July 2002.
- [14]. B. Noble and J. W. Daniel, *Applied Linear Algebra*, Prentice-Hall, 1988.
- [15]. J. Zander, "Distributed cochannel interference control in cellular radio systems", *IEEE Trans. on Veh. Technol.*, vol. 41, no. 3, pp. 305-311, Aug. 1992.
- [16]. J. Zander, "Performance of optimum transmitter power control in cellular radio systems", *IEEE Trans. on Veh. Technol.*, vol. 41, no. 1, pp. 57-62, Feb. 1992.
- [17]. E. Seneta, *Non-negative Matrices and Markov Chains*, Springer Verlag, 1981.
- [18]. J. L. Massey and T. Mittelholzer, "Welch's bound and sequence sets for code-division multiple-access systems", *Sequences II: Methods in Communication, Security and computer Science*, R. Capocelli, A. De Santis and U. Vaccaro, Eds. New York: Springer-Verlag, 1991.
- [19]. M. Rubf and J. L. Massey, "Optimum sequence multisets for synchronous code-division multiple-access channels", *IEEE Trans. Inform. Theory*, vol. 40, no. 4, pp. 1261-1266, July 1994.
- [20]. S. Ulukus, "Optimum signature sequence sets for asynchronous CDMA systems", *38th Allerton Conference on Communication, Control, and Computing*, pp. 317-326, 2000.
- [21]. S. Ulukus and R. D. Yates, "Iterative construction of optimum signature sequence sets in synchronous CDMA systems", *IEEE Trans. Inform. Theory*, vol. 47, no. 5, pp. 1989-1998, July 2001.
- [22]. Roy D. Yates, "A framework for uplink power control in cellular radio systems", *IEEE J. Select. Areas Commun.*, vol. 13, no. 7, pp. 638-644, Sept. 1995.
- [23]. J. F. Hayes, "Adaptive feedback communications," *IEEE Trans. Commun. Technol.*, vol. COM-16, pp. 29-34, Feb. 1968.
- [24]. B. Vucetic, "An adaptive coding scheme for time-varying channels," *IEEE Trans. Commun.*, vol. 39, pp. 653-663, May 1991.
- [25]. V. K. N. Lau and S. V. Maric, "Variable rate adaptive modulation for DS-SS-CDMA," *IEEE Trans. Commun.*, vol. 47, no. 4, pp. 577-589, Apr. 1999.
- [26]. J. K. Cavers, "Variable-rate transmission for Rayleigh fading channels," *IEEE*

- Trans. Commun., vol. 20, pp. 15-22, Feb. 1972.
- [27]. W. T. Webb and R. Steele, "Variable rate QAM for mobile radio," *IEEE Trans. Commun.*, vol. 43, pp. 2223-2230, Jul. 1995.
- [28]. S. Otsuki, S. Sampei, and N. Morinaga, "Performance of modulation-level-controlled adaptive modulation systems," *Electronics & Communications in Japan, Part I: Communications*, vol. 79, no. 7, pp. 81-93, Jul. 1996.
- [29]. T. Ue, S. Sampei, N. Morinaga, and K. Hamaguchi, "Symbol rate and modulation level-controlled adaptive modulation/TDMA/TDD system for high-bit-rate wireless data transmission," *IEEE Trans. Veh. Technol.*, vol. 47, no. 4, pp. 1134-1147, Nov. 1998.
- [30]. J. Goldsmith and S. Chua, "Variable-rate variable-power MQAM for fading channels," *IEEE Trans. Commun.*, vol. 45, pp. 1218-1230, Oct. 1997.
- [31]. S. M. Alamouti and S. Kallel, "Adaptive trellis-coded multiple-phased-shift keying for Rayleigh fading channels," *IEEE Trans. Commun.*, vol. 42, pp. 2305-2314, Jun. 1994.
- [32]. M. B. Pursley and J. M. Shea, "Nonuniform Phase-Shift-Key modulation for multimedia multicast transmission in mobile wireless networks," *IEEE J. Select. Areas Commun.*, vol. 17, pp.774-783, May 1999.
- [33]. L. Wei, "Coded modulation with unequal error protection," *IEEE Trans. Commun.*, vol. 41, pp. 1439-1449, Oct. 1993.
- [34]. D. Stamatelos and A. Ephremides, "Combating performance degradation in highly mobile networks using rate control," *The 1st Annual Advanced Telecommunications/Information Distribution Research Program Conference*, Jan. 1997.
- [35]. J. G. Proakis, *Digital Communications*, 3rd Edition McGraw-Hill, 1995.
- [36]. X. Dong, N. C. Beaulieu, and P. H. Wittke, "Error probabilities of two-dimensional M-ary signaling in fading," *IEEE Trans. Commun.*, vol. 47, pp. 352-355, Mar. 1999.
- [37]. J. W. Craig, "A new simple and exact result for calculating the probability of error for two-dimensional signal constellations," *MILCOM'91*, pp. 571-575, 1991.
- [38]. S. Shakkottai, T. S. Rappaport, and P. C. Karlsson, "Cross-layer design for wireless networks," *IEEE Commun. Mag.*, vol. 41, no. 10, pp. 74-80, Oct. 2003.
- [39]. S. Toumpis and A. J. Goldsmith, "Performance, optimization, and cross-layer design of media access protocols for wireless Ad hoc networks," *IEEE ICC*, vol. 3, pp. 2234-2240, May 2003.

- [40]. A. Safwat, H. Hassanein, and H. Moutah, "Optimal cross-layer designs for energy-efficient wireless ad hoc and sensor networks," *IEEE International Performance, Computing and Communications Conference, Proceedings*, pp. 123-128, Apr. 2003.
- [41]. A. Iwata, et al., "Scalable routing strategies for ad hoc wireless networks," *IEEE J. Select Areas Commun.*, vol. 17, no. 8, pp. 1369-1379, Aug. 1999.
- [42]. C. R. Lin and J. S. Liu, "QoS routing in ad hoc wireless networks," *IEEE J. Select. Areas Commun.*, vol. 17, no. 8, pp. 1426-1438, Aug. 1999.
- [43]. S. Lal, and E. S. Sousa, "Distributed resource allocation for DS-CDMA-based multimedia ad hoc wireless LAN's," *IEEE J. Select Areas Commun.*, vol. 17, no. 5, pp. 947-967, May 1999.
- [44]. D. Ayyagari, A. Michail, and A. Ephremides, "Unified approach to scheduling, access control and routing for ad-hoc wireless networks," *IEEE Vehicular Technology Conference*, vol. 1, pp 380-384, May 2000.
- [45]. Girici, and A. Ephremides, "Joint routing and scheduling metrics for wireless ad hoc networks," *Collaborative Technology Alliances Conference 2003 Proceedings –Communications and Networks*, Apr. 2003.
- [46]. A. V. Santhanam and R. L. Cruz, "Optimal routing, link scheduling and power control in multi-hop wireless networks," *IEEE INFOCOM*, vol. 1, pp. 702-711, Mar. 2003.
- [47]. K. Wang, C. F. Chiasserini, R. R. Rao, and J. G. Proakis, "A distributed joint scheduling and power control algorithm for multicasting in wireless Ad Hoc networks," *IEEE ICC.*, vol. 1, pp. 725-731, May, 2003.
- [48]. T. Elbatte and A. Ephremides, "Joint Scheduling and Power Control for Wireless Ad Hoc Networks," *IEEE Trans. Wireless Commun.*, vol. 3, no. 1, pp. 74-85, Jan. 2004.
- [49]. D. Bertsekas and R. Gallager, "Data networks," Prentice-Hall, 1992.
- [50]. S. Ulukus and R. D. Yates, "Stochastic power control for cellular radio systems," *IEEE Trans. Commun.*, vol. 46, no. 6, pp. 784-798, Jun. 1998.